Electronic Supplementary Material (ESI) for RSC Advances.

Activation of C=P bond in phosphanylphosphaalkenes (C=P–P bond system) in the reaction with nucleophilic reagents: MeLi, *n*BuLi and *t*BuLi

Aleksandra Ziółkowska, Natalia Szynkiewicz, Łukasz Ponikiewski*

Department of Inorganic Chemistry, Chemical Faculty, Gdansk University of Technology, 11/12 Gabriela Narutowicza Str, 80-233 Gdansk, Poland.

PART A. X-ray data

The X-ray intensity data for **1a***, **2_1** and **3** were measured with an IPDS2T diffractometer equipped with an STOE image plate detector system and microfocus X-ray sources providing K*α* radiation by high-grade multi-layer X-ray mirror optics for Mo (λ = 0.71073 Å) wavelengths. The measurements were carried out at 120 K. The structures of the compounds were solved by direct methods and refined against F^2 with the Shelxs-2008 and Shelxl-2008 programs[1] run under WinGX.[2] Non-hydrogen atoms were refined with anisotropic displacement parameters. The isotropic displacement parameters of all hydrogens were fixed to 1.2 U_{eq} for aromatic, CH, CH_2 (1.5 times for methyl) groups.

The crystallographic data for the structures of **1a***, **2_1** and **3** reported in this paper have been deposited in the Cambridge Crystallographic Data Centre as supplementary publication No. CCDC 2114106, 2114107 and 2163558. Copies of the data can be obtained free of charge upon application to the CCDC, 12 Union Road, Cambridge CB2 1EZ, UK (Fax: (+44) 1223-336-033; E mail: deposit@ccdc.cam.ac.uk).

Table S1. Crystallographic data for **1a***, **2_1** and **3**.

	1a*	**2_1**	**3**
Empirical formula	$C_{84}H_{11}8Li_2O_6P_6$	$C_{41}H_{76}Li_1O_6P_3$	$C_{23}H_{40}P_2$
Formula weight	1423.48	764.86	378.49
Radiation source	Mo-$K\alpha$	Mo-$K\alpha$	Mo-$K\alpha$
Wavelength [Å]	0.71073	0.71073	0.71073
Crystal System	triclinic	triclinic	orthorhombic
Space group	*P*-1	*P*-1	$P2_12_12_1$
a [Å]	12.1986(5)	11.4465(8)	11.8649(3)
b [Å]	19.2100(8)	15.6595(16)	12.6361(4)
c [Å]	20.5903(9)	16.0158(10)	15.6655(4)
α [°]	115.094(3)	61.528(6)	90
β [°]	100.381(3)	71.074(5)	90
γ [°]	98.093(3)	68.526(7)	90
V [Å3]	4168.4(3)	2308.7(4)	2348.67(11)
Z	2	2	4
Calculated Density [g·cm-1]	1.134	1.100	1.07
T [K]	120(2)	120(2)	120(2)
μ [mm-1]	0.177	0.169	0.189
Theta range for data collection [°]	2.23-29.52	2.65-29.51	2.35-29.35
Index ranges	-16 ≤ h ≤ 16 -25 ≤ k ≤ 25 -27 ≤ l ≤ 27	-13 ≤ h ≤ 15 -20 ≤ k ≤ 20 -21 ≤ l ≤ 21	-15 ≤ h ≤ 15 -16 ≤ k ≤ 16 -19 ≤ l ≤20
Data / restraints / parameters	19849/0/905	11083/0/478	5657/0/238
Goodness-of-fit on F^2	1.026	0.967	1.046
Final R indices	0.0836	0.0468	0.0364
[*I*>2σ(I)]	0.2091	0.1065	0.0784
R indices (all data)	0.1587	0.0910	0.0489
[*I*>2σ(I)] (all data)	0.2549	0.1179	0.0828
Largest diff. peak and hole [e.Å-3]	0.741 and -0.47	0.414 and -0.362	0.041 and -0.202
CCDC	**2114107**	**2114106**	**2163558**

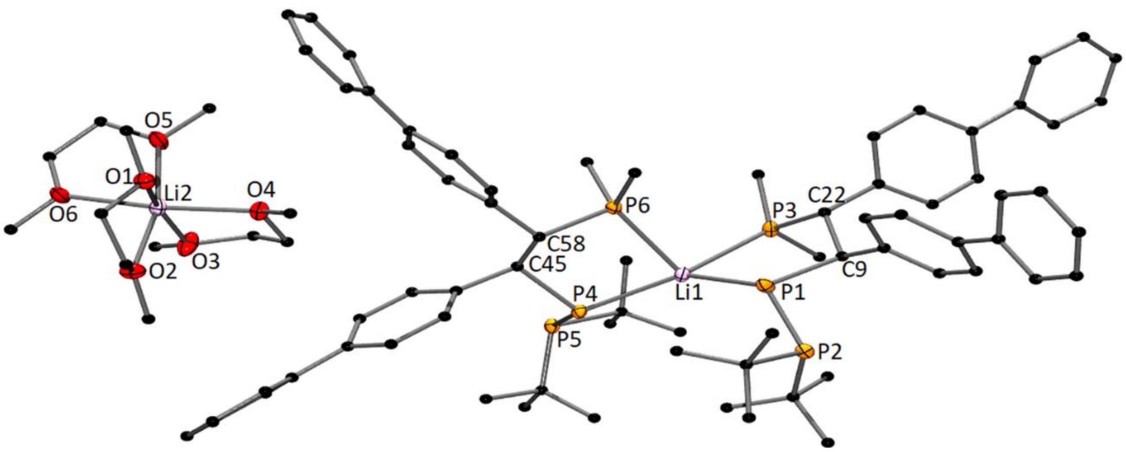

Figure S1. Molecular structure of [Li(DME)$_3$]$^+$[{P(Me)$_2$–CH(biph)–CH(biph)–P(P*t*Bu$_2$)}$_2$]$^-$ (**1a***) (ellipsoids 30%, the H atoms have been omitted for clarity). Important distances (Å) and angles (deg): Li1-P1 2.479(7), Li1-P3 2.556(6), Li1-P4 2.517(6), Li1-P6 2.531(7), P1-P2 2.1585(15), P4-P5 2.1685(15), C9-C22 1.531(5), C45-C58 1.548(5), Li2-O1 2.174(8), Li2-O2 2.119(8). Li2-03 2.088(8), Li2-O4 2.146(7), Li2-O5 2.101(8), Li2-O6 2.146(8); P1-Li1-P4 133.7(3), P1-Li-P3 79.08(19), P1-Li1-P6 108.4(3), P3-Li1-P4 145.6(3), P4-Li1-P6 81.62(19), P2-P1-C9 98.49(13), P5-P4-C45 98.62(13).

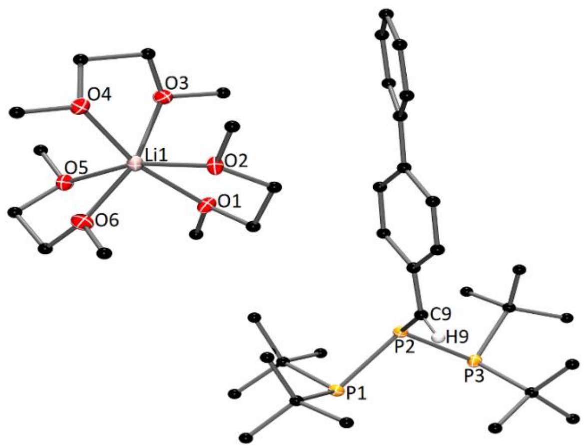

Figure S2. The molecular structure of [Li(DME)$_3$]$^+$[*t*Bu$_2$P–P{C(H)–biph}–P*t*Bu$_2$]$^-$ (**2_1**) (ellipsoids 30%, the H atoms have been omitted for clarity). Important distances (Å) and angles (deg): P1-P2 2.2465(7), P2-P3 2.2107(7), P2-C9 1.7612(19), Li1-O1 2.140(3), Li1-O2 2.118(4), Li1-O3 2.2107(7), Li1-O4 2.138(3), Li1-O5 2.132(4), Li1-O6 2.121(4); P1-P2-P3 97.39(3), P1-P2-C9 116.20(6), P3-P2-C9 114.27(7).

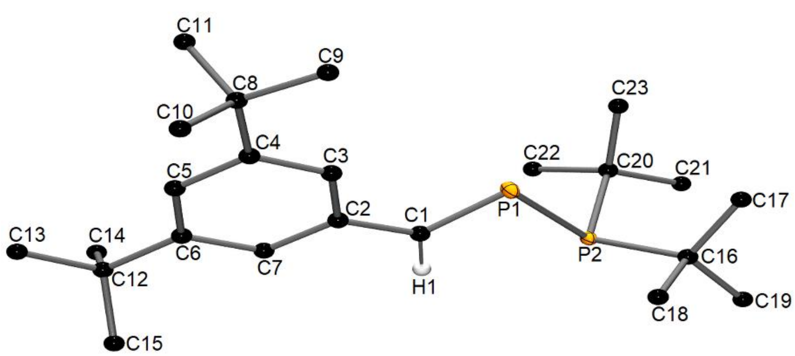

Figure S3. Molecular structure of (3,5-*t*Bu$_2$C$_6$H$_3$)(H)C=P–P*t*Bu$_2$ (**3**) (ellipsoids are drawn at the 50% probability level; hydrogen atoms are omitted except H1 atom; carbon atoms are drawn as sphere for clarity). Important distances (Å) and angles (deg): P1-P2 2.2092(8), C1-P1 1.678(2); C1-P1-P2 99.99(8).

PART B. NMR spectra

1. Reaction of (biph)(H)C=P–P*t*Bu$_2$ (**1**).

a) with MeLi

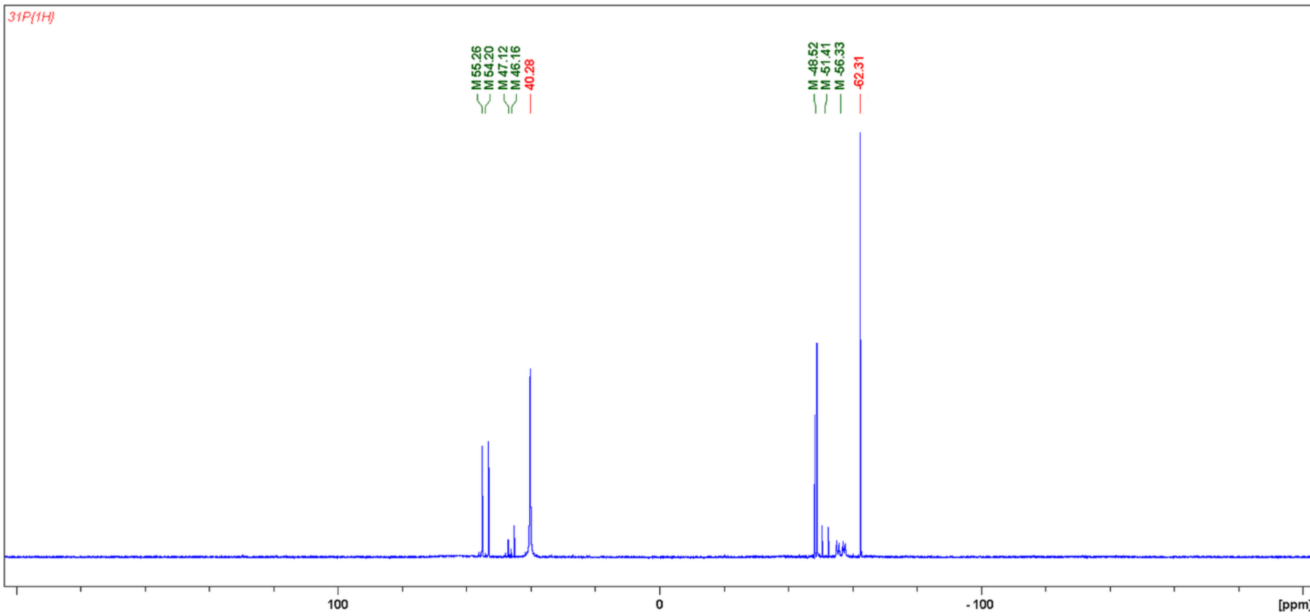

Figure S4. ^{31}P{^{1}H} NMR spectrum of reaction mixture of (biph)(H)C=P–P*t*Bu$_2$ (**1**) with MeLi in THF-d$_8$.

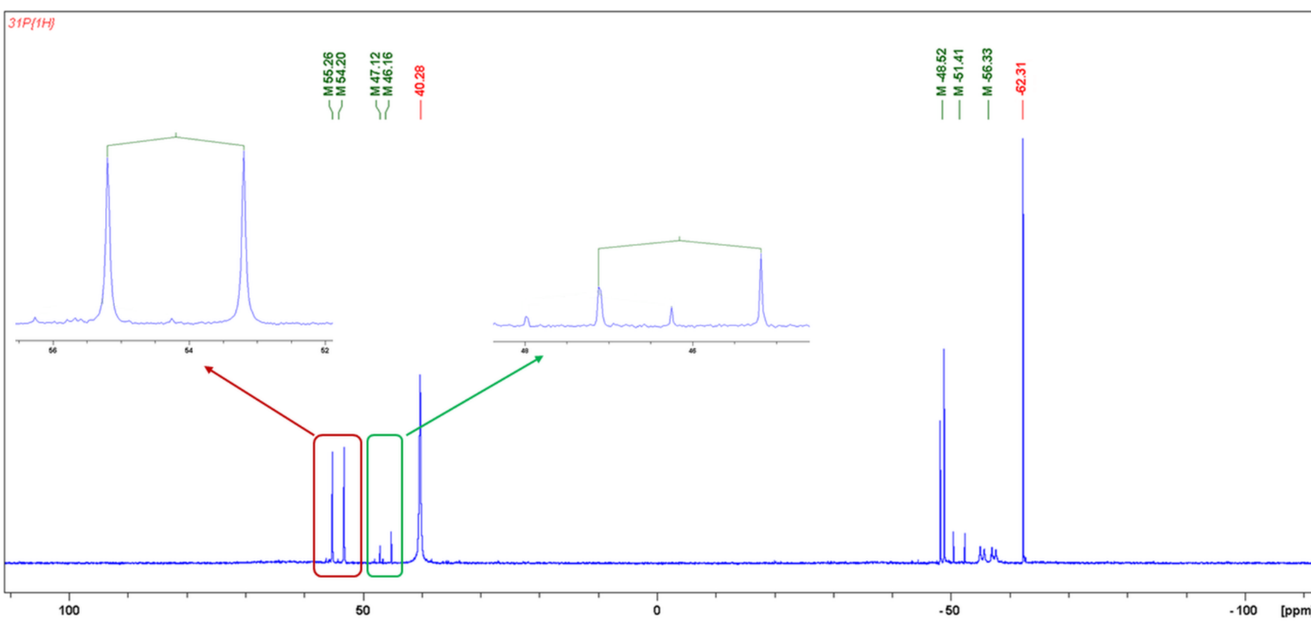

Figure S5. ^{31}P{^{1}H} NMR spectrum of reaction mixture of (biph)(H)C=P–P*t*Bu$_2$ (**1**) with MeLi in THF-d$_8$ in narrow range (from 100 ppm to -100 ppm).

Table S2. Description of signals observed on the ^{31}P{^{1}H} NMR spectrum - **Figure S4** and **S5**.

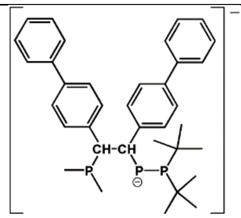	[P(Me)$_2$–CH(biph)–CH(biph)–P–(P*t*Bu$_2$)]$^{-}$ (**1a”**)
➢ 54.20 ppm, d, J_{PP} = 325.2 Hz, [P(Me)$_2$–CH(biph)–CH(biph)–P–(**P***t*Bu$_2$)]$^{-}$; ➢ -48.52 ppm, d, J_{PP} = 108.4 Hz, [**P**(Me)$_2$–CH(biph)–CH(biph)–P–(P*t*Bu$_2$)]$^{-}$; ➢ -56.33 ppm, broad dd, J_{PP} = 325.2 Hz, J_{PP} = 108.4 Hz [P(Me)$_2$–CH(biph)–CH(biph)–**P**–(P*t*Bu$_2$)]$^{-}$;	
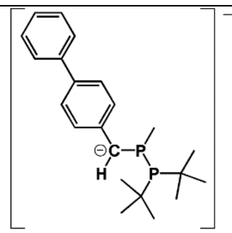	[(biph)(H)C–P(Me)–P*t*Bu$_2$]$^{-}$ (**1a**)
➢ 46.16 ppm, d, J_{PP} = 313.2 Hz, [(biph)(H)C–P(Me)–**P***t*Bu$_2$]$^{-}$; ➢ -51.41 ppm, d, J_{PP} = 313.2 Hz, [(biph)(H)C–**P**(Me)–P*t*Bu$_2$]$^{-}$;	
*t*Bu$_2$PLi ➢ 40.28 ppm, s;	
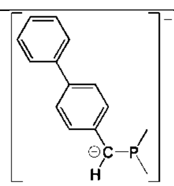	[(biph)(H)C–P(Me)$_2$]$^{-}$ (**1a’**)
➢ -62.31 ppm, s, [(biph)(H)C–**P**(Me)$_2$]$^{-}$;	

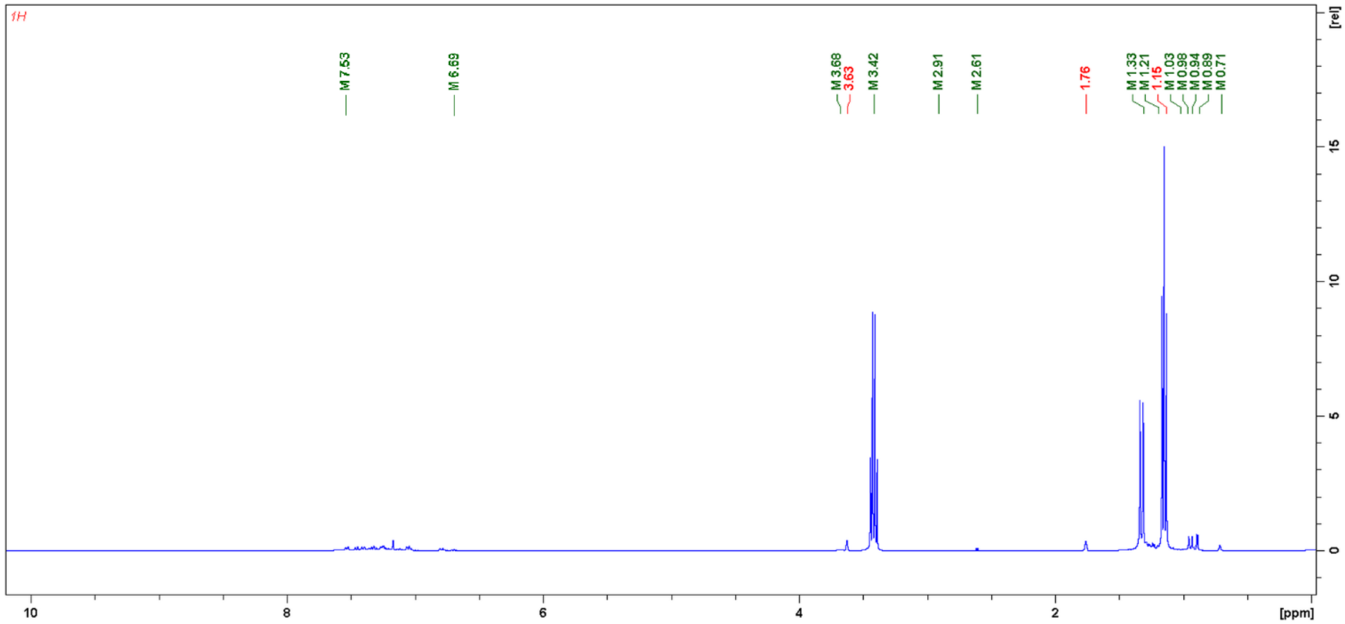

Figure S6. [1]H NMR spectrum of reaction mixture of (biph)(H)C=P–P*t*Bu_2 (**1**) with MeLi in THF-d_8.

Table S3. Description of signals observed on the ^{1}H NMR spectrum - **Figure S6**.

➢ 7.53 ppm – 6.69 ppm – aromatic protons;
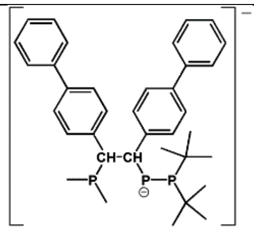 [P(Me)$_2$–CH(biph)–CH(biph)–P–(P*t*Bu$_2$)]$^-$ (**1a”**) ➢ 3.68 ppm, broad m, 2H, [P(Me)$_2$–C**H**(biph)–C**H**(biph)–P–(P*t*Bu$_2$)]$^-$; ➢ 0.94 ppm, d, J_{PH} = 10.1 Hz, 18H, [P(Me)$_2$–CH(biph)–CH(biph)–P–(P***t*Bu**$_2$)]$^-$; ➢ 0.71 ppm, d, J_{PH} = 2.9 Hz, 6H, [P(**Me**)$_2$–CH(biph)–CH(biph)–P–(P*t*Bu$_2$)]$^-$;
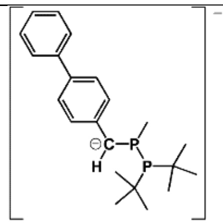 [(biph)(H)C–P(Me)–P*t*Bu$_2$]$^-$ (**1a**) ➢ 2.91 ppm, dd, J_{PH} = 7.4 Hz, J_{PH} = 1.9 Hz, 1H, [(biph)(**H**)C–P(Me)–P*t*Bu$_2$]$^-$; ➢ 1.21 ppm, d, J_{PH} = 10.6 Hz, 18 H, [(biph)(H)C–P(Me)–P***t*Bu**$_2$]$^-$; ➢ 1.03 ppm, d, J_{PH} = 3.1 Hz, 3H, [(biph)(H)C–P(**Me**)–P*t*Bu$_2$]$^-$;
*t*Bu$_2$PLi ➢ 1.33 ppm, d, J_{PH} = 10.1 Hz, ***t*Bu**$_2$PLi;
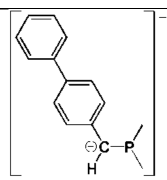 [(biph)(H)C–P(Me)$_2$]$^-$ (**1a’**) ➢ 2.61 ppm, d, J_{PH} = 5.2 Hz, 1H, [(biph)(**H**)C–P(Me)$_2$]$^-$; ➢ 0.98 ppm, d, J_{PH} = 2.4 Hz, 3H, [(biph)(H)C–P(**Me**)$_2$]$^-$; ➢ 0.89 ppm, d, J_{PH} = 2.9 Hz, 3H, [(biph)(H)C–P(**Me**)$_2$]$^-$;
[Li(DME)$_3$]$^+$ ➢ 3.42 ppm, q, J_{HH} = 7.1 Hz; ➢ 1.15 ppm, t, J_{HH} = 7.1 Hz;
Additional signals of small amounts of THF (from THF-d$_8$) were visible at – 3.63 ppm and 1.76 ppm.

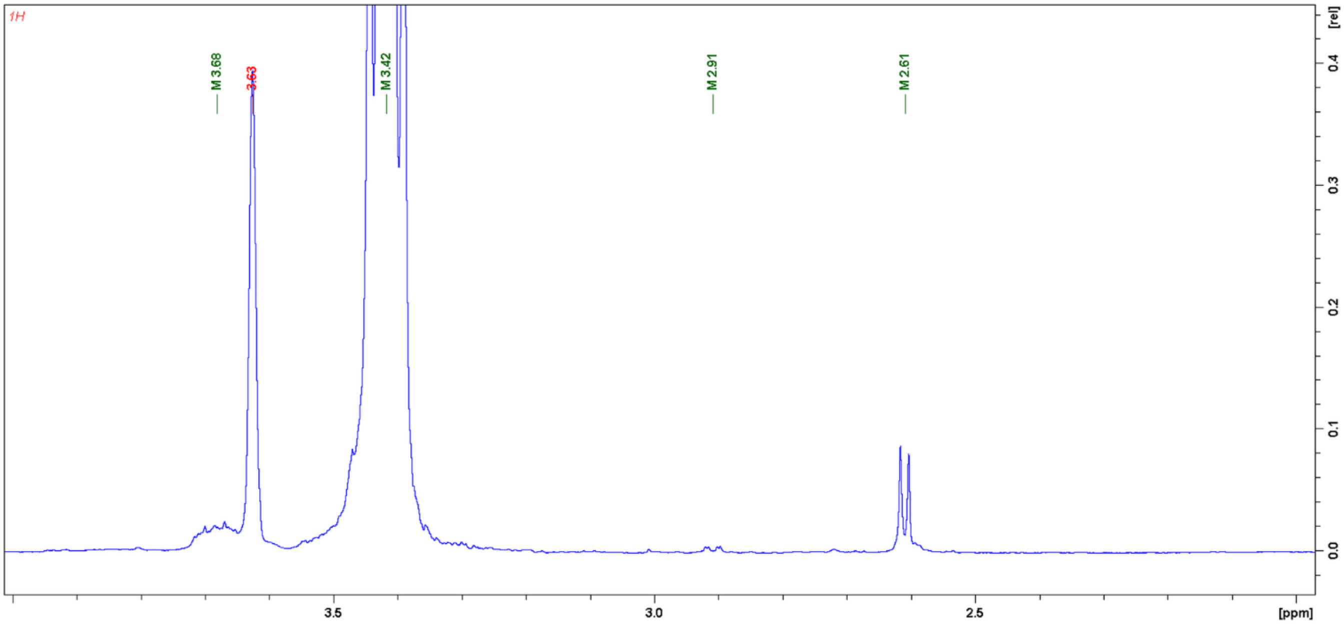

Figure S7. ^{1}H NMR spectrum of reaction mixture of (biph)(H)C=P–P*t*Bu$_2$ (**1**) with MeLi in THF-d$_8$ in the range from 4 ppm to 2 ppm.

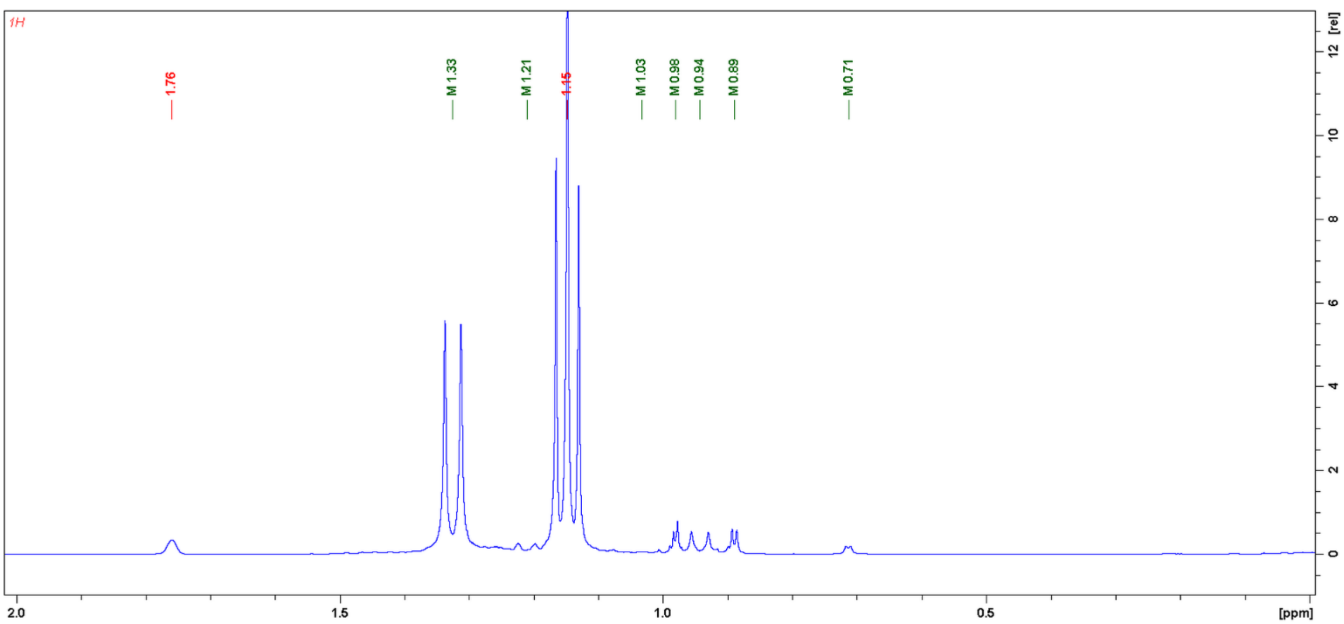

Figure S8. ^{1}H NMR spectrum of reaction mixture of (biph)(H)C=P–P*t*Bu$_2$ (**1**) with MeLi in THF-d$_8$ in the range from 2 ppm to 0 ppm.

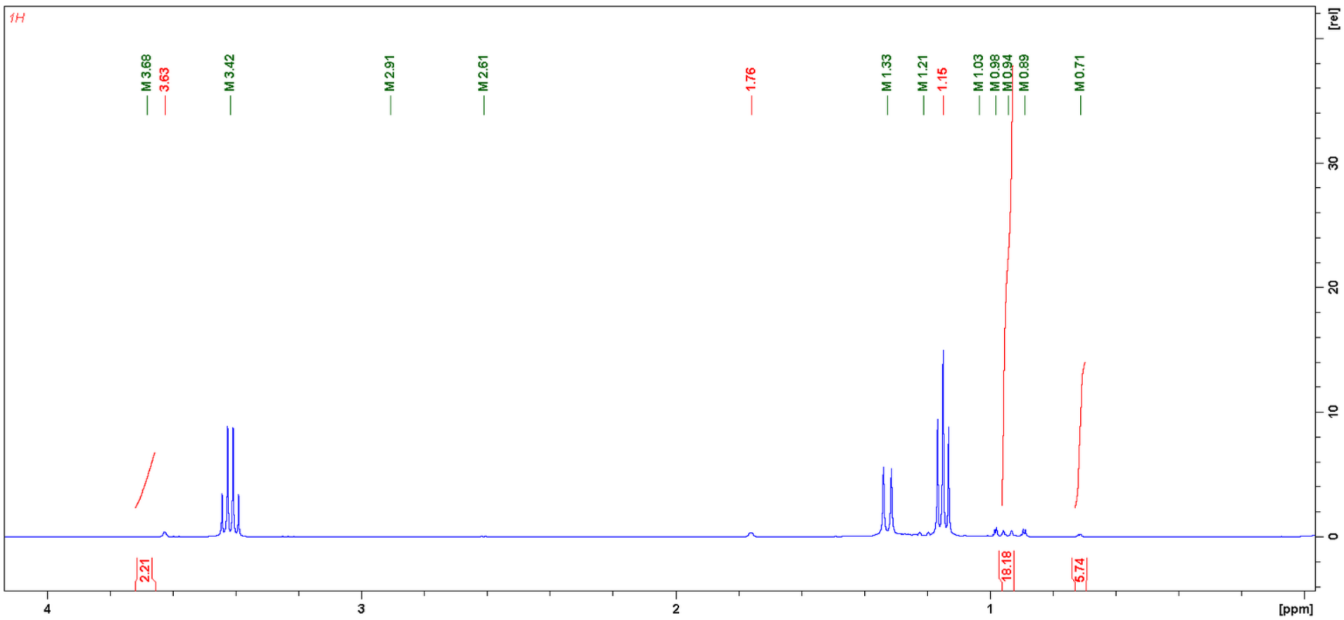

Figure S9. ^{1}H NMR spectrum of reaction mixture of (biph)(H)C=P–P*t*Bu$_2$ (**1**) with MeLi in THF-d$_8$ in the range from 4 ppm to 0 ppm with marked integration for [P(Me)$_2$–CH(biph)–CH(biph)–P–(P*t*Bu$_2$)]$^-$ (**1a”**).

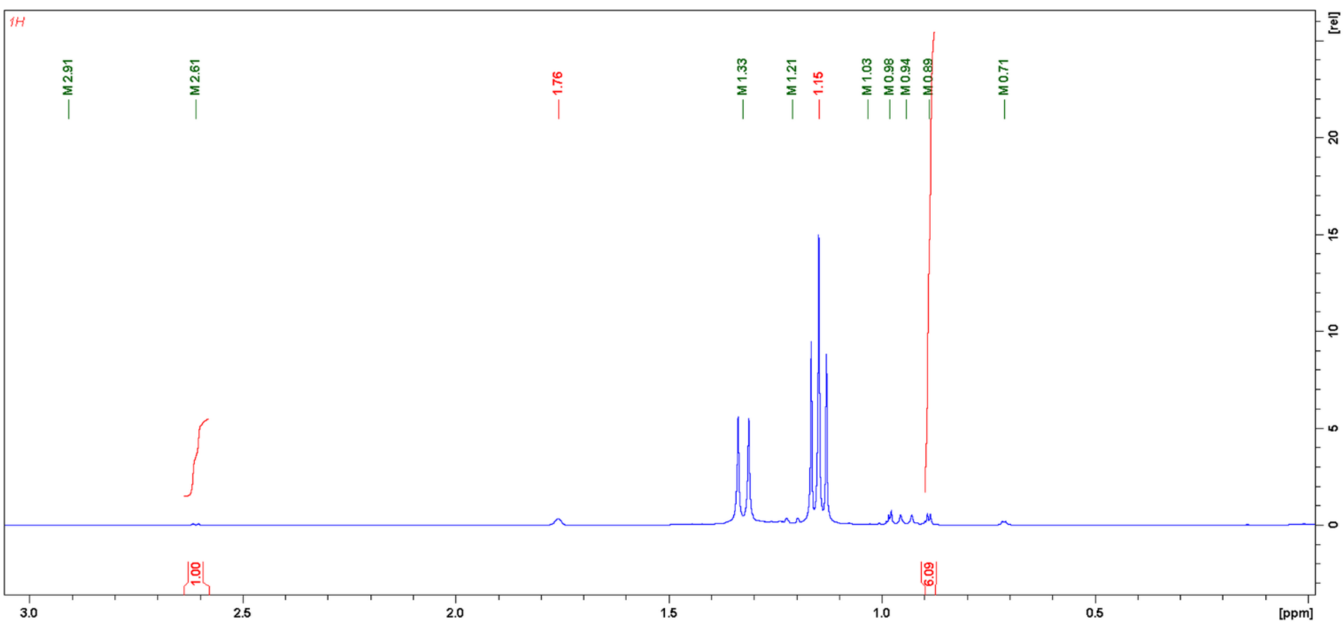

Figure S10. ^{1}H NMR spectrum of reaction mixture of (biph)(H)C=P–P*t*Bu$_2$ (**1**) with MeLi in THF-d$_8$ in the range from 4 ppm to 0 ppm with marked integration for [(biph)(H)C–P(Me)$_2$]$^-$ (**1a’**).

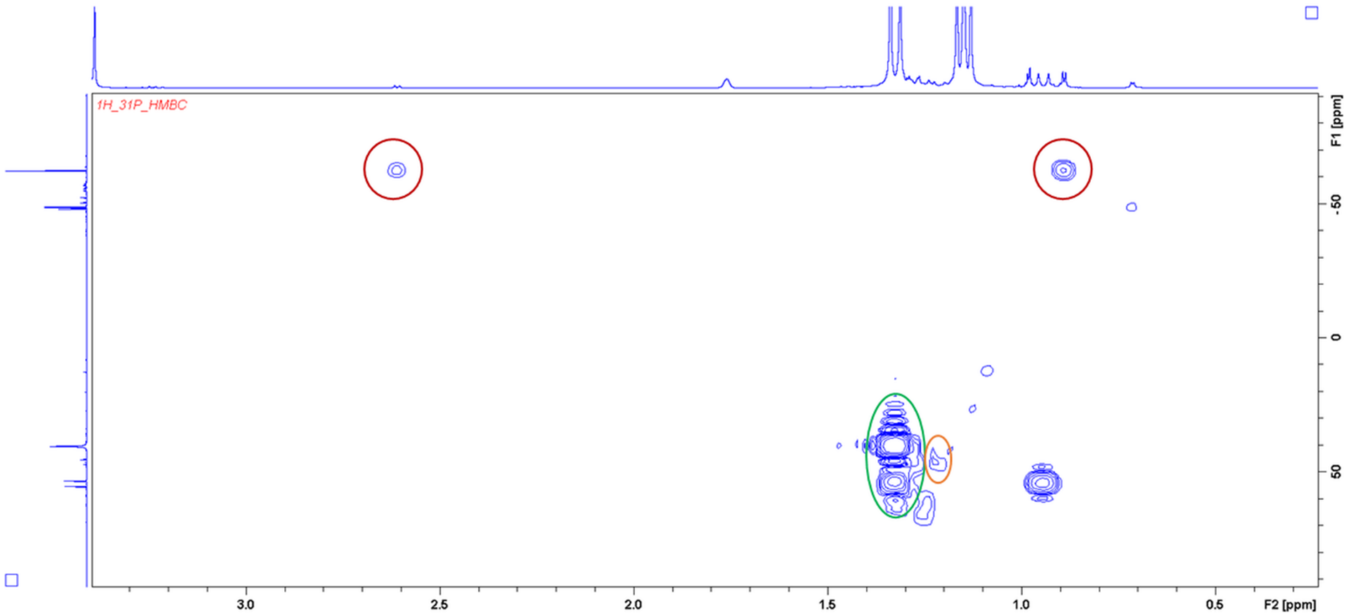

Figure S11. $^{31}P\{^{1}H\}/^{1}H$ HMQC NMR spectrum presenting the correlation of protons from *t*Bu groups with phosphorus atom in $[(biph)(H)C–P(Me)–PtBu_2]^-$ (**1a**, orange color ring); correlation of protons from *t*Bu groups with phosphorus atom in tBu_2PLi (green); correlation of protons from methine and methyl groups with phosphorus atom in $[(biph)(H)C–P(Me)_2]^-$ (**1a'**, red);

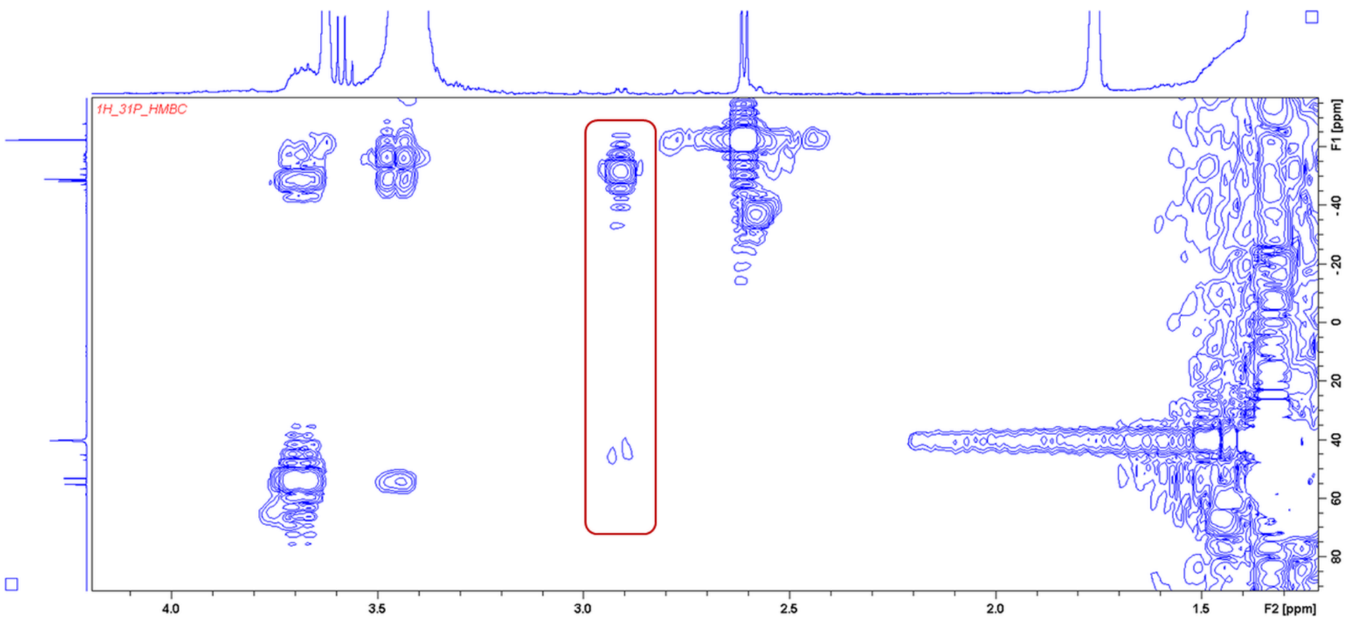

Figure S12. $^{31}P\{^{1}H\}/^{1}H$ HMQC NMR spectrum presenting the correlation of methine protons with phosphorus atom in $[(biph)(H)C–P(Me)–PtBu_2]^-$ (**1a**).

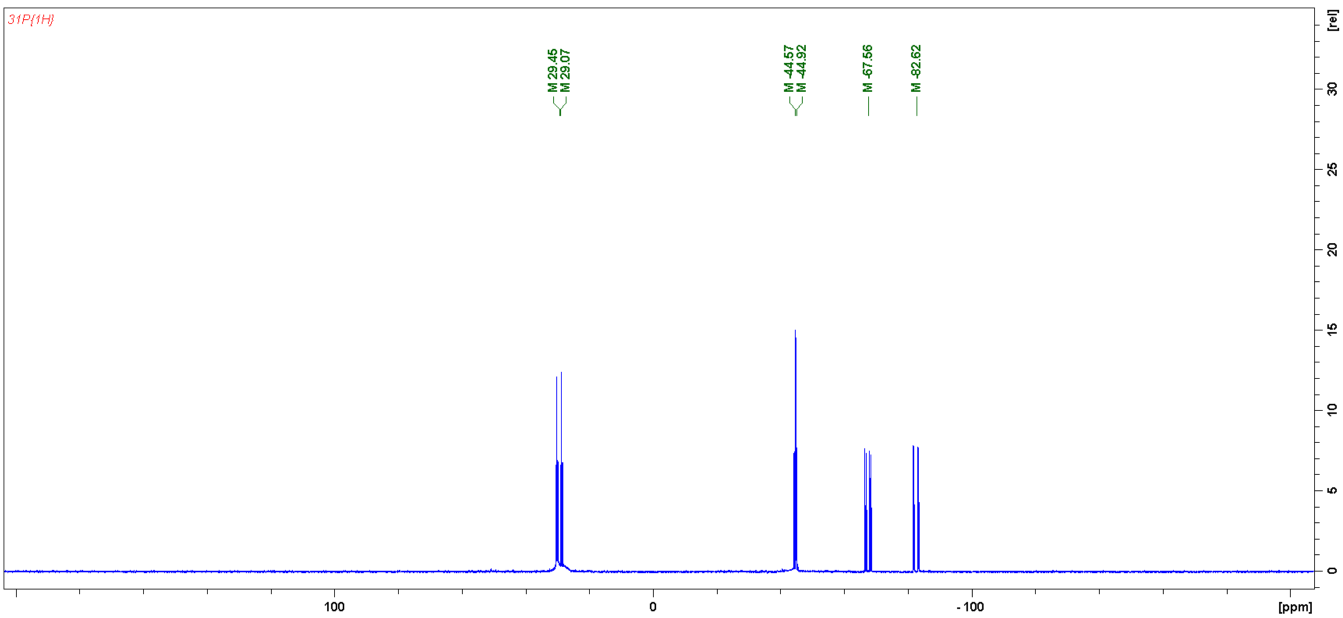

Figure S13. $^{31}P\{^1H\}$ NMR spectrum of isolated crystals of **1a*** dissolved in THF-d_8.

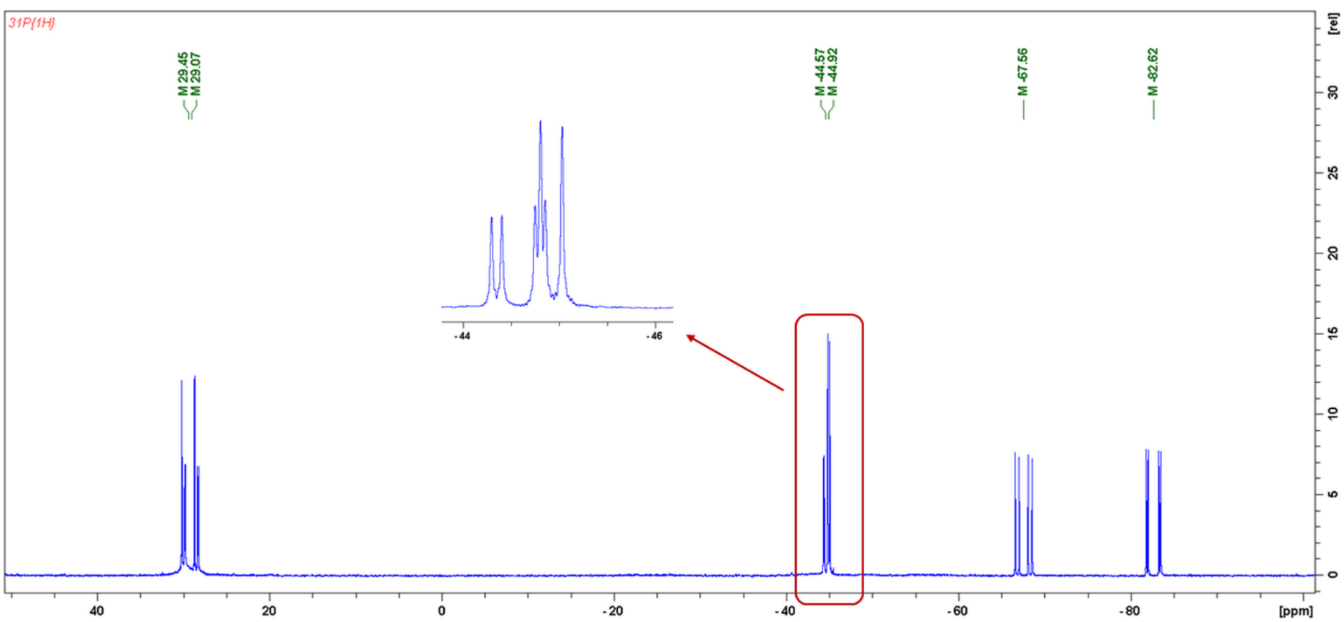

Figure S14. $^{31}P\{^1H\}$ NMR spectrum of isolated crystals of **1a*** dissolved in THF-d_8 in the range from 50 ppm to -100 ppm.

Table S4. Description of signals observed on the ^{31}P{^{1}H} NMR spectrum of isolated crystals of **1a*- Figure S13** and **S14**.

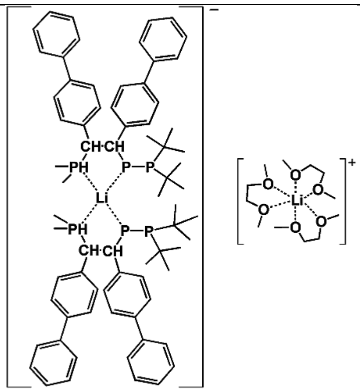

[Li(DME)$_3$]$^+$[{P(Me$_2$)–CH(biph)–CH(biph)–P(P*t*Bu$_2$)}$_2$Li]$^-$
(1**a***)

- 29.45 ppm, d, J_{PP} = 239.3 Hz, [Li(DME)$_3$]$^+$[{P(Me$_2$)–CH(biph)–CH(biph)–P(**P***t*Bu$_2$)}$_2$Li]$^-$;
- 29.07 ppm, dd, J_{PP} = 245.7 Hz, J_{PP} = 17.2 Hz, [Li(DME)$_3$]$^+$[{P(Me$_2$)–CH(biph)–CH(biph)–P(**P***t*Bu$_2$)}$_2$Li]$^-$;
- -44.57 ppm, dd, J_{PP} = 73.4 Hz, J_{PP} = 17.2 Hz, [Li(DME)$_3$]$^+$[{**P**(Me$_2$)–CH(biph)–CH(biph)–P(P*t*Bu$_2$)}$_2$Li]$^-$;
- -44.92 ppm, d, J_{PP} = 36.5 Hz, [Li(DME)$_3$]$^+$[{**P**(Me$_2$)–CH(biph)–CH(biph)–P(P*t*Bu$_2$)}$_2$Li]$^-$;
- -67.56 ppm, dd, J_{PP} = 245.7 Hz, J_{PP} = 73.4 Hz, [Li(DME)$_3$]$^+$[{P(Me$_2$)–CH(biph)–CH(biph)–**P**(P*t*Bu$_2$)}$_2$Li]$^-$;
- -82.62 ppm, dd, J_{PP} = 239.3 Hz, J_{PP} = 36.5 Hz, [Li(DME)$_3$]$^+$[{P(Me$_2$)–CH(biph)–CH(biph)–**P**(P*t*Bu$_2$)}$_2$Li]$^-$;

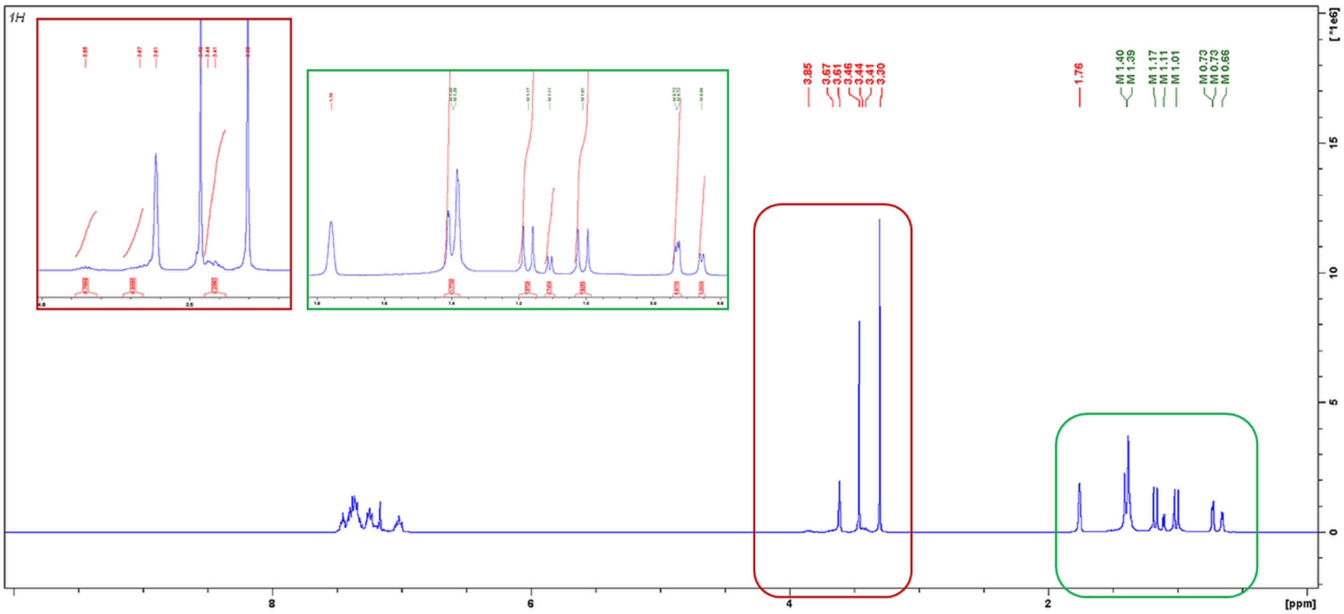

Figure S15. [1]H NMR spectrum of isolated crystals of **1a*** dissolved in THF-d_8.

Table S5. Description of signals observed on the ^{1}H NMR spectrum of isolated crystals of **1a***- Figure S15.

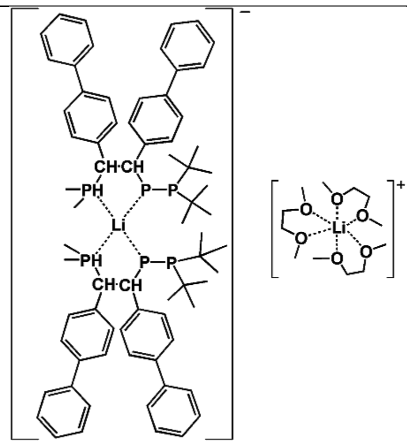

[Li(DME)$_3$]$^+$[{P(Me$_2$)–CH(biph)–CH(biph)–P(P*t*Bu$_2$)}$_2$Li]$^-$ (**1a***)

- 7.5 ppm – 6.98 ppm – aromatic protons;
- 3.85 ppm, m, 1 H, [Li(DME)$_3$]$^+$[{P(Me)$_2$–C**H**(biph)–C**H**(biph)–P(P*t*Bu$_2$)}$_2$Li]$^-$;
- 3.67 ppm, m, 1H, [Li(DME)$_3$]$^+$[{P(Me)$_2$–C**H**(biph)–C**H**(biph)–P(P*t*Bu$_2$)}$_2$Li]$^-$;
- 3.61 ppm, small amount of THF from THF-d$_8$;
- 3.46 ppm, DME protons;
- 3.44 ppm, m, 1H, [Li(DME)$_3$]$^+$[{P(Me)$_2$–C**H**(biph)–C**H**(biph)–P(P*t*Bu$_2$)}$_2$Li]$^-$;
- 3.41 ppm, m, 1H, [Li(DME)$_3$]$^+$[{P(Me)$_2$–C**H**(biph)–C**H**(biph)–P(P*t*Bu$_2$)}$_2$Li]$^-$;
- 3.30 ppm, DME protons;
- 1.76 ppm, small amount of THF from THF-d$_8$;
- 1.40 ppm, d, J_{PH} = 11.2 Hz, 9H, [Li(DME)$_3$]$^+$[{P(Me)$_2$–CH(biph)–CH(biph)–P(P***t*Bu**$_2$)}$_2$Li]$^-$;
- 1.39 ppm, d, J_{PH} = 11.0 Hz, 9H, [Li(DME)$_3$]$^+$[{P(Me)$_2$–CH(biph)–CH(biph)–P(P***t*Bu**$_2$)}$_2$Li]$^-$;
- 1.17 ppm, d, J_{PH} = 11.2 Hz, 9H, [Li(DME)$_3$]$^+$[{P(Me)$_2$–CH(biph)–CH(biph)–P(P***t*Bu**$_2$)}$_2$Li]$^-$;
- 1.11 ppm, d, J_{PH} = 4.5 Hz, 3H, [Li(DME)$_3$]$^+$[{P(**Me**)$_2$–CH(biph)–CH(biph)–P(P*t*Bu$_2$)}$_2$Li]$^-$;
- ppm, d, J_{PH} = 11.6 Hz, 9H, [Li(DME)$_3$]$^+$[{P(Me)$_2$–CH(biph)–CH(biph)–P(P***t*Bu**$_2$)}$_2$Li]$^-$;
- 0.73 ppm, d, J_{PH} = 3.9 Hz, 3H, [Li(DME)$_3$]$^+$[{P(**Me**)$_2$–CH(biph)–CH(biph)–P(P*t*Bu$_2$)}$_2$Li]$^-$;
- 0.73 ppm, d, J_{PH} = 4.3 Hz, 3H, [Li(DME)$_3$]$^+$[{P(**Me**)$_2$–CH(biph)–CH(biph)–P(P*t*Bu$_2$)}$_2$Li]$^-$;
- 0.66 ppm, d, J_{PH} = 4.0 Hz, 3H, [Li(DME)$_3$]$^+$[{P(**Me**)$_2$–CH(biph)–CH(biph)–P(P*t*Bu$_2$)}$_2$Li]$^-$;

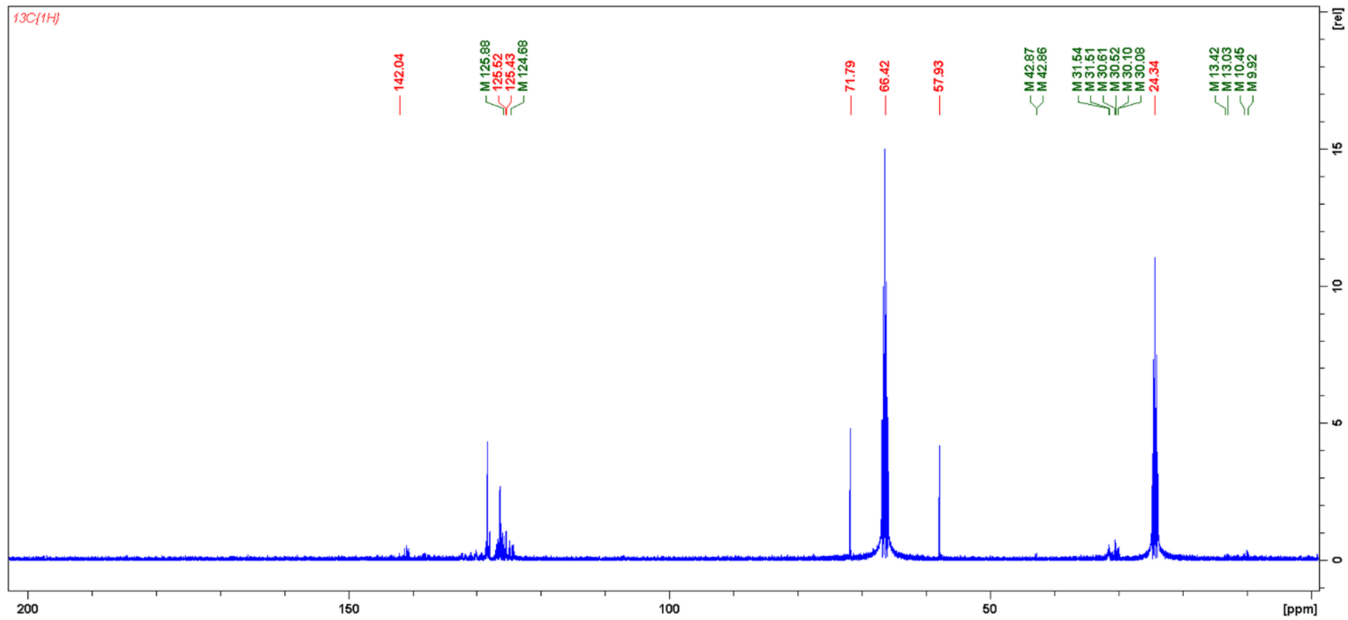

Figure S16. $^{13}C\{^1H\}$ NMR spectrum of isolated crystals of **1a*** dissolved in THF-d_8.

Table S6. Description of signals observed on the $^{13}C\{^{1}H\}$ NMR spectrum of isolated crystals of **1a*- Figure S16**.

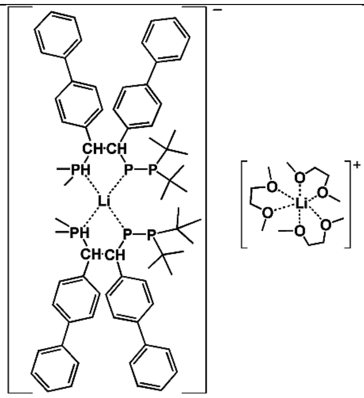

[Li(DME)$_3$]$^+$[{P(Me$_2$)–CH(biph)–CH(biph)–P(P*t*Bu$_2$)}$_2$Li]$^-$
(**1a***)

- 142.04 ppm – 125.43 ppm – aromatic C-atoms;
- 71.79 ppm, DME;
- 66.42 ppm, THF-d$_8$;
- 57.93 ppm, DME;
- 52.79 ppm, d, J_{PC} = 19.4 Hz, [Li(DME)$_3$]$^+$[{P(Me)$_2$–**C**H(biph)–**C**H(biph)–P(P*t*Bu$_2$)}$_2$Li]$^-$;
- 52.72 ppm, d, J_{PC} = 17.8 Hz, [Li(DME)$_3$]$^+$[{P(Me)$_2$–**C**H(biph)–**C**H(biph)–P(P*t*Bu$_2$)}$_2$Li]$^-$;
- 44.67 ppm, d, J_{PC} = 16.2 Hz, [Li(DME)$_3$]$^+$[{P(Me)$_2$–**C**H(biph)–**C**H(biph)–P(P*t*Bu$_2$)}$_2$Li]$^-$;
- 42.87 ppm, d, J_{PC} = 18.7 Hz, [Li(DME)$_3$]$^+$[{P(Me)$_2$–**C**H(biph)–**C**H(biph)–P(P*t*Bu$_2$)}$_2$Li]$^-$;
- 31.54 ppm, dd, J_{PC} = 28.8 Hz, J_{PC} = 1.7 Hz, [Li(DME)$_3$]$^+$[{P(Me)$_2$–CH(biph)–CH(biph)–P(P{**C**(CH$_3$)$_3$}$_2$)}$_2$Li]$^-$;
- 31.51 ppm, dd, J_{PC} = 28.7 Hz, J_{PC} = 3.7 Hz, [Li(DME)$_3$]$^+$[{P(Me)$_2$–CH(biph)–CH(biph)–P(P{**C**(CH$_3$)$_3$}$_2$)}$_2$Li]$^-$;
- 30.61 ppm, dd, J_{PC} = 15.0 Hz, J_{PC} = 1.6 Hz, [Li(DME)$_3$]$^+$[{P(Me)$_2$–CH(biph)–CH(biph)–P(P{C(**C**H$_3$)$_3$}$_2$)$_2$Li]$^-$;
- 30.52 ppm, dd, J_{PC} = 14.0 Hz, J_{PC} = 0.8 Hz, [Li(DME)$_3$]$^+$[{P(Me)$_2$–CH(biph)–CH(biph)–P(P{C(**C**H$_3$)$_3$}$_2$)}$_2$Li]$^-$;
- 30.10 ppm, dd, J_{PC} = 13.1 Hz, J_{PC} = 8.6 Hz, [Li(DME)$_3$]$^+$[{P(Me)$_2$–CH(biph)–CH(biph)–P(P{C(**C**H$_3$)$_3$}$_2$)}$_2$Li]$^-$;
- 30.08 ppm, dd, J_{PC} = 14.3 Hz, J_{PC} = 1.2 Hz, [Li(DME)$_3$]$^+$[{P(Me)$_2$–CH(biph)–CH(biph)–P(P{C(**C**H$_3$)$_3$}$_2$)}$_2$Li]$^-$;
- 24.34 ppm, THF-d$_8$;
- 13.42 ppm, d, J_{PC} = 17.5 Hz, [Li(DME)$_3$]$^+$[{P(**Me**)$_2$–CH(biph)–CH(biph)–P(P*t*Bu$_2$)}$_2$Li]$^-$;
- 13.03 ppm, d, J_{PC} = 15.5 Hz, [Li(DME)$_3$]$^+$[{P(**Me**)$_2$–CH(biph)–CH(biph)–P(P*t*Bu$_2$)}$_2$Li]$^-$;
- 10.45 ppm, d, J_{PC} = 18.7 Hz, [Li(DME)$_3$]$^+$[{P(**Me**)$_2$–CH(biph)–CH(biph)–P(P*t*Bu$_2$)}$_2$Li]$^-$;
- 9.92 ppm, d, J_{PC} = 19.5 Hz, [Li(DME)$_3$]$^+$[{P(**Me**)$_2$–CH(biph)–CH(biph)–P(P*t*Bu$_2$)}$_2$Li]$^-$;

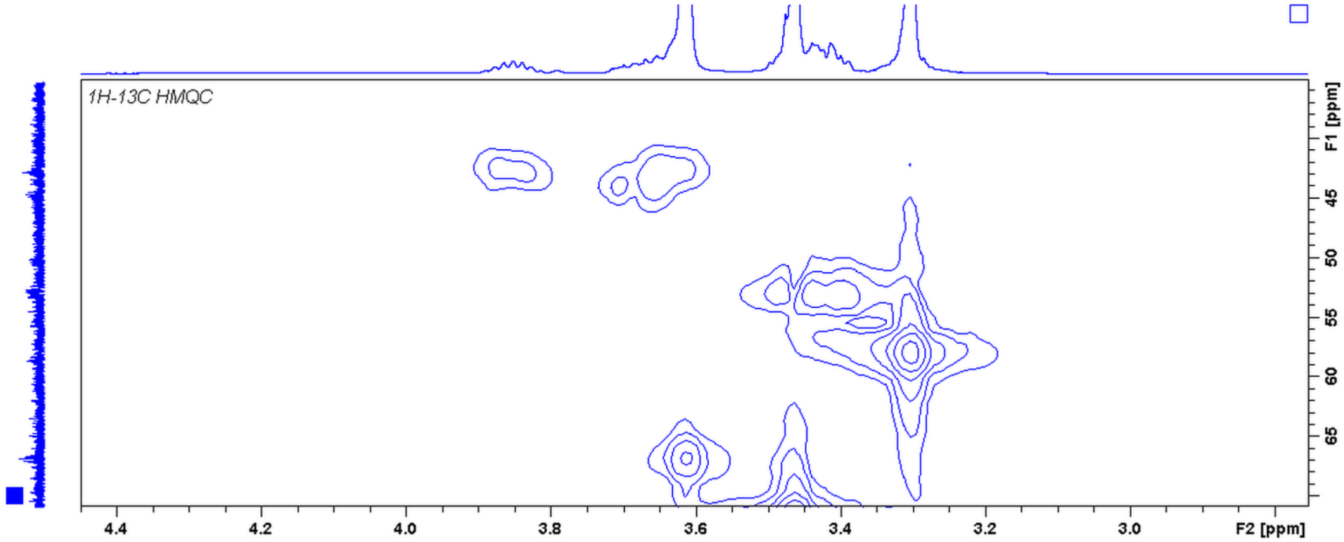

Figure S17. $^{13}C\{^{1}H\}$-dept 90/^{1}H HMQC NMR spectrum of isolated crystals of **1a*** dissolved in THF-d_8 presenting the correlation of methine protons with carbon atoms.

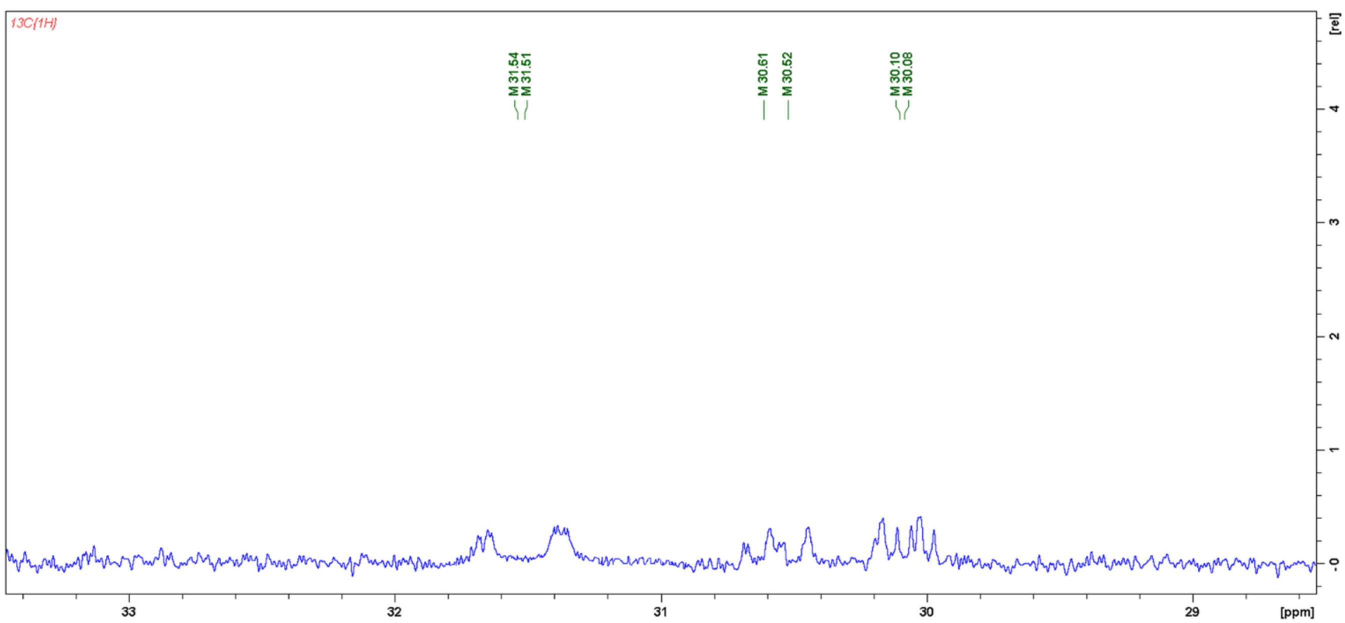

Figure S18. $^{13}C\{^{1}H\}$ NMR spectrum of isolated crystals of **1a*** dissolved in THF-d_8 in the range of 33 ppm to 29 ppm.

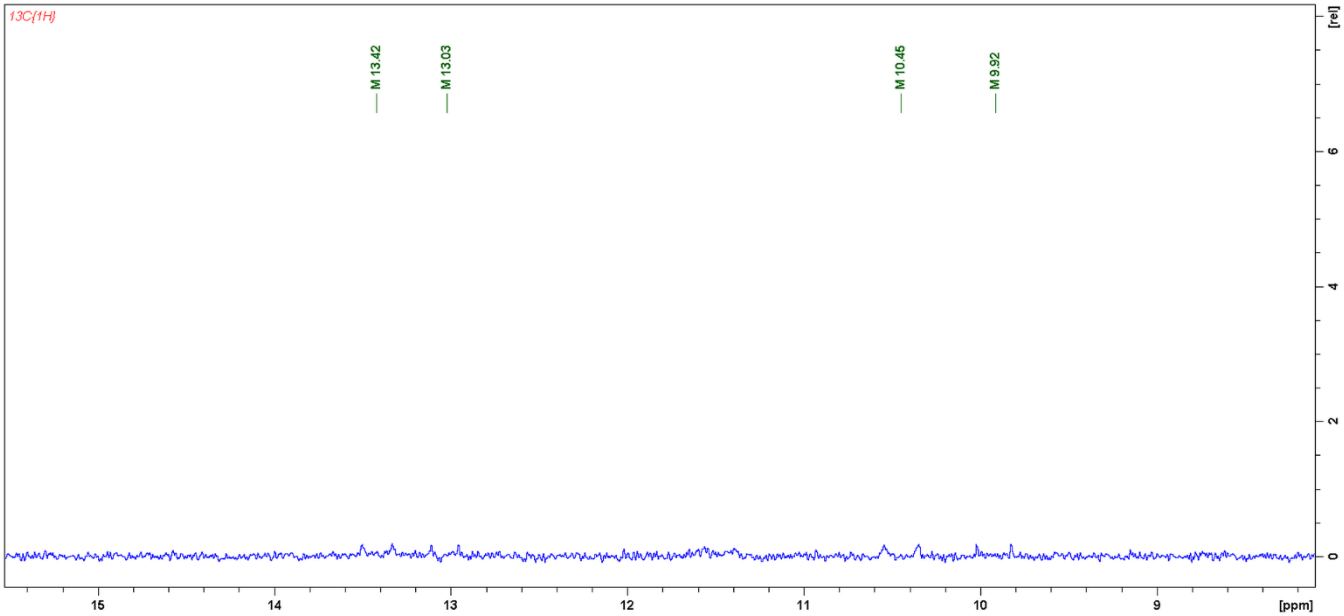

Figure S19. $^{13}C\{^1H\}$ NMR spectrum of isolated crystals of **1a*** dissolved in THF-d_8 in the range of 15 ppm to 8 ppm.

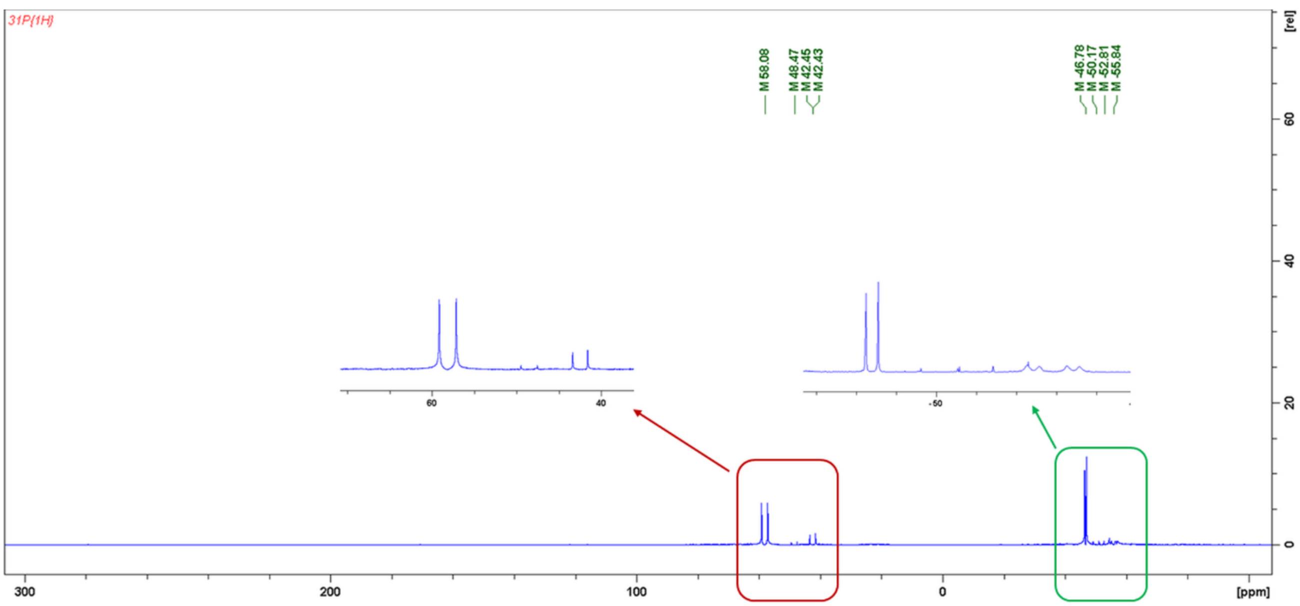

Figure S20. $^{31}P\{^1H\}$ NMR spectrum of reaction mixture of (biph)(H)C=P–P*t*Bu_2 (**1**) with MeLi in THF-d_8 with a lower concentration of reagents.

Table S7. Description of signals observed on the ^{31}P{^{1}H} NMR spectrum - **Figure S20**.

<table>
<tr><td>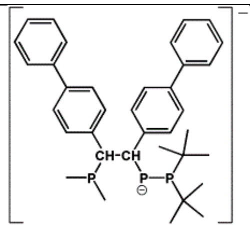
[P(Me)$_2$–CH(biph)–CH(biph)–P–(P*t*Bu$_2$)]$^–$ (**1a”**)
➢ 58.08 ppm, d, J_{PP} = 325.2 Hz, [P(Me)$_2$–CH(biph)–CH(biph)–P–(**P***t*Bu$_2$)]$^–$;
➢ -46.78 ppm, d, J_{PP} = 108.4 Hz, [**P**(Me)$_2$–CH(biph)–CH(biph)–P–(P*t*Bu$_2$)]$^–$;
➢ -55.84 ppm, broad dd, J_{PP} = 325.2 Hz, J_{PP} = 108.4 Hz [P(Me)$_2$–CH(biph)–CH(biph)–**P**–(P*t*Bu$_2$)]$^–$;</td></tr>
<tr><td>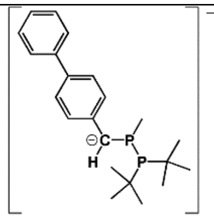
[(biph)(H)C–P(Me)–P*t*Bu$_2$]$^–$ (**1a**)
➢ 48.47 ppm, d, J_{PP} = 313.2 Hz, [(biph)(H)C–P(Me)–**P***t*Bu$_2$]$^–$;
➢ -50.17 ppm, d, J_{PP} = 313.2 Hz, [(biph)(H)C–**P**(Me)–P*t*Bu$_2$]$^–$;</td></tr>
<tr><td>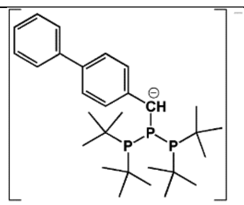
[*t*Bu$_2$P–P–{C(H)(biph)}–P*t*Bu$_2$]$^–$ (**2_1**)
➢ -52.81 ppm, dd, J_{PP} = 285.4 Hz, J_{PP} = 284.8 Hz, [*t*Bu$_2$P–**P**–{C(H)(biph)}–P*t*Bu$_2$]$^–$;
➢ 42.43 ppm, d, J_{PP} = 285.4 Hz, [*t*Bu$_2$**P**–P–{C(H)(biph)}–P*t*Bu$_2$]$^–$;
➢ 42.45 ppm, d, J_{PP} = 284.8 Hz, [*t*Bu$_2$P–P–{C(H)(biph)}–**P***t*Bu$_2$]$^–$;</td></tr>
</table>

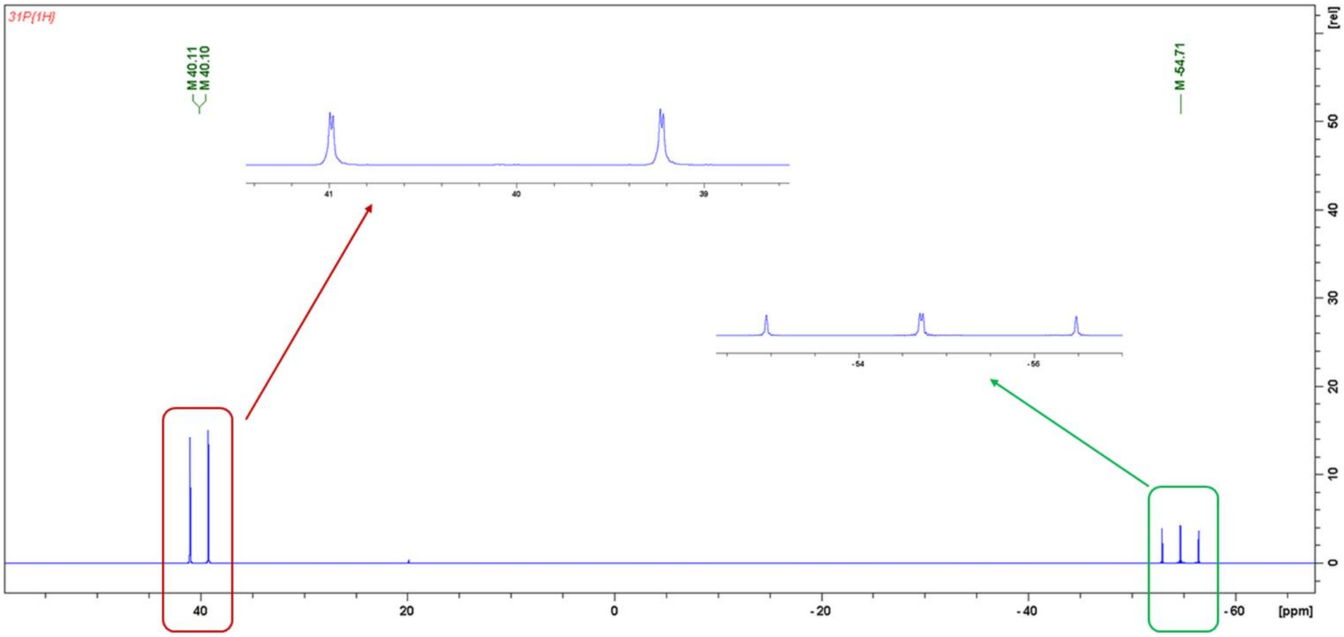

Figure S21. $^{31}P\{^{1}H\}$ NMR spectrum of isolated crystals of $[Li(DME)_3]^+[t\text{Bu}_2\text{P–P–}\{C(H)(biph)\}\text{–P}t\text{Bu}_2]^-$ (**2_1**) dissolved in THF-d_8.

Table S8. Description of signals observed on the $^{31}P\{^{1}H\}$ NMR spectrum - **Figure S21**.

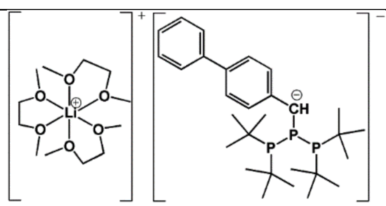

$[Li(DME)_3]^+[t\text{Bu}_2\text{P–P–}\{C(H)(biph)\}\text{–P}t\text{Bu}_2]^-$ (**2_1**)

- 40.11 ppm, d, J_{PP} = 285.4 Hz, $[Li(DME)_3]^+[t\text{Bu}_2\mathbf{P}\text{–P–}\{C(H)(biph)\}\text{–P}t\text{Bu}_2]^-$;
- 40.10 ppm, d, J_{PP} = 284.8 Hz, $[Li(DME)_3]^+[t\text{Bu}_2\text{P–P–}\{C(H)(biph)\}\text{–}\mathbf{P}t\text{Bu}_2]^-$;
- -54.71 ppm, dd, J_{PP} = 285.4 Hz, JPP = 284.8 Hz, $[Li(DME)_3]^+[t\text{Bu}_2\text{P–}\mathbf{P}\text{–}\{C(H)(biph)\}\text{–P}t\text{Bu}_2]^-$;

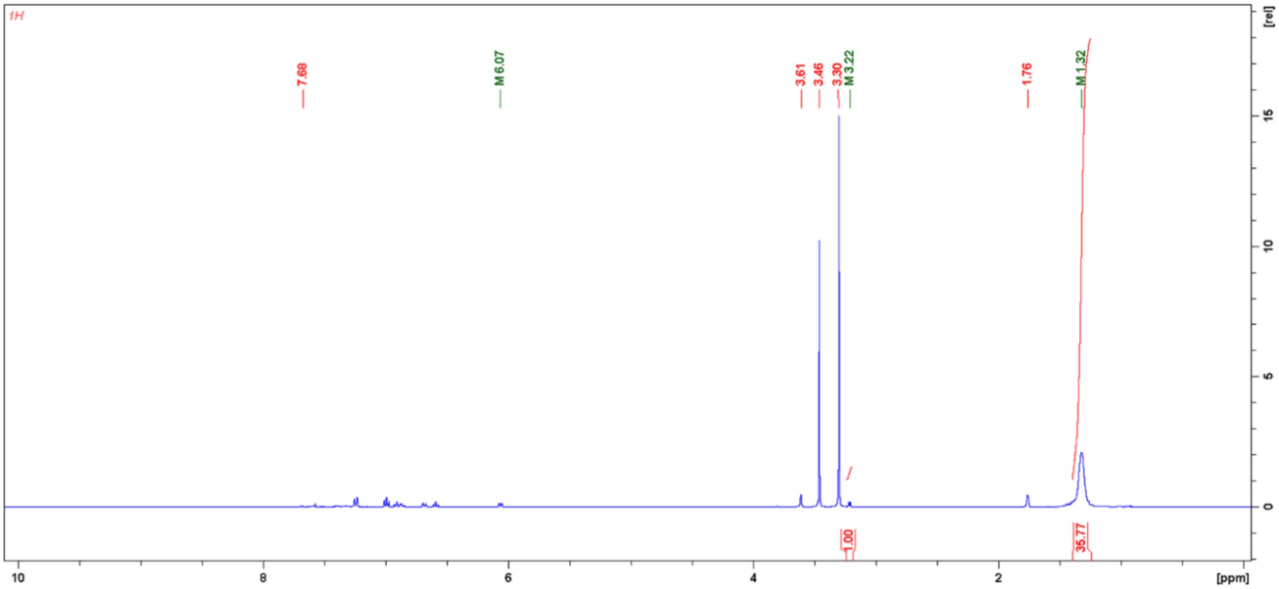

Figure S22. [1]H NMR spectrum of isolated crystals of $[Li(DME)_3]^+[t\text{Bu}_2\text{P–P–\{C(H)(biph)\}–P}t\text{Bu}_2]^-$ (**2_1**) dissolved in THF-d_8.

Table S9. Description of signals observed on the [1]H NMR spectrum - **Figure S22**.

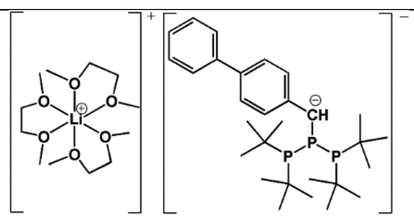

$[Li(DME)_3]^+[t\text{Bu}_2\text{P–P–\{C(H)(biph)\}–P}t\text{Bu}_2]^-$ (**2_1**)

- 7.68 ppm – 6.07 ppm – aromatic protons;
- 3.61 ppm, broad s, THF protons (from THF-d_8);
- 3.46 ppm, s, DME protons;
- 3.30 ppm, s, DME protons;
- 3.22 ppm, broad d, J_{PH} = 5.3 Hz, 1H, $[Li(DME)_3]^+[t\text{Bu}_2\text{P–P–\{C(}\mathbf{H}\text{)(biph)\}–P}t\text{Bu}_2]^-$;
- 1.76 ppm, broad s, THF protons (from THF-d_8);
- 1.32 ppm, broad s, 36 H, $[Li(DME)_3]^+[\boldsymbol{t}\mathbf{Bu}_2\text{P–P–\{C(H)(biph)\}–P}\boldsymbol{t}\mathbf{Bu}_2]^-$;

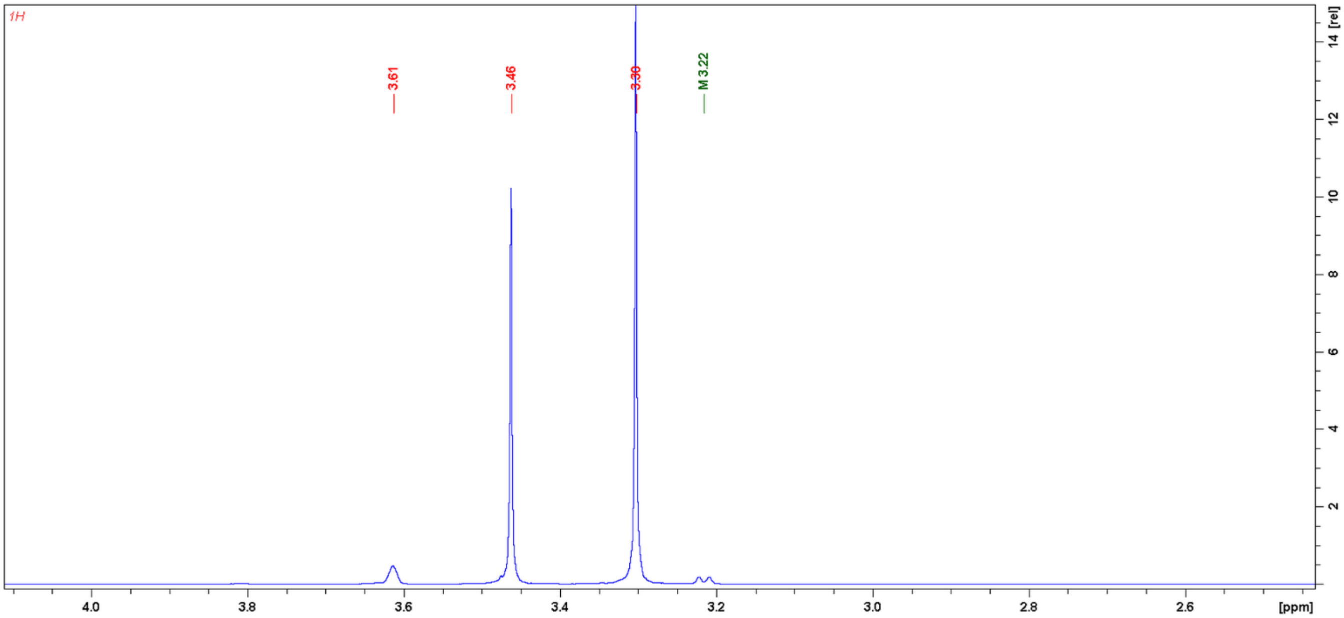

Figure S23. ^{1}H NMR spectrum of isolated crystals of $[Li(DME)_3]^+[t\text{Bu}_2\text{P–P–\{C(H)(biph)\}–P}t\text{Bu}_2]^-$ (**2_1**) dissolved in THF-d_8 in the range from 4.0 ppm to 2.5 ppm.

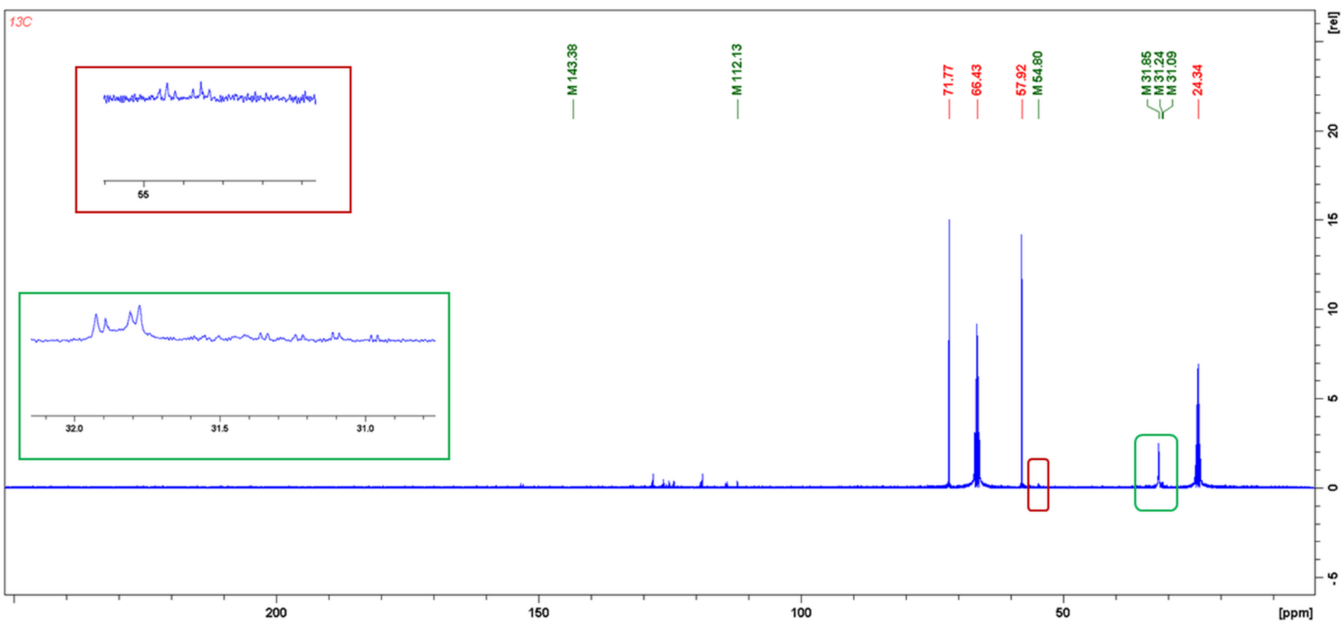

Figure S24. $^{13}C\{^{1}H\}$ NMR spectrum of isolated crystals of $[Li(DME)_3]^+[t\text{Bu}_2\text{P–P–\{C(H)(biph)\}–P}t\text{Bu}_2]^-$ (**2_1**) dissolved in THF-d_8.

Table S10. Description of signals observed on the $^{13}C\{^1H\}$ NMR spectrum - **Figure S24**.

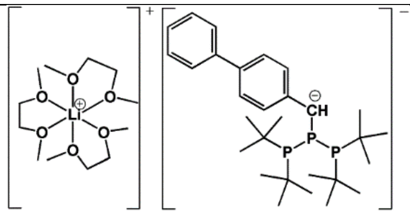

$[Li(DME)_3]^+[tBu_2P–P–\{C(H)(biph)\}–PtBu_2]^–$ (**2_1**)

- 143.38 ppm – 112.13 ppm – aromatic C-atoms;
- 71.79 ppm, s, DME;
- 66.42 ppm, THF-d_8;
- 57.92 ppm, s, DME;
- 54.80 ppm, dt, J_{PC} = 17.4 Hz, J_{PC} = 3.9 Hz, $[Li(DME)_3]^+[tBu_2P–P–\{\mathbf{C}(H)(biph)\}–PtBu_2]^–$;
- 31.85 ppm, broad dd, J_{PC} = 15.0 Hz, J_{PC} = 7.0 Hz, $[Li(DME)_3]^+[\{(H_3\mathbf{C})_3C\}_2P–P–\{C(H)(biph)\}–P\{C(\mathbf{C}H_3)_3\}_2]^–$;
- 31.24 ppm, dd, J_{PC} = 24.9 Hz, J_{PC} = 2.3 Hz, $[Li(DME)_3]^+[\{(H_3C)_3\mathbf{C}\}_2P–P–\{C(H)(biph)\}–P\{\mathbf{C}(CH_3)_3\}_2]^–$;
- 31.09 ppm, dd, J_{PC} = 28.2 Hz, J_{PC} = 2.4 Hz, $[Li(DME)_3]^+[\{(H_3C)_3\mathbf{C}\}_2P–P–\{C(H)(biph)\}–P\{\mathbf{C}(CH_3)_3\}_2]^–$;
- 24.34 ppm, THF-d_8;

b) with *n*BuLi

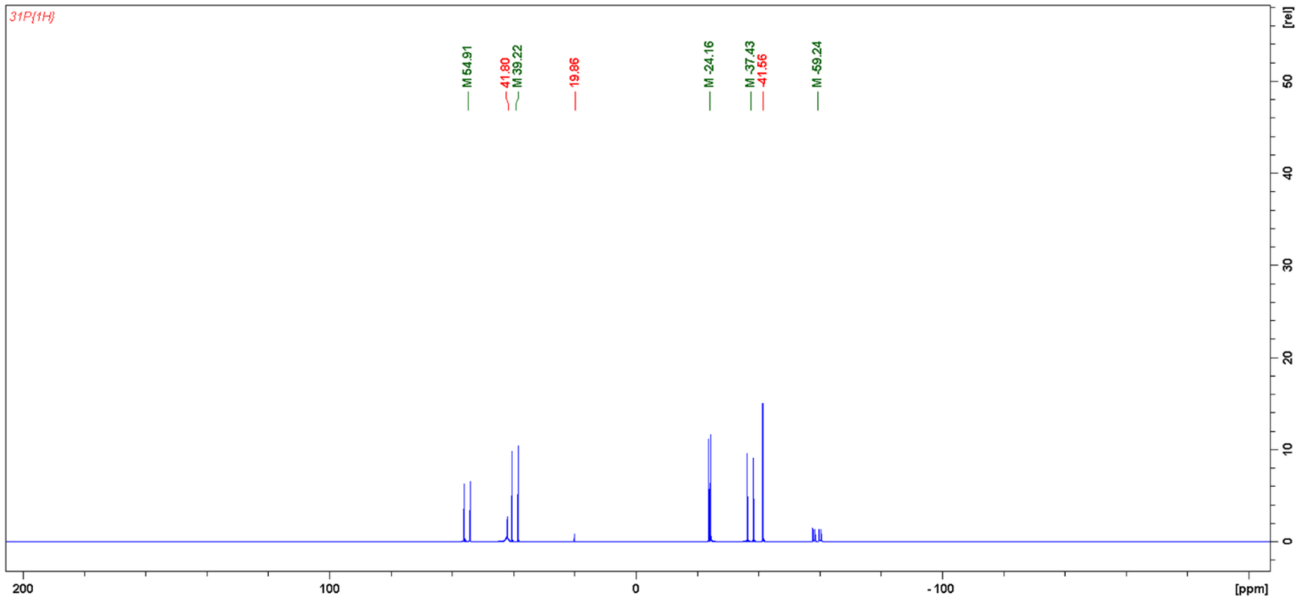

Figure S25. $^{31}P\{^{1}H\}$ NMR spectrum of reaction mixture of (biph)(H)C=P–P*t*Bu$_2$ (**1**) with *n*BuLi in THF-d$_8$.

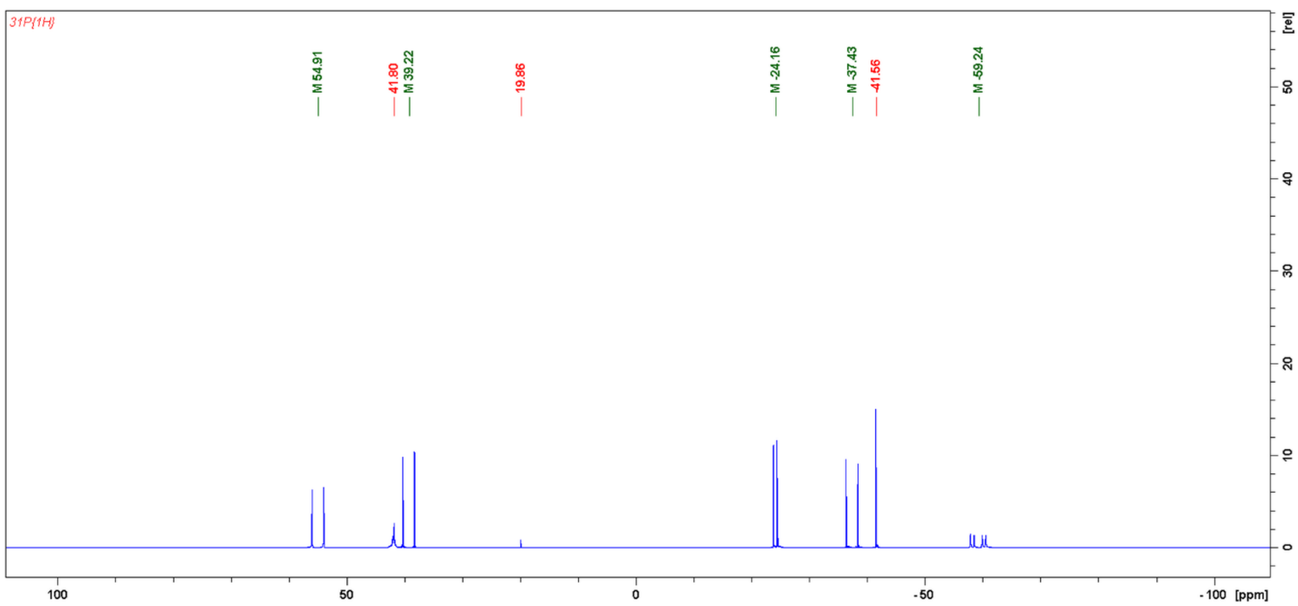

Figure S26. $^{31}P\{^{1}H\}$ NMR spectrum of reaction mixture of (biph)(H)C=P–P*t*Bu$_2$ (**1**) with *n*BuLi in THF-d$_8$ in narrow range (from 100 ppm to -100 ppm).

Table S11. Description of signals observed on the $^{31}P\{^1H\}$ NMR spectrum of reaction mixture of (biph)(H)C=P–P*t*Bu$_2$ with *n*BuLi in THF-d$_8$ – **Figure S25** and **S26**.

<table>
<tr><td>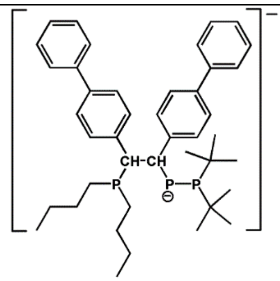
[P(nBu)$_2$–CH(biph)–CH(biph)–P–(PtBu$_2$)]$^–$ (1b”)
➢ 54.91 ppm, d, J_{PP} = 326.0 Hz, [P(nBu)$_2$–CH(biph)–CH(biph)–P–(PtBu$_2$)]$^–$;
➢ -24.16 ppm, d, J_{PP} = 102.4 Hz, [P(nBu)$_2$–CH(biph)–CH(biph)–P–(PtBu$_2$)]$^–$;
➢ -59.24 ppm, dd, J_{PP} = 102.4 Hz, J_{PP} = 326.0 Hz, [P(nBu)$_2$–CH(biph)–CH(biph)–P–(PtBu$_2$)]$^–$;</td></tr>
<tr><td>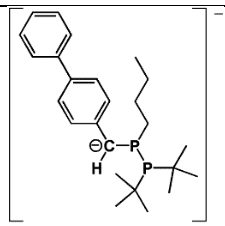
[(biph)(H)C–P(nBu)–PtBu$_2$]$^–$ (1b)
➢ 39.22 ppm, d, J_{PP} = 326.3 Hz, [(biph)(H)C–P(nBu)–PtBu$_2$]$^–$;
➢ -37.43 ppm, d, J_{PP} = 326.3 Hz, [(biph)(H)C–P(nBu)–PtBu$_2$]$^–$;</td></tr>
<tr><td>tBu$_2$PLi
➢ 41.80 ppm, broad singlet, tBu$_2$PLi;</td></tr>
<tr><td>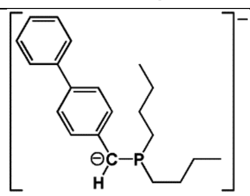
[(biph)(H)C–P(nBu)$_2$]$^–$ (1b’)
➢ -41.56 ppm, s, [(biph)(H)C–P(nBu)$_2$]$^–$;</td></tr>
</table>

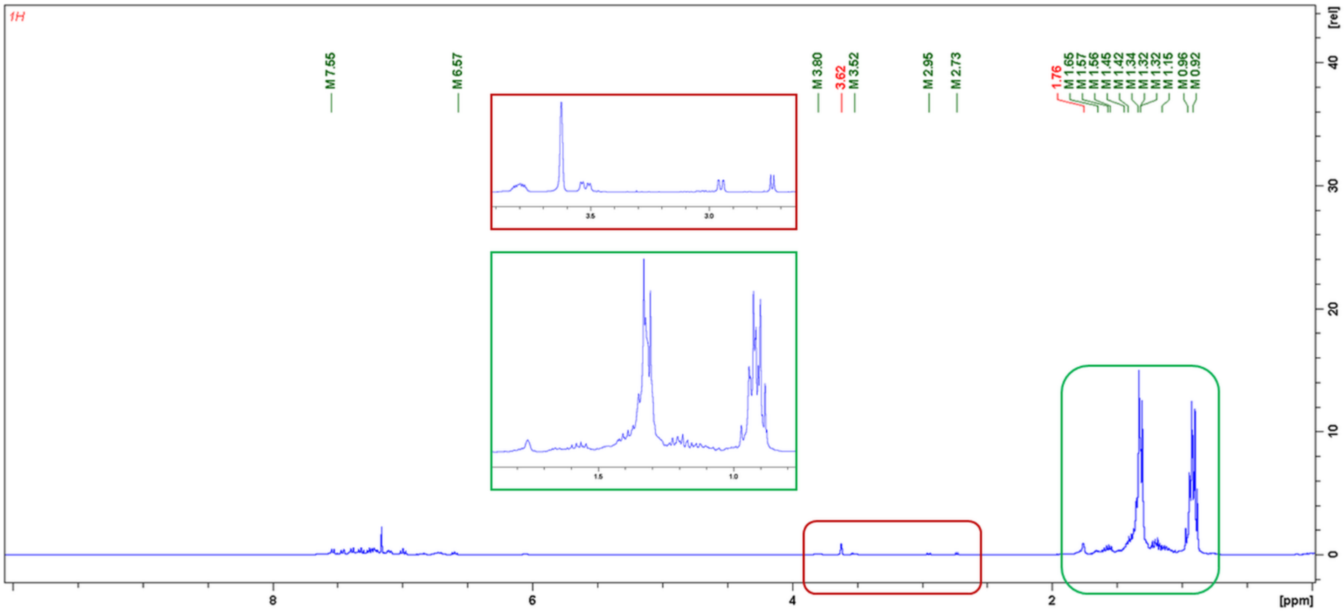

Figure S27. ^{1}H NMR spectrum of reaction mixture of (biph)(H)C=P–P*t*Bu_2 (**1**) with *n*BuLi in THF-d_8.

Table S12. Description of signals observed on the ^{1}H NMR spectrum reaction mixture of (biph)(H)C=P–P*t*Bu$_2$ **(**1**)** with *n*BuLi in THF-d$_8$ – **Figure S27**.

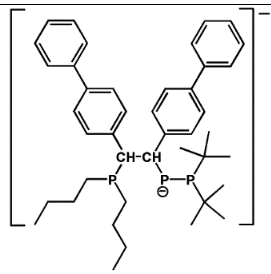

[P(*n*Bu)$_2$–CH(biph)–CH(biph)–P–(P*t*Bu$_2$)]$^-$ (**1b”**)

- 3.80 ppm, broad m, 1H, [P(*n*Bu)$_2$–C**H**(biph)–CH(biph)–P–(P*t*Bu$_2$)]$^-$;
- 3.52 ppm, dd, J_{PH} = 11.5 Hz, J_{PH} = 3.7 Hz, 1H, [P(*n*Bu)$_2$–CH(biph)–C**H**(biph)–P–(P*t*Bu$_2$)]$^-$;
- 1.65 ppm, broad m, [P(***n*Bu**)$_2$–CH(biph)–CH(biph)–P–(P*t*Bu$_2$)]$^-$;
- 1.57 ppm, broad m, [P(***n*Bu**)$_2$–CH(biph)–CH(biph)–P–(P*t*Bu$_2$)]$^-$;
- 1.45 ppm, broad m, [P(***n*Bu**)$_2$–CH(biph)–CH(biph)–P–(P*t*Bu$_2$)]$^-$;
- 1.34 ppm, d, J_{PH} = 12.2 Hz, 18H, [P(*n*Bu$_2$)–CH(biph)–CH(biph)–P–(P***t*Bu$_2$**)]$^-$;
- 1.15 ppm, broad m, [P(***n*Bu$_2$**)–CH(biph)–CH(biph)–P–(P*t*Bu$_2$)]$^-$;
- 0.96 ppm, d, J_{PH} = 11.6 Hz, 18H, [P(*n*Bu$_2$)–CH(biph)–CH(biph)–P–(P***t*Bu$_2$**)]$^-$;

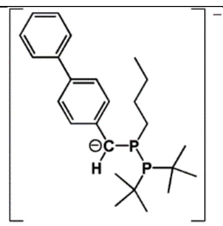

[(biph)(H)C–P(*n*Bu)–P*t*Bu$_2$]$^-$ (**1b**)

- 2.95 ppm, dd, J_{PH} = 7.8 Hz, J_{PH} = 1.5 Hz, 1H, [(biph)(**H**)C–P(*n*Bu)–P*t*Bu$_2$]$^-$;
- 1.56 ppm, broad m, [(biph)(H)C–P(***n*Bu**)–P*t*Bu$_2$]$^-$;
- 1.32 ppm, d, J_{PH} = 12.2 Hz, 18H, [(biph)(H)C–P(*n*Bu)–P***t*Bu$_2$**]$^-$;

*t*Bu$_2$PLi

- 1.32 ppm, d, J_{PH} = 10.9 Hz, 18H, *t*Bu$_2$PLi;

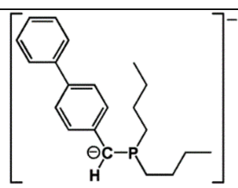

[(biph)(H)C–P(*n*Bu)$_2$]$^-$ (**1b’**)

- 2.73 ppm, d, J_{PH} = 5.3 Hz, [(biph)(**H**)C–P(*n*Bu)$_2$]$^-$;
- 1.48 ppm, broad m, [(biph)(H)C–P(***n*Bu**)$_2$]$^-$;
- 1.42 ppm, broad m, [(biph)(H)C–P(***n*Bu**)$_2$]$^-$;

Another signals

- 7.55 ppm - 6.57 ppm – aromatic protons;
- 3.62 ppm, THF-d$_8$;
- 1.76 ppm, THF-d$_8$;
- 1.32 ppm, DME protons;
- 0.92 ppm, DME protons;

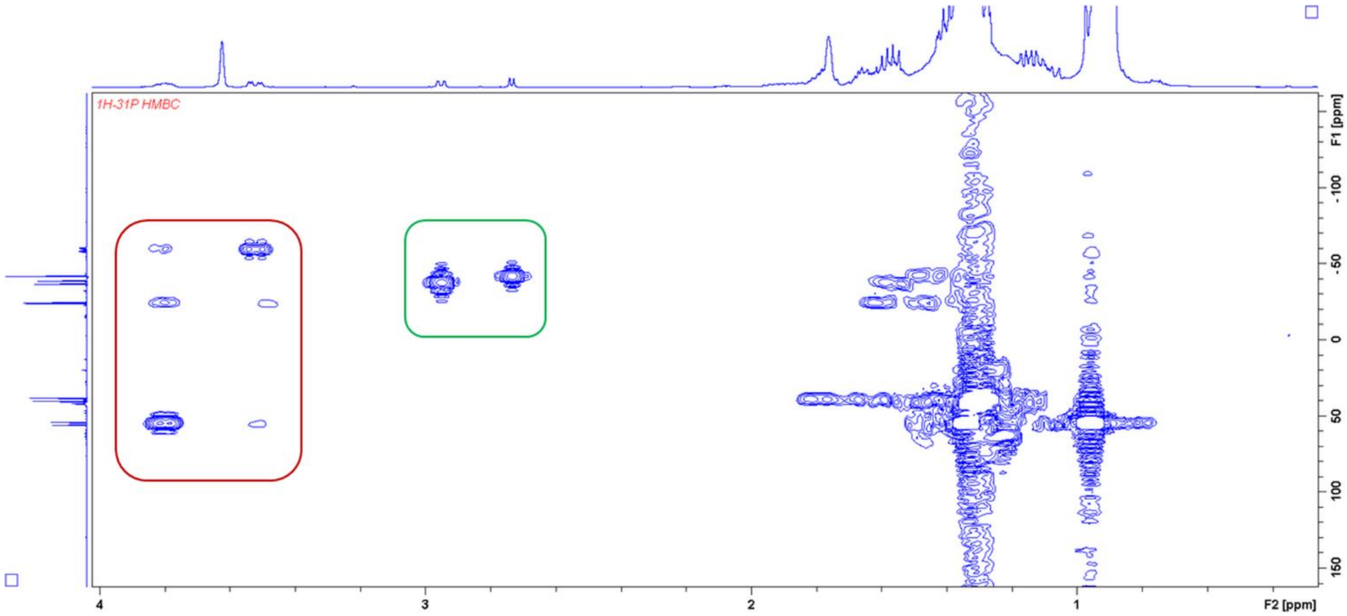

Figure S28. ${}^{31}P\{{}^{1}H\}/{}^{1}H$ HMQC NMR spectrum presenting the correlation of methine protons with phosphorus atoms in the anion $[P(n\mathrm{Bu}_2)–CH(biph)–CH(biph)–P–(Pt\mathrm{Bu}_2)]^{-}$ (**1b''**) (red color box), correlation of methine protons with phosphorus atoms in the anions $[(biph)(H)C–P(n\mathrm{Bu})–Pt\mathrm{Bu}_2]^{-}$ (**1b**) and $[(biph)(H)C–P(n\mathrm{Bu})_2]^{-}$ (**1b'**) (green box).

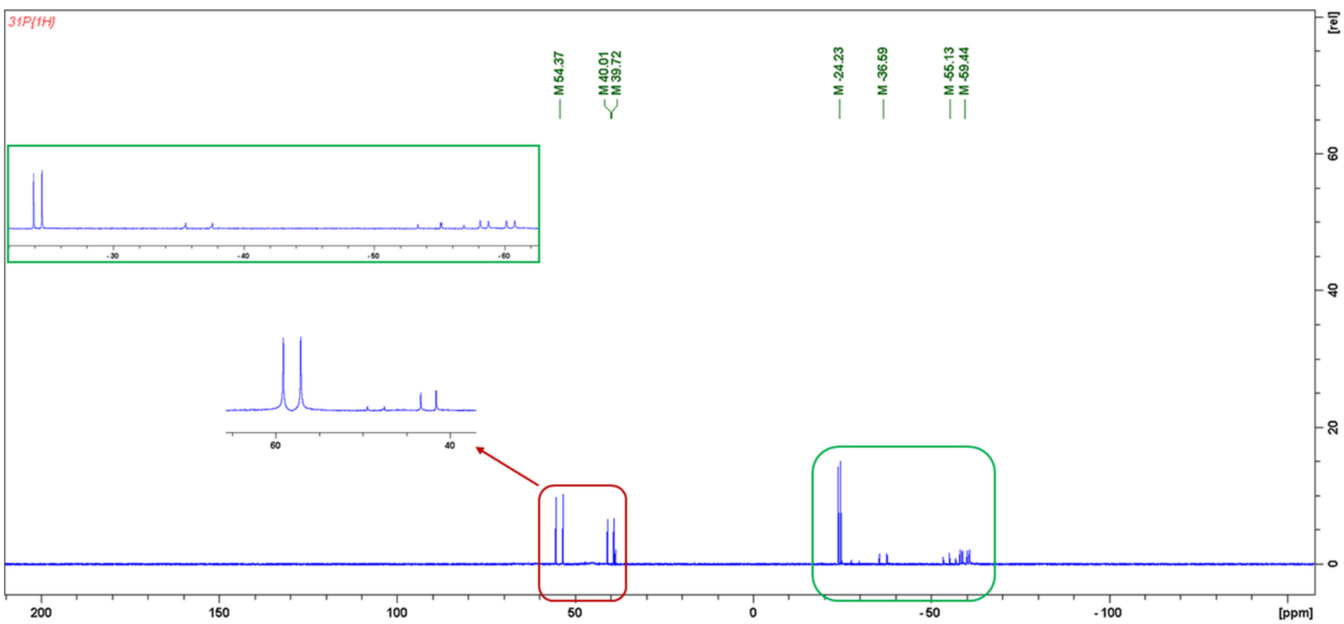

Figure S29. ${}^{31}P\{{}^{1}H\}$ NMR spectrum of reaction mixture of (biph)(H)C=P–PtBu$_2$ (**1**) with nBuLi in THF-d_8 with a lower concentration of reagents.

Table S13. Description of signals observed on the ^{31}P{^{1}H} NMR spectrum of reaction mixture of (biph)(H)C=P–P*t*Bu$_2$ **(1)** with *n*BuLi in THF-d$_8$ with a lower concentration of reagents – **Figure S29**.

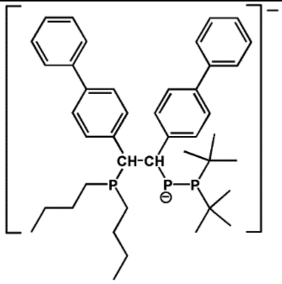

[P(*n*Bu)$_2$–CH(biph)–CH(biph)–P–(P*t*Bu$_2$)]$^{-}$ (**1b”**)

- 54.37 ppm, d, J_{PP} = 326.0 Hz, [P(*n*Bu)$_2$–CH(biph)–CH(biph)–P–(**P***t*Bu$_2$)]$^{-}$;
- -24.23 ppm, d, J_{PP} = 102.4 Hz, [**P**(*n*Bu)$_2$–CH(biph)–CH(biph)–P–(P*t*Bu$_2$)]$^{-}$;
- -59.44 ppm, dd, J_{PP} = 102.4 Hz, J_{PP} = 326.0 Hz, [P(*n*Bu)$_2$–CH(biph)–CH(biph)–**P**–(P*t*Bu$_2$)]$^{-}$;

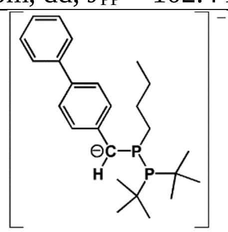

[(biph)(H)C–P(*n*Bu)–P*t*Bu$_2$]$^{-}$ (**1b**)

- 39.72 ppm, d, J_{PP} = 326.3 Hz, [(biph)(H)C–P(*n*Bu)–**P***t*Bu$_2$]$^{-}$;
- -36.59 ppm, d, J_{PP} = 326.3 Hz, [(biph)(H)C–**P**(*n*Bu)–P*t*Bu$_2$]$^{-}$;

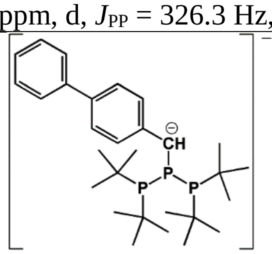

[*t*Bu$_2$P–P–{C(H)(biph)}–P*t*Bu$_2$]$^{-}$ (**2_1**)

- 40.01 ppm, broad d, J_{PP} = 285.1 Hz, [*t*Bu$_2$**P**–P–{C(H)(biph)}–P*t*Bu$_2$]$^{-}$;
- -55.13 ppm, dd, J_{PP} = 285.4 Hz, J_{PP} = 284.8 Hz, [*t*Bu$_2$P–**P**–{C(H)(biph)}–P*t*Bu$_2$]$^{-}$;

c) with *t*BuLi

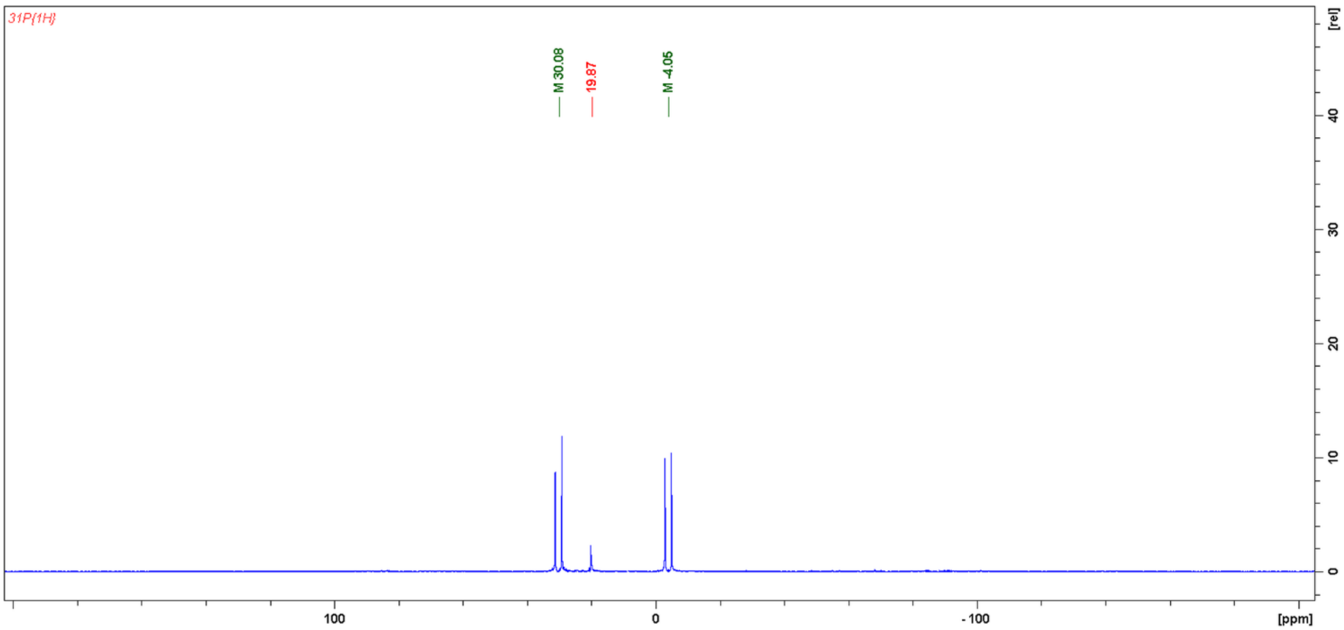

Figure S30. ^{31}P{^{1}H} NMR spectrum of reaction mixture of (biph)(H)C=P–P*t*Bu$_2$ (**1**) with *t*BuLi in THF-d$_8$.

Table S14. Description of signals observed on the ^{31}P{^{1}H} NMR spectrum reaction mixture of (biph)(H)C=P–P*t*Bu$_2$ **(1)** with *t*BuLi in THF-d$_8$ – **Figure S30**.

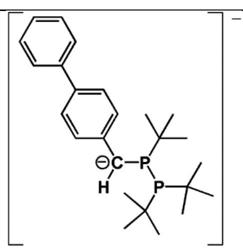	[(biph)(H)C–P(*t*Bu)–P*t*Bu$_2$]$^{-}$ **(1c)**
➢ 30.08 ppm, d, J_{PP} = 333.28 Hz, [(biph)(H)C–P(*t*Bu)–**P***t*Bu$_2$]$^{-}$; ➢ -4.05 ppm, d, J_{PP} = 333.28 Hz, [(biph)(H)C–**P**(*t*Bu)–P*t*Bu$_2$]$^{-}$;	
*t*Bu$_2$PH ➢ 19.87 ppm, s, *t*Bu$_2$**P**H;	

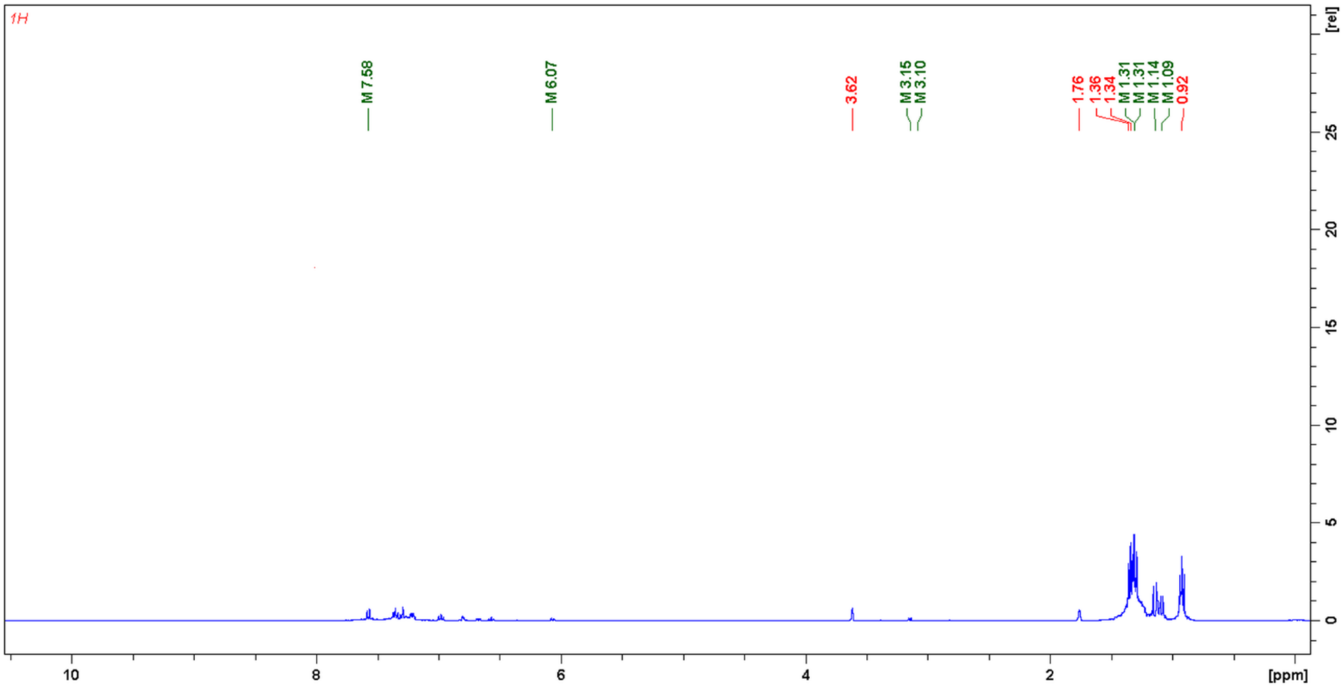

Figure S31. ^{1}H NMR spectrum of reaction mixture of (biph)(H)C=P–P*t*Bu$_2$ (**1**) with *t*BuLi in THF-d$_8$.

Table S15. Description of signals observed on the ^{1}H NMR spectrum reaction mixture of (biph)(H)C=P–P*t*Bu$_2$ **(1)** with *t*BuLi in THF-d$_8$ – **Figure S31**.

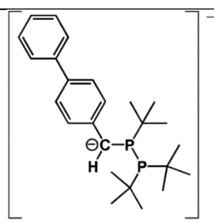

[(biph)(H)C–P(*t*Bu)–P*t*Bu$_2$]$^-$ **(1c)**

- 7.58 ppm – 6.07 ppm – aromatic protons;
- 3.15 ppm, dd, J_{PH} = 7.6 Hz, J_{PH} = 1.3 Hz, 1H, [(biph)(**H**)C–P(*t*Bu)–P*t*Bu$_2$]$^-$;
- 1.31, ppm, d, J_{PH} = 13.2 Hz, [(biph)(H)C–P(*t*Bu)–P***t*Bu**$_2$]$^-$;
- 1.31 ppm, J_{PH} = 13.7 Hz, [(biph)(H)C–P(*t*Bu)–P***t*Bu**$_2$]$^-$;
- 1.14 ppm, d, J_{PH} = 12.7 Hz, [(biph)(H)C–P(***t*Bu**)–P*t*Bu$_2$]$^-$;

*t*Bu$_2$PH

- 3.10 ppm, d, J_{PH} = 198.4 Hz, *t*Bu$_2$P**H**;
- 1.09 ppm, d, J_{PH} = 12.3 Hz, ***t*Bu**$_2$PH;

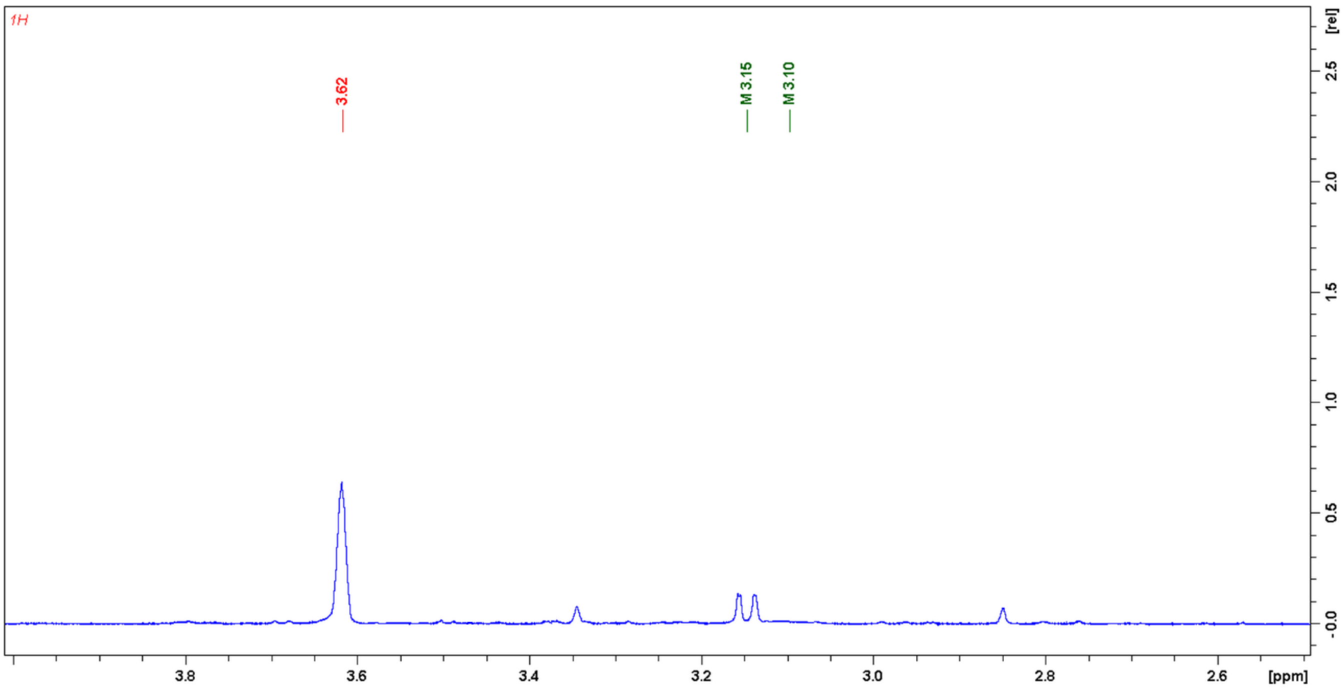

Figure S32. ^{1}H NMR spectrum of reaction mixture of (biph)(H)C=P–P*t*Bu_2 (**1**) with *t*BuLi in THF-d_8 in the range from 4 ppm to 3 ppm.

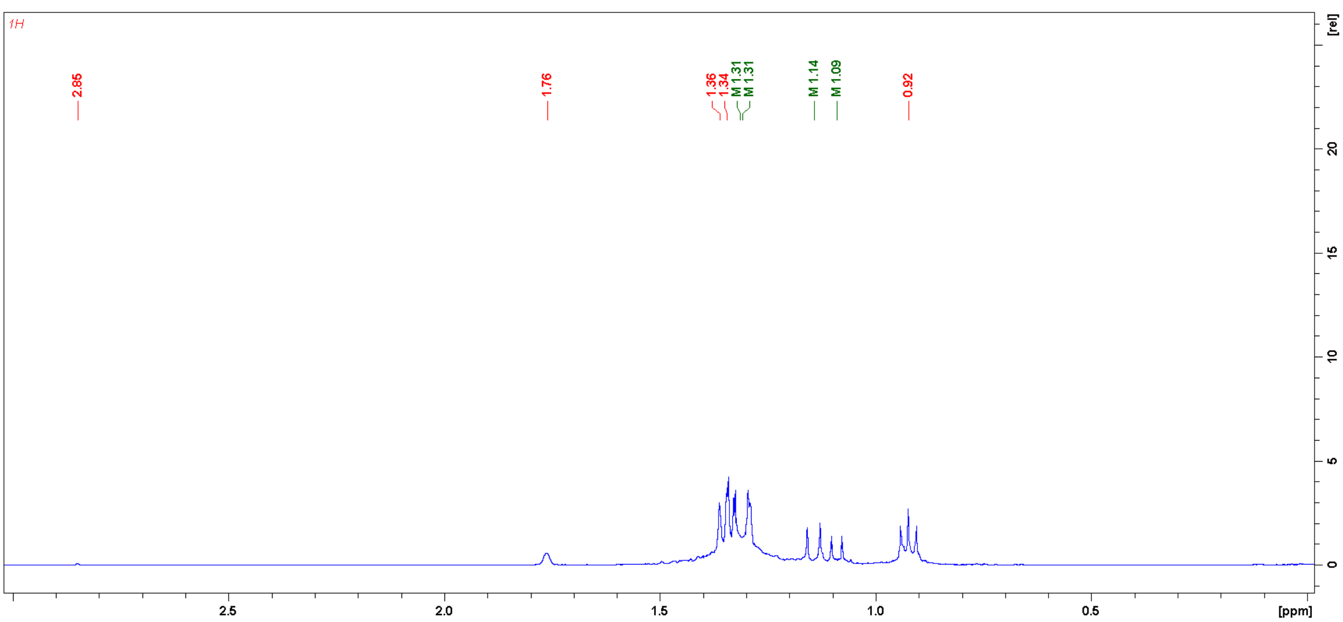

Figure S33. ^{1}H NMR spectrum of reaction mixture of (biph)(H)C=P–PtBu$_2$ (**1**) with *t*BuLi in THF-d_8 in the range from 3 ppm to 0 ppm.

2. Reaction of (3,5-tBu$_2$C$_6$H$_3$)(H)C=P–PtBu$_2$ **(3).**

a) with MeLi

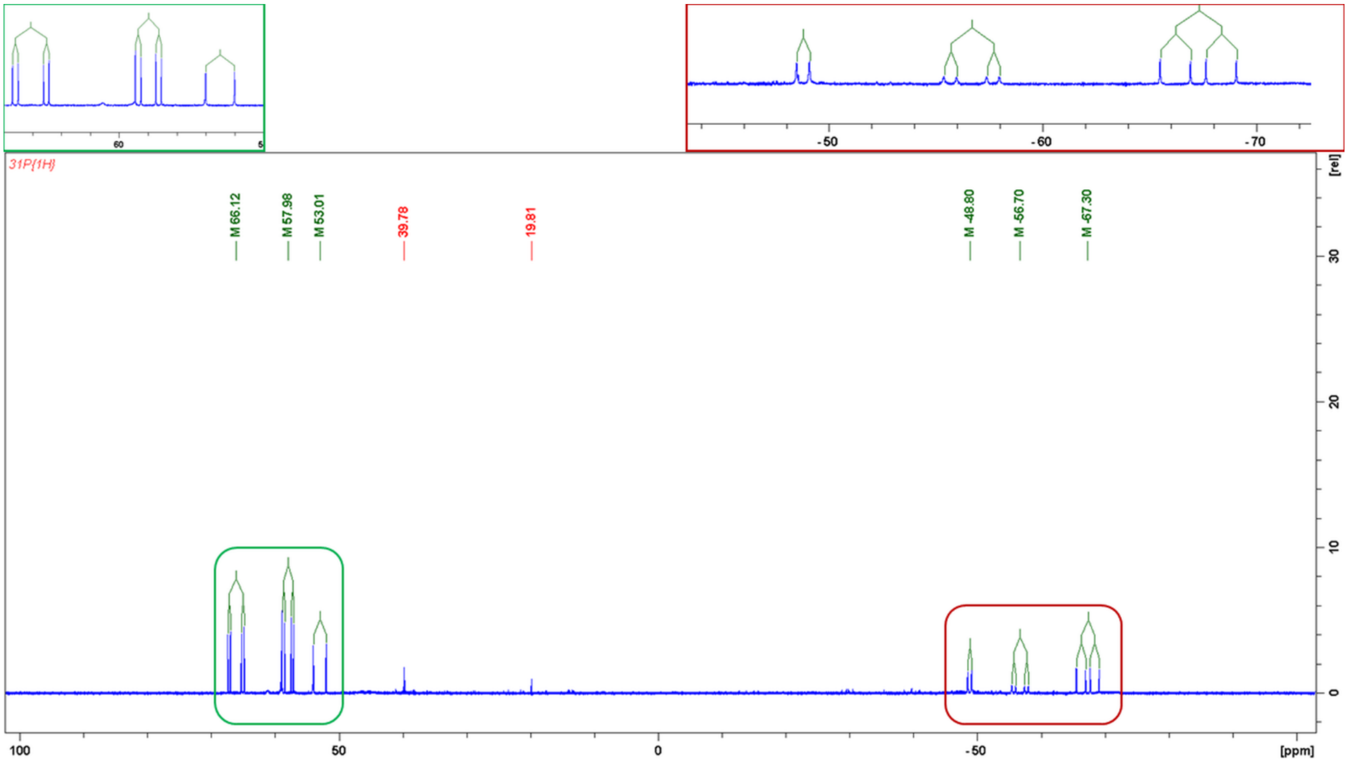

Figure S34. ^{31}P{^{1}H} NMR spectrum of reaction mixture of (3,5-tBu$_2$C$_6$H$_3$)(H)C=P–PtBu$_2$ (**3**) with MeLi in THF-d$_8$.

Table S16. Description of signals observed on the $^{31}P\{^{1}H\}$ NMR spectrum - **Figure S34**.

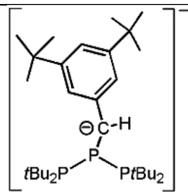

[*t*Bu$_2$P–P–{C(H)(3,5-*t*Bu$_2$C$_6$H$_3$)}–P*t*Bu$_2$]$^-$ (**2_3**)

- 66.12 ppm, dd, J_{PP} = 347.5 Hz, J_{PP} = 62.5 Hz, [*t*Bu$_2$**P**–P–{C(H)(3,5-*t*Bu$_2$C$_6$H$_3$)}–P*t*Bu$_2$]$^-$;
- 57.98 ppm, dd, J_{PP} = 231.7 Hz, J_{PP} = 62.5 Hz, [*t*Bu$_2$P–P–{C(H)(3,5-*t*Bu$_2$C$_6$H$_3$)}–**P***t*Bu$_2$]$^-$;
- -67.30 ppm, dd, J_{PP} = 347.5 Hz, J_{PP} = 231.7 Hz, [[*t*Bu$_2$P–**P**–{C(H)(3,5-*t*Bu$_2$C$_6$H$_3$)}–P*t*Bu$_2$]$^-$;

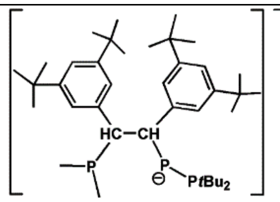

[P(Me)$_2$–CH(3,5-*t*Bu$_2$C$_6$H$_3$)–CH(3,5-*t*Bu$_2$C$_6$H$_3$)–P–(P*t*Bu$_2$)]$^-$ (**3a”**)

- 53.01 ppm, d, J_{PP} = 324.1 Hz, [P(Me)$_2$–CH(3,5-*t*Bu$_2$C$_6$H$_3$)–CH(3,5-*t*Bu$_2$C$_6$H$_3$)–P–(**P***t*Bu$_2$)]$^-$;
- -48.80 ppm, d, J_{PP} = 97.6 Hz, [**P**(Me)$_2$–CH(3,5-*t*Bu$_2$C$_6$H$_3$)–CH(3,5-*t*Bu$_2$C$_6$H$_3$)–P–(P*t*Bu$_2$)]$^-$;
- -56.70 ppm, broad dd, J_{PP} = 324.1 Hz, J_{PP} = 97.6 Hz [P(Me)$_2$–CH(3,5-*t*Bu$_2$C$_6$H$_3$)–CH(3,5-*t*Bu$_2$C$_6$H$_3$)–**P**–(P*t*Bu$_2$)]$^-$;

*t*Bu$_2$PLi

- 39.78 ppm, s;

*t*Bu$_2$PH

- 19.81 ppm, s;

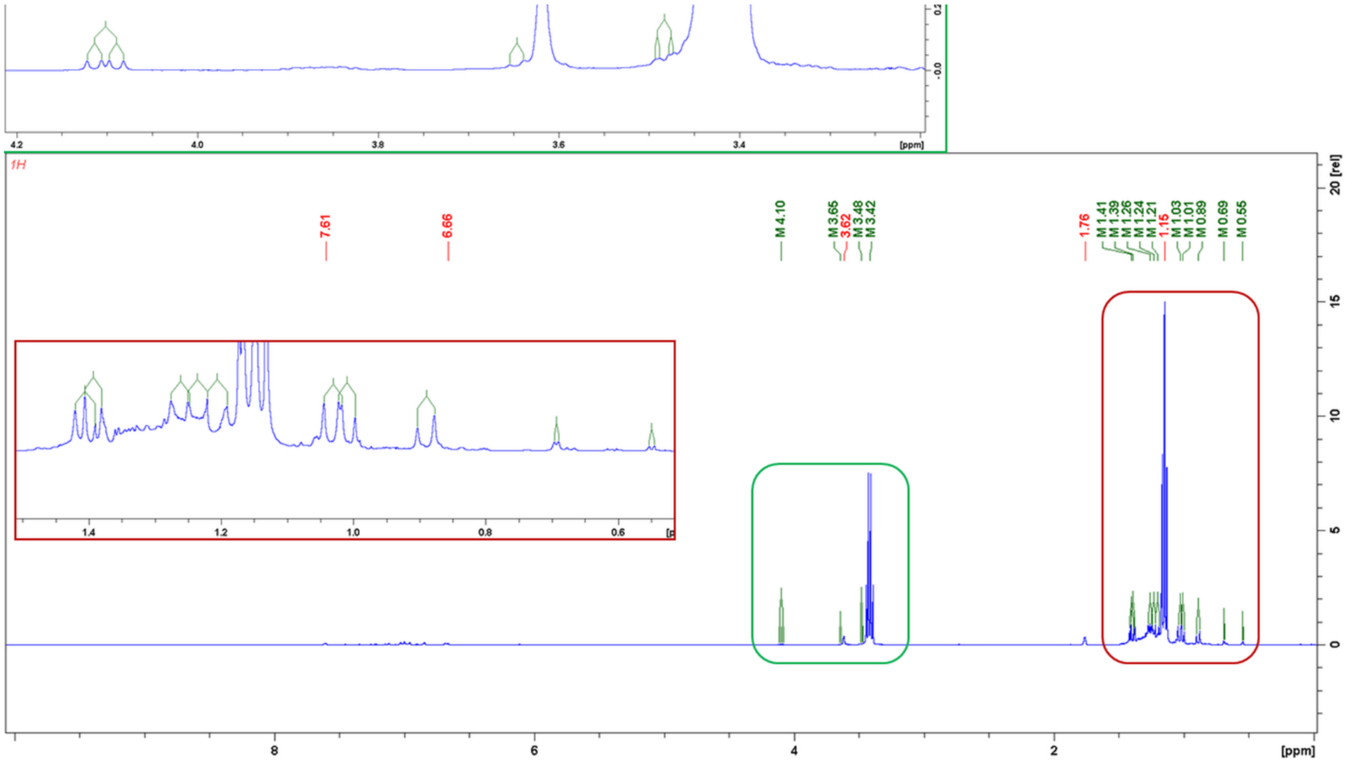

Figure 35. [1]H NMR spectrum of reaction mixture of (3,5-tBu$_2$C$_6$H$_3$)(H)C=P–PtBu$_2$ (**3**) with MeLi in THF-d$_8$.

Table 17. Description of signals observed on the [1]H NMR spectrum of reaction mixture of (3,5-tBu$_2$C$_6$H$_3$)(H)C=P–PtBu$_2$ **(3)** with nBuLi in THF-d$_8$ – **Figure S35**.

- ➢ from 7.61 ppm to 6.66 ppm - aromatic protons;

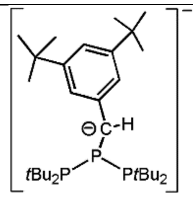

[tBu$_2$P–P–{C(H)(3,5-tBu$_2$C$_6$H$_3$)}–PtBu$_2$]$^-$ (**2_3**)

- ➢ 4.10 ppm, dd, J_{PH} = 9.8 Hz, J_{HH} = 6.4 Hz [tBu$_2$P–P–{C(**H**)(3,5-tBu$_2$C$_6$H$_3$)}–PtBu$_2$]$^-$;
- ➢ 1.39 ppm, d, J_{PH} = 10.1 Hz, [***t*Bu**$_2$P–P–{C(H)(3,5-tBu$_2$C$_6$H$_3$)}–P***t*Bu**$_2$]$^-$;
- ➢ 1.24 ppm, d, J_{PH} = 11.1 Hz, [***t*Bu**$_2$P–P–{C(H)(3,5-tBu$_2$C$_6$H$_3$)}–P***t*Bu**$_2$]$^-$;
- ➢ 1.03 ppm, d, J_{PH} = 10.9 Hz, [tBu$_2$P–P–{C(H)(3,5-***t*Bu**$_2$C$_6$H$_3$)}–PtBu$_2$]$^-$;
- ➢ 1.01 ppm, d, J_{PH} = 10.9 Hz, [tBu$_2$P–P–{C(H)(3,5-***t*Bu**$_2$C$_6$H$_3$)}–PtBu$_2$]$^-$;

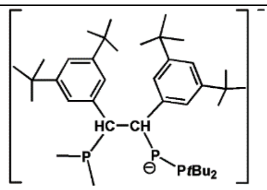

[P(Me)$_2$–CH(3,5-tBu$_2$C$_6$H$_3$)–CH(3,5-tBu$_2$C$_6$H$_3$)–P–(PtBu$_2$)]$^-$ (**3a”**)

- ➢ 3.65 ppm, broad d, J_{HH} = 6.1 Hz, [P(Me)$_2$–CH(3,5-tBu$_2$C$_6$H$_3$)–C**H**(3,5-tBu$_2$C$_6$H$_3$)–P–(PtBu$_2$)]$^-$;
- ➢ 3.48 ppm, broad dd, J_{HH} = 6.0 Hz, J_{PH} = 1.9 Hz [P(Me)$_2$–C**H**(3,5-tBu$_2$C$_6$H$_3$)–CH(3,5-tBu$_2$C$_6$H$_3$)–P–(PtBu$_2$)]$^-$;
- ➢ 1.26 ppm, broad d, J_{PH} = 11.3 Hz, [P(Me)$_2$–CH(3,5-tBu$_2$C$_6$H$_3$)–CH(3,5-tBu$_2$C$_6$H$_3$)–P–(P***t*Bu**$_2$)]$^-$;
- ➢ 1.21 ppm, broad d, J_{PH} = 11.3 Hz, [P(Me)$_2$–CH(3,5-tBu$_2$C$_6$H$_3$)–CH(3,5-tBu$_2$C$_6$H$_3$)–P–(P***t*Bu**$_2$)]$^-$;
- ➢ 0.89 ppm, J_{PH} = 12.3 Hz, [P(Me)$_2$–CH(3,5-***t*Bu**$_2$C$_6$H$_3$)–CH(3,5-***t*Bu**$_2$C$_6$H$_3$)–P–(PtBu$_2$)]$^-$;
- ➢ 0.69 ppm, d, J_{PH} = 2.4 Hz, [P(**Me**)$_2$–CH(3,5-tBu$_2$C$_6$H$_3$)–CH(3,5-tBu$_2$C$_6$H$_3$)–P–(PtBu$_2$)]$^-$;
- ➢ 0.55 ppm, d, J_{PH} = 2.4 Hz, [P(**Me**)$_2$–CH(3,5-tBu$_2$C$_6$H$_3$)–CH(3,5-tBu$_2$C$_6$H$_3$)–P–(PtBu$_2$)]$^-$;

tBu$_2$PLi

- ➢ 1.41 ppm, d, J_{PH} = 11.7 Hz;

Another signals

- ➢ 3.62 ppm and 1.76 ppm, THF-d$_8$;
- ➢ 3.42 ppm and 1.15 ppm, Et$_2$O signals from the 1.6 M solution of MeLi in Et$_2$O;

b) with *n*BuLi

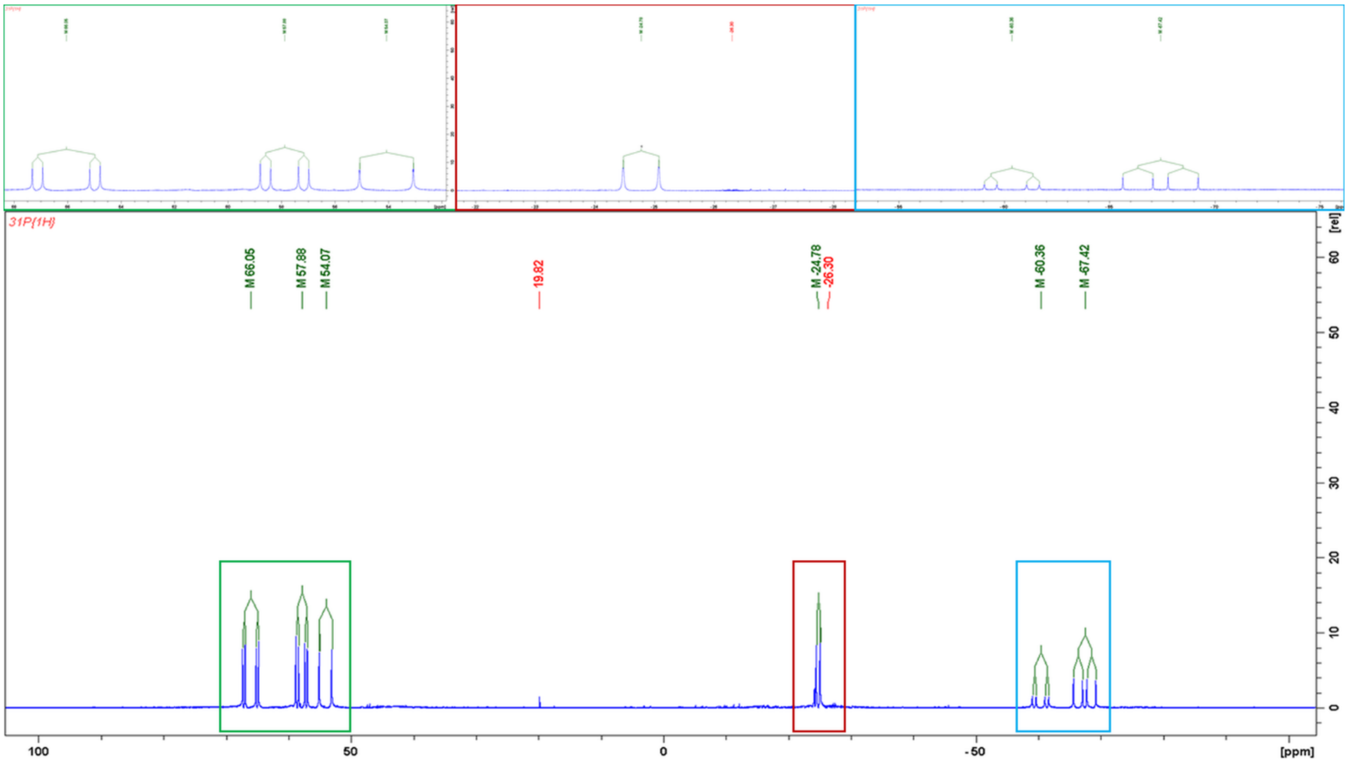

Figure 36. $^{31}P\{^1H\}$ NMR spectrum of reaction mixture of (3,5-*t*$Bu_2C_6H_3$)(H)C=P–P*t*Bu_2 (**3**) with *n*BuLi in THF-d_8.

Table S18. Description of signals observed on the ^{31}P{^{1}H} NMR spectrum of reaction mixture of (3,5-*t*Bu$_2$C$_6$H$_3$)(H)C=P–P*t*Bu$_2$ **(3)** with *n*BuLi in THF-d$_8$ – **Figure S36**.

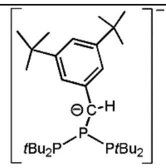	[*t*Bu$_2$P–P–{C(H)(3,5-*t*Bu$_2$C$_6$H$_3$)}–P*t*Bu$_2$]$^-$ (**2_3**)
➢ 66.05 ppm, dd, J_{PP} = 347.5 Hz, J_{PP} = 62.5 Hz, [*t*Bu$_2$**P**–P–{C(H)(3,5-*t*Bu$_2$C$_6$H$_3$)}–P*t*Bu$_2$]$^-$; ➢ 57.88 ppm, dd, J_{PP} = 231.7 Hz, J_{PP} = 62.5 Hz, [*t*Bu$_2$P–P–{C(H)(3,5-*t*Bu$_2$C$_6$H$_3$)}–**P***t*Bu$_2$]$^-$; ➢ -67.42 ppm, dd, J_{PP} = 347.5 Hz, J_{PP} = 231.7 Hz, [[*t*Bu$_2$P–**P**–{C(H)(3,5-*t*Bu$_2$C$_6$H$_3$)}–P*t*Bu$_2$]$^-$;	
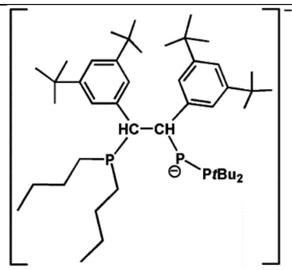	[P(*n*Bu)$_2$–CH(3,5-*t*Bu$_2$C$_6$H$_3$)–CH(3,5-*t*Bu$_2$C$_6$H$_3$)–P–(P*t*Bu$_2$)]$^-$ (**3b”**)
➢ 54.07 ppm, dd, J_{PP} = 325.2 Hz, J_{PP} = 2.6 Hz, [P(*n*Bu)$_2$–CH(3,5-*t*Bu$_2$C$_6$H$_3$)–CH(3,5-*t*Bu$_2$C$_6$H$_3$)–P–(**P***t*Bu$_2$)]$^-$; ➢ -24.07 ppm, dd, J_{PP} = 96.8 Hz, J_{PP} = 2.6 Hz, [**P**(*n*Bu)$_2$–CH(3,5-*t*Bu$_2$C$_6$H$_3$)–CH(3,5-*t*Bu$_2$C$_6$H$_3$)–P–(P*t*Bu$_2$)]$^-$; ➢ -60.36 ppm, dd, J_{PP} = 325.2 Hz, J_{PP} = 96.8 Hz, [P(*n*Bu)$_2$–CH(3,5-*t*Bu$_2$C$_6$H$_3$)–CH(3,5-*t*Bu$_2$C$_6$H$_3$)–P–(P*t*Bu$_2$)]$^-$;	

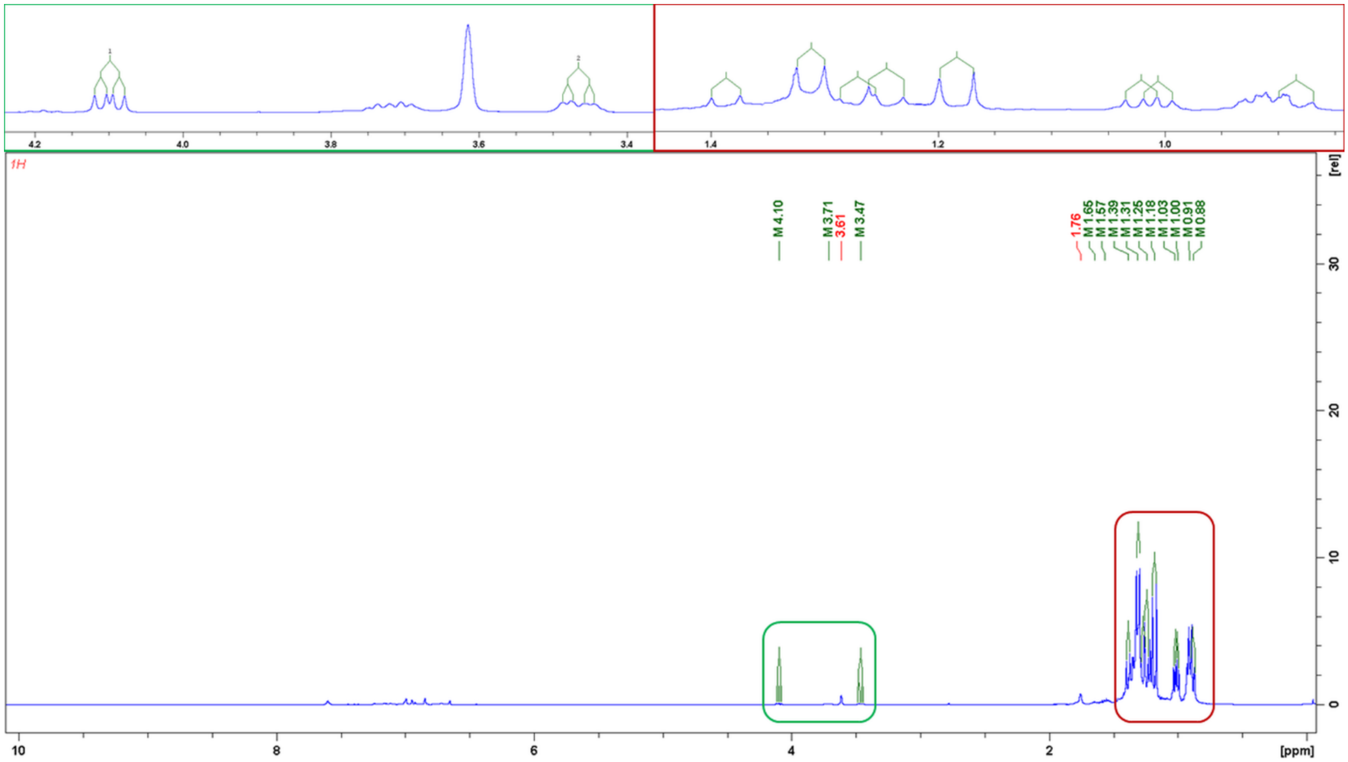

Figure S37. ¹H NMR spectrum of reaction mixture of (3,5-tBu$_2$C$_6$H$_3$)(H)C=P–PtBu$_2$ (**3**) with nBuLi in THF-d$_8$.

Table 19. Description of signals observed on the ^{1}H NMR spectrum of reaction mixture of (3,5-tBu$_2$C$_6$H$_3$)(H)C=P–PtBu$_2$ **(3)** with nBuLi in THF-d$_8$ – **Figure S37**.

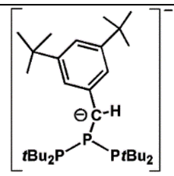

[tBu$_2$P–P–{C(H)(3,5-tBu$_2$C$_6$H$_3$)}–PtBu$_2$]$^-$ (**2_3**)

- 4.10 ppm, dd, J_{PH} = 9.8 Hz, J_{HH} = 6.4 Hz [tBu$_2$P–P–{C(**H**)(3,5-tBu$_2$C$_6$H$_3$)}–PtBu$_2$]$^-$;
- 1.39 ppm, d, J_{PH} = 10.3 Hz, [***t*Bu**$_2$P–P–{C(H)(3,5-tBu$_2$C$_6$H$_3$)}–P***t*Bu**$_2$]$^-$;
- 1.25 ppm, d, J_{PH} = 12.2 Hz, [***t*Bu**$_2$P–P–{C(H)(3,5-tBu$_2$C$_6$H$_3$)}–P***t*Bu**$_2$]$^-$;
- 1.03 ppm, d, J_{PH} = 11.0 Hz, [tBu$_2$P–P–{C(H)(3,5-***t*Bu**$_2$C$_6$H$_3$)}–PtBu$_2$]$^-$;
- 1.00 ppm, d, J_{PH} = 10.9 Hz, [tBu$_2$P–P–{C(H)(3,5-***t*Bu**$_2$C$_6$H$_3$)}–PtBu$_2$]$^-$

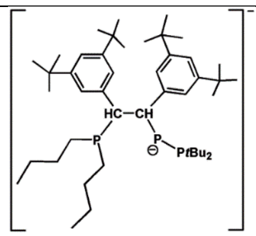

[P(nBu)$_2$–CH(3,5-tBu$_2$C$_6$H$_3$)–CH(3,5-tBu$_2$C$_6$H$_3$)–P–(PtBu$_2$)]$^-$ (**3b”**)

- 3.71 ppm, broad m, [P(nBu)$_2$–CH(3,5-tBu$_2$C$_6$H$_3$)–C**H**(3,5-tBu$_2$C$_6$H$_3$)–P–(PtBu$_2$)]$^-$;
- 3.47 ppm, broad dd, J_{PH} = 9.8 Hz, J_{HH} = 6.4 Hz [P(nBu)$_2$–C**H**(3,5-tBu$_2$C$_6$H$_3$)–CH(3,5-tBu$_2$C$_6$H$_3$)–P–(PtBu$_2$)]$^-$;
- 1.65 ppm, broad m, [P(***n*Bu**)$_2$–CH(3,5-tBu$_2$C$_6$H$_3$)–CH(3,5-tBu$_2$C$_6$H$_3$)–P–(PtBu$_2$)]$^-$;
- 1.57 ppm, broad m, [P(***n*Bu**)$_2$–CH(3,5-tBu$_2$C$_6$H$_3$)–CH(3,5-tBu$_2$C$_6$H$_3$)–P–(PtBu$_2$)]$^-$;
- 1.31 ppm, broad d, J_{PH} = 10.3 Hz, [P(nBu)$_2$–CH(3,5-tBu$_2$C$_6$H$_3$)–CH(3,5-tBu$_2$C$_6$H$_3$)–P–(P***t*Bu**$_2$)]$^-$;
- 1.27 ppm, broad d, J_{PH} = 12.5 Hz, [P(nBu)$_2$–CH(3,5-tBu$_2$C$_6$H$_3$)–CH(3,5-tBu$_2$C$_6$H$_3$)–P–(P***t*Bu**$_2$)]$^-$;
- 1.18 ppm, broad d, [P(nBu)$_2$–CH(3,5-***t*Bu**$_2$C$_6$H$_3$)–CH(3,5-***t*Bu**$_2$C$_6$H$_3$)–P–(PtBu$_2$)]$^-$;
- 1.03 ppm, broad m, [P(***n*Bu**)$_2$–CH(3,5-tBu$_2$C$_6$H$_3$)–CH(3,5-tBu$_2$C$_6$H$_3$)–P–(PtBu$_2$)]$^-$;
- 0.91 ppm, broad m, [P(***n*Bu**)$_2$–CH(3,5-tBu$_2$C$_6$H$_3$)–CH(3,5-tBu$_2$C$_6$H$_3$)–P–(PtBu$_2$)]$^-$;
- 0.88 ppm, broad d, J_{PH} = 12.1 Hz, [P(nBu)$_2$–CH(3,5-***t*Bu**$_2$C$_6$H$_3$)–CH(3,5-***t*Bu**$_2$C$_6$H$_3$)–P–(PtBu$_2$)]$^-$;

a) with *t*BuLi

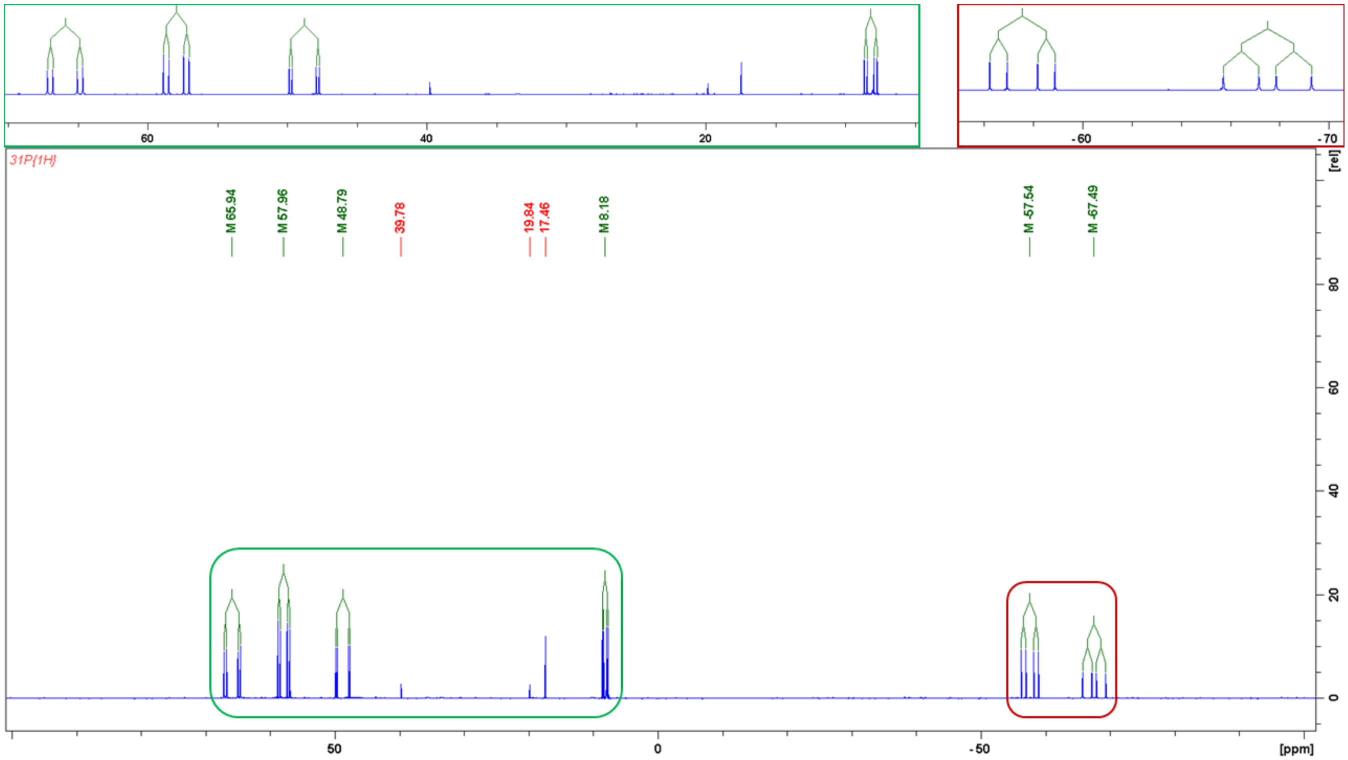

Figure S38. $^{31}P\{^{1}H\}$ NMR spectrum of reaction mixture of (3,5-tBu$_2$C$_6$H$_3$)(H)C=P–PtBu$_2$ (**3**) with *t*BuLi in THF-d$_8$.

Table S20. Description of signals observed on the ^{31}P{^{1}H} NMR spectrum of reaction mixture of (3,5-*t*Bu$_2$C$_6$H$_3$)(H)C=P–P*t*Bu$_2$ **(3)** with *n*BuLi in THF-d$_8$ – **Figure 38**.

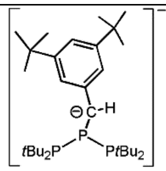

[*t*Bu$_2$P–P–{C(H)(3,5-*t*Bu$_2$C$_6$H$_3$)}–P*t*Bu$_2$]$^{-}$ (**2_3**)

- 65.94 ppm, dd, J_{PP} = 347.5 Hz, J_{PP} = 62.5 Hz, [*t*Bu$_2$**P**–P–{C(H)(3,5-*t*Bu$_2$C$_6$H$_3$)}–P*t*Bu$_2$]$^{-}$;
- 57.96 ppm, dd, J_{PP} = 231.7 Hz, J_{PP} = 62.5 Hz, [*t*Bu$_2$P–P–{C(H)(3,5-*t*Bu$_2$C$_6$H$_3$)}–**P***t*Bu$_2$]$^{-}$;
- -67.49 ppm, dd, J_{PP} = 347.5 Hz, J_{PP} = 231.7 Hz, [[*t*Bu$_2$P–**P**–{C(H)(3,5-*t*Bu$_2$C$_6$H$_3$)}–P*t*Bu$_2$]$^{-}$;

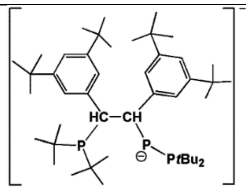

[P(*t*Bu)$_2$–CH(3,5-*t*Bu$_2$C$_6$H$_3$)–CH(3,5-*t*Bu$_2$C$_6$H$_3$)–P–(P*t*Bu$_2$)]$^{-}$ (**3c”**)

- 48.79 ppm, dd, J_{PP} = 314.6 Hz, J_{PP} = 35.3 Hz, [P(*t*Bu)$_2$–CH(3,5-*t*Bu$_2$C$_6$H$_3$)–CH(3,5-*t*Bu$_2$C$_6$H$_3$)–P–(**P***t*Bu$_2$)]$^{-}$;
- 8.18 ppm, dd, J_{PP} = 114.7 Hz, J_{PP} = 35.3 Hz, [**P**(*t*Bu)$_2$–CH(3,5-*t*Bu$_2$C$_6$H$_3$)–CH(3,5-*t*Bu$_2$C$_6$H$_3$)–P–(P*t*Bu$_2$)]$^{-}$;
- -67.54 ppm, dd, J_{PP} = 314.6 Hz, J_{PP} = 114.7 Hz, [P(*t*Bu)$_2$–CH(3,5-*t*Bu$_2$C$_6$H$_3$)–CH(3,5-*t*Bu$_2$C$_6$H$_3$)–**P**–(P*t*Bu$_2$)]$^{-}$;

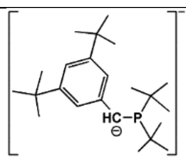

[(3,5-*t*Bu$_2$C$_6$H$_3$)(H)C–P(*t*Bu$_2$)$_2$]$^{-}$ (**3a’**)

- 17.46 ppm, s, [(3,5-*t*Bu$_2$C$_6$H$_3$)(H)C–**P**(*t*Bu$_2$)$_2$]$^{-}$;

*t*Bu$_2$PLi

- 39.78 ppm, s;

*t*Bu$_2$PH

- 19.84 ppm, s;

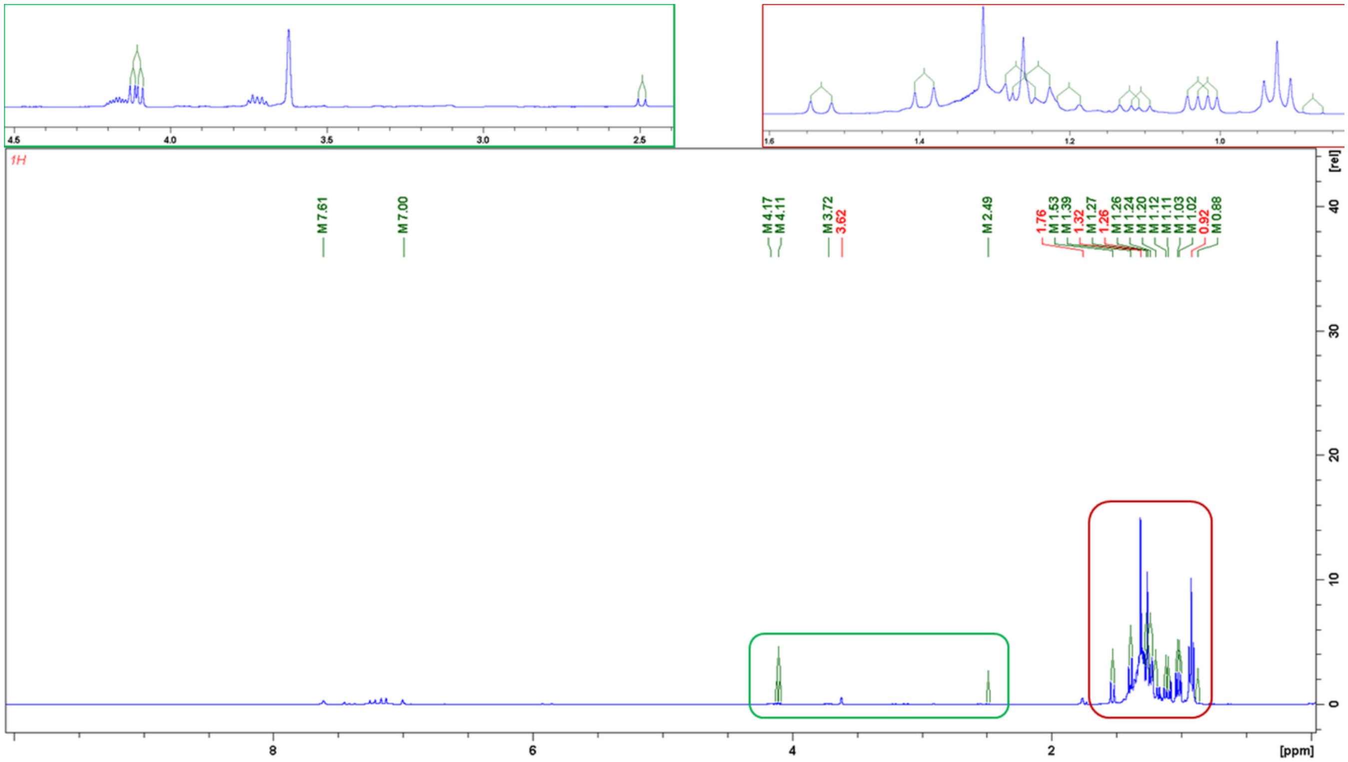

Figure S39. [1]H NMR spectrum of reaction mixture of (3,5-*t*$Bu_2C_6H_3$)(H)C=P–P*t*Bu_2 (**3**) with *t*BuLi in THF-d_8.

Table S21. Description of signals observed on the ^{1}H NMR spectrum of reaction mixture of (3,5-*t*Bu$_2$C$_6$H$_3$)(H)C=P–P*t*Bu$_2$ **(4)** with *t*BuLi in THF-d$_8$ – **Figure S39**.

- from 7.61 ppm to 7.00 ppm – aromatic protons;

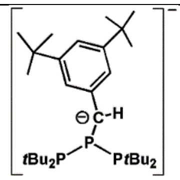

[*t*Bu$_2$P–P–{C(H)(3,5-*t*Bu$_2$C$_6$H$_3$)}–P*t*Bu$_2$]$^-$ (**2_3**)

- 4.11 ppm, dd, J_{PH} = 9.8 Hz, J_{HH} = 6.4 Hz [*t*Bu$_2$P–P–{C(**H**)(3,5-*t*Bu$_2$C$_6$H$_3$)}–P*t*Bu$_2$]$^-$;
- 1.39 ppm, d, J_{PH} = 10.3 Hz, [***t*Bu**$_2$P–P–{C(H)(3,5-*t*Bu$_2$C$_6$H$_3$)}–P***t*Bu**$_2$]$^-$;
- 1.24 ppm, d, J_{PH} = 12.2 Hz, [***t*Bu**$_2$P–P–{C(H)(3,5-*t*Bu$_2$C$_6$H$_3$)}–P***t*Bu**$_2$]$^-$;
- 1.03 ppm, d, J_{PH} = 10.9 Hz, [*t*Bu$_2$P–P–{C(H)(3,5-***t*Bu**$_2$C$_6$H$_3$)}–P*t*Bu$_2$]$^-$;
- 1.02 ppm, d, J_{PH} = 10.1 Hz, [*t*Bu$_2$P–P–{C(H)(3,5-***t*Bu**$_2$C$_6$H$_3$)}–P*t*Bu$_2$]$^-$

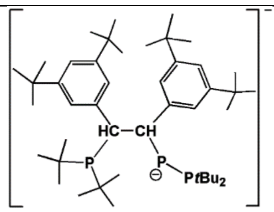

[P(*t*Bu)$_2$–CH(3,5-*t*Bu$_2$C$_6$H$_3$)–CH(3,5-*t*Bu$_2$C$_6$H$_3$)–P–(P*t*Bu$_2$)]$^-$ (**3c”**)

- 4.17 ppm, broad m, [P(*t*Bu)$_2$–CH(3,5-*t*Bu$_2$C$_6$H$_3$)–C**H**(3,5-*t*Bu$_2$C$_6$H$_3$)–P–(P*t*Bu$_2$)]$^-$;
- 3.72 ppm, broad m, [P(*n*Bu)$_2$–C**H**(3,5-*t*Bu$_2$C$_6$H$_3$)–CH(3,5-*t*Bu$_2$C$_6$H$_3$)–P–(P*t*Bu$_2$)]$^-$;
- 1.53 ppm, d, J_{PH} = 11.2 Hz, [P(*t*Bu)$_2$–CH(3,5-*t*Bu$_2$C$_6$H$_3$)–CH(3,5-*t*Bu$_2$C$_6$H$_3$)–P–(P***t*Bu**$_2$)]$^-$;
- 1.27 ppm, broad d, J_{PH} = 11.3 Hz, [P(*t*Bu)$_2$–CH(3,5-*t*Bu$_2$C$_6$H$_3$)–CH(3,5-*t*Bu$_2$C$_6$H$_3$)–P–(P***t*Bu**$_2$)]$^-$;
- 1.26 ppm, d, J_{PH} = 11.7 Hz, [P(***t*Bu**)$_2$–CH(3,5-*t*Bu$_2$C$_6$H$_3$)–CH(3,5-*t*Bu$_2$C$_6$H$_3$)–P–(P*t*Bu$_2$)]$^-$;
- 1.20 ppm, d, broad d, J_{PH} = 12.1 Hz, [P(***t*Bu**)$_2$–CH(3,5-*t*Bu$_2$C$_6$H$_3$)–CH(3,5-*t*Bu$_2$C$_6$H$_3$)–P–(P*t*Bu$_2$)]$^-$;
- 0.88 ppm, broad d, J_{PH} = 10.6 Hz, [P(*t*Bu)$_2$–CH(3,5-***t*Bu**$_2$C$_6$H$_3$)–CH(3,5-***t*Bu**$_2$C$_6$H$_3$)–P–(P*t*Bu$_2$)]

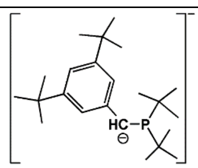

[(3,5-*t*Bu$_2$C$_6$H$_3$)(H)C–P(*t*Bu$_2$)$_2$]$^-$ (**3c’**)

- 2.49 ppm, d, J_{PH} = 10.4 Hz, [(3,5-*t*Bu$_2$C$_6$H$_3$)(**H**)C–P(*t*Bu$_2$)$_2$]$^-$;
- 1.12 ppm, d, J_{PH} = 10.4 Hz, [(3,5-*t*Bu$_2$C$_6$H$_3$)(H)C–P(***t*Bu**$_2$)$_2$]$^-$;
- 1.11 ppm, d, J_{PH} = 9.8 Hz, [(3,5-*t*Bu$_2$C$_6$H$_3$)(H)C–P(***t*Bu**$_2$)$_2$]$^-$;

The weak signals of the *t*Bu group from 3 and 5 positions in the phenyl ring were not found (probably obscured by pentane signals)

Another signals

- 1.32 ppm, 1.26 ppm, 0.92 ppm, signals from the pentane solution of *t*BuLi;
- 3.62 ppm and 1.76 ppm, THF-d$_8$;

3. Reaction of (p-Me_2N-C_6H_4)(H)C=P–P$t$$Bu_2$ **(4).**

a) with MeLi

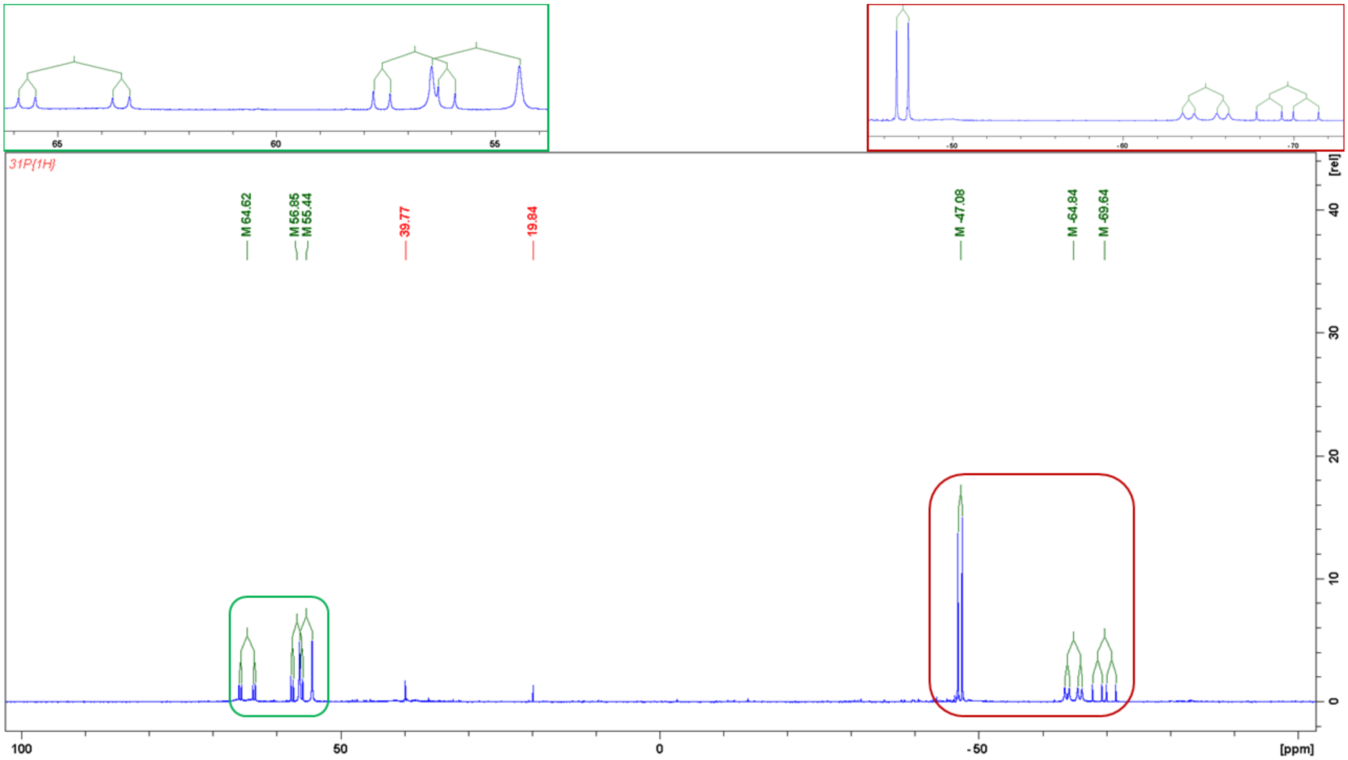

Figure S40. ^{31}P{^{1}H} NMR spectrum of reaction mixture of (p-Me_2N-C_6H_4)(H)C=P–P$t$$Bu_2$ (**4**) with MeLi in THF-d_8.

Table S22. Description of signals observed on the $^{31}P\{^1H\}$ NMR spectrum of reaction mixture of (p-Me_2N-C_6H_4)(H)C=P–P*t*Bu$_2$ **(4)** with MeLi in THF-d_8 – **Figure S40**.

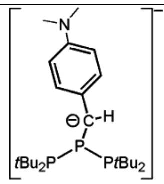

[*t*Bu$_2$P–P–{C(H)(p-Me_2N-C_6H_4)}–P*t*Bu$_2$]$^–$ (**2_4**)

- 64.62 ppm, dd, J_{PP} = 348.2 Hz, J_{PP} = 62.6 Hz, [*t*Bu$_2$**P**–P–{C(H)(p-Me_2N-C_6H_4)}–P*t*Bu$_2$]$^–$;
- 56.85 ppm, dd, J_{PP} = 239.6 Hz, J_{PP} = 62.6 Hz, [*t*Bu$_2$P–P–{C(H) (p-Me_2N-C_6H_4)}–**P***t*Bu$_2$]$^–$;
- -69.64 ppm, dd, J_{PP} = 348.2 Hz, J_{PP} = 239.6 Hz, [*t*Bu$_2$P–**P**–{C(H) (p-Me_2N-C_6H_4)}–P*t*Bu$_2$]$^–$;

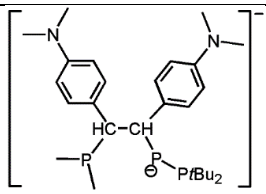

[P(Me)$_2$–CH(p-Me_2N-C_6H_4)–CH(p-Me_2N-C_6H_4)–P–(P*t*Bu$_2$)]$^–$ (**4a”**)

- 54.44 ppm, d, J_{PP} = 324.7 Hz, [P(Me)$_2$–CH(p-Me_2N-C_6H_4)–CH(p-Me_2N-C_6H_4)–P–(**P***t*Bu$_2$)]$^–$;
- -47.08 ppm, d, J_{PP} = 111.51 Hz, [**P**(Me)$_2$–CH(p-Me_2N-C_6H_4)–CH(p-Me_2N-C_6H_4)–P–(P*t*Bu$_2$)]$^–$;
- -64.84 ppm, dd, J_{PP} = 324.7 Hz, J_{PP} = 111.51 Hz, [P(Me)$_2$–CH(p-Me_2N-C_6H_4)–CH(p-Me_2N-C_6H_4)–**P**–(P*t*Bu$_2$)]$^–$;

*t*Bu$_2$PLi

- 39.77 ppm, s;

*t*Bu$_2$PH

- 19.84 ppm, s;

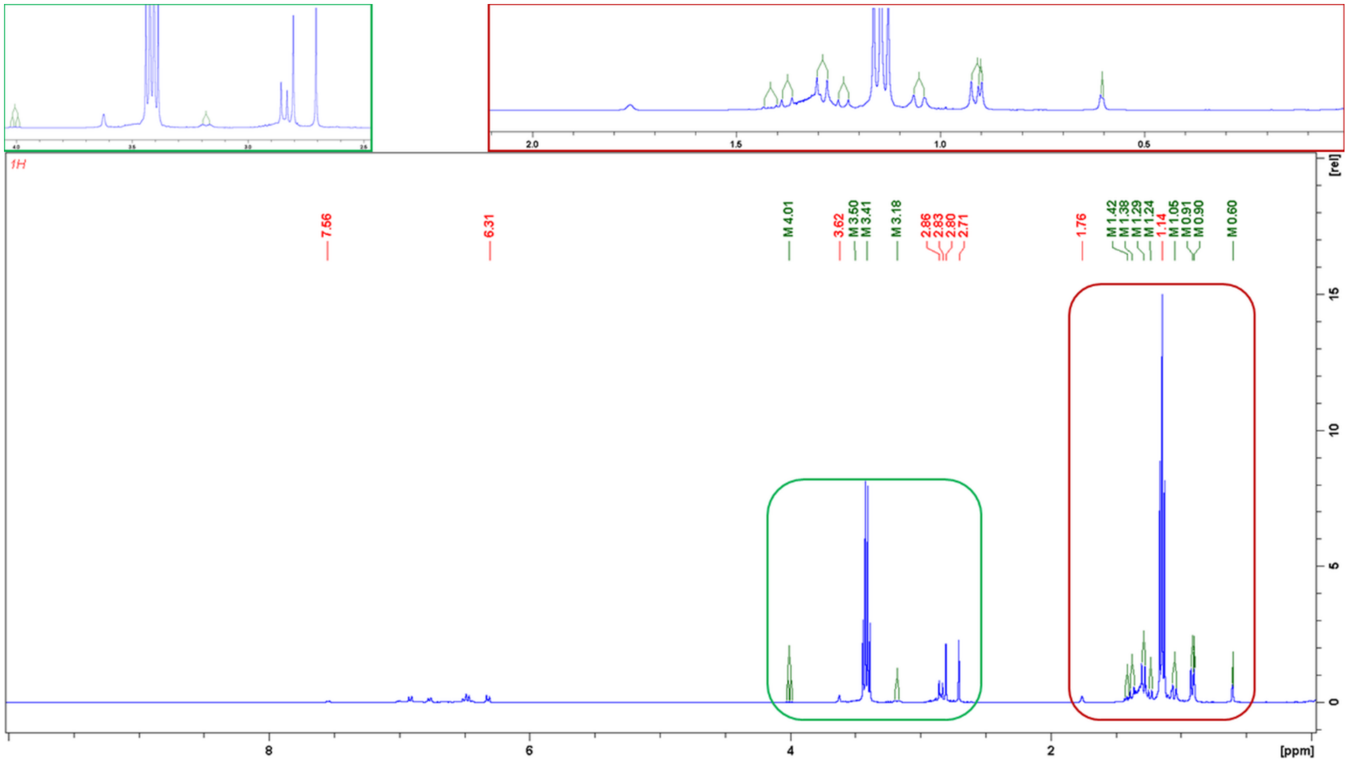

Figure S41. ^{1}H NMR spectrum of reaction mixture of (*p*-Me_2N-C_6H_4)(H)C=P–P*t*Bu_2 (**4**) with MeLi in THF-d_8.

Table S23. Description of signals observed on the [1]H NMR spectrum of reaction mixture of (p-Me_2N-C_6H_4)(H)C=P–P*t*Bu_2 **(4)** with nBuLi in THF-d_8 – **Figure S41**.

- from 7.56 ppm to 6.31 ppm - aromatic protons;

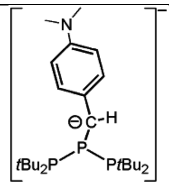

[*t*Bu_2P–P–{C(H)(*p*-Me_2N-C_6H_4)}–P*t*Bu_2]$^-$ (**2_4**)

- 4.01 ppm, dd, J_{PH} = 9.5 Hz, J_{HH} = 6.4 Hz [*t*Bu_2P–P–{C(**H**)(*p*-Me_2N-C_6H_4)}–P*t*Bu_2]$^-$;
- 2.86 ppm, s, [*t*Bu_2P–P–{C(H)(*p*-**Me**$_2$N-C_6H_4)}–P*t*Bu_2]$^-$;
- 2.83 ppm, s, [*t*Bu_2P–P–{C(H)(*p*-**Me**$_2$N-C_6H_4)}–P*t*Bu_2]$^-$;
- 1.38 ppm, d, J_{PH} = 9.9 Hz, [***t*Bu**$_2$P–P–{C(H)(*p*-Me_2N-C_6H_4)}–P***t*Bu**$_2$]$^-$;
- 1.24 ppm, d, J_{PH} = 9.8 Hz, [***t*Bu**$_2$P–P–{C(H)(*p*-Me_2N-C_6H_4)}–P***t*Bu**$_2$]$^-$;

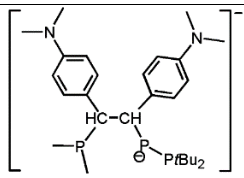

[P(Me)$_2$–CH(*p*-Me_2N-C_6H_4)–CH(*p*-Me_2N-C_6H_4)–P–(P*t*Bu_2)]$^-$ (**4a”**)

- 3.50 ppm, broad m, [P(Me)$_2$–CH(*p*-Me_2N-C_6H_4)–C**H**(*p*-Me_2N-C_6H_4)–P–(P*t*Bu_2)]$^-$;
- 3.18 ppm, broad d, J_{PH} = 11.6 Hz, [P(Me)$_2$–C**H**(*p*-Me_2N-C_6H_4)–CH(*p*-Me_2N-C_6H_4)–P–(P*t*Bu_2)]$^-$;
- 2.80 ppm, s, [P(Me)$_2$–CH(*p*-Me_2N-C_6H_4)–CH(*p*-**Me**$_2$N-C_6H_4)–P–(P*t*Bu_2)]$^-$;
- 2.71 ppm, s, [P(Me)$_2$–CH(*p*-Me_2N-C_6H_4)–CH(*p*-**Me**$_2$N-C_6H_4)–P–(P*t*Bu_2)]$^-$;
- 1.29 ppm, broad d, J_{PH} = 11.3 Hz, [P(Me)$_2$–CH(*p*-Me_2N-C_6H_4)–CH(*p*-Me_2N-C_6H_4)–P–(P***t*Bu**$_2$)]$^-$;
- 0.91 ppm, d, J_{PH} = 10.3 Hz, [P(Me)$_2$–CH(*p*-Me_2N-C_6H_4)–CH(*p*-Me_2N-C_6H_4)–P–(P***t*Bu**$_2$)]$^-$;
- 0.90 ppm, d, J_{PH} = 3.0 Hz, [P(**Me**)$_2$–CH(*p*-Me_2N-C_6H_4)–CH(*p*-Me_2N-C_6H_4)–P–(P*t*Bu_2)]$^-$;
- 0.60 ppm, d, J_{PH} = 2.3 Hz, [P(**Me**)$_2$–CH(*p*-Me_2N-C_6H_4)–CH(*p*-Me_2N-C_6H_4)–P–(P*t*Bu_2)]$^-$;

tBu_2PLi

- 1.42 ppm, d, J_{PH} = 11.7 Hz;

tBu_2PH

- 1.05 ppm, d, J_{PH} = 10.0 Hz;

Another signals

- 3.41 ppm and 1.14 ppm, Et_2O protons from the 1.6 M solution of MeLi in Et_2O;
- 3.62 ppm and 1.76 ppm, THF-d_8;

b) with *n*BuLi

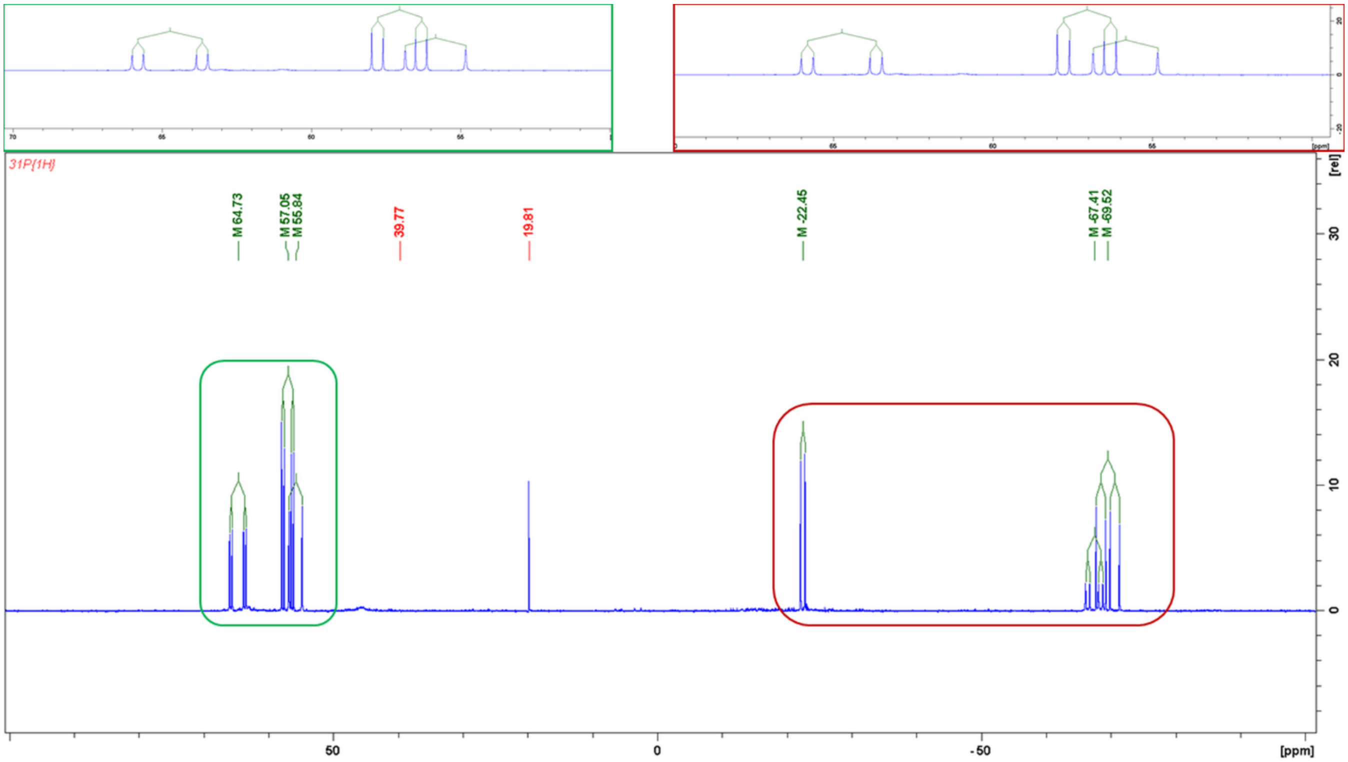

Figure S42. $^{31}P\{^{1}H\}$ NMR spectrum of reaction mixture of (*p*-Me_2N-C_6H_4)(H)C=P–P*t*Bu_2 (**4**) with *n*BuLi in THF-d_8.

Table S24. Description of signals observed on the $^{31}P\{^1H\}$ NMR spectrum of reaction mixture of (p-Me_2N-C_6H_4)(H)C=P–P$t$$Bu_2$ **(4)** with nBuLi in THF-d_8 – **Figure S42**.

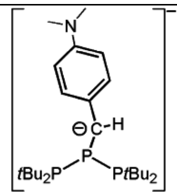

[$t$$Bu_2$P–P–{C(H)($p$-$Me_2N$-$C_6H_4$)}–P$t$$Bu_2$]$^-$ **(2_4)**

- 64.73 ppm, dd, J_{PP} = 348.2 Hz, J_{PP} = 62.6 Hz, [$t$$Bu_2$**P**–P–{C(H)($p$-$Me_2N$-$C_6H_4$)}–P$t$$Bu_2$]$^-$;
- 57.05 ppm, dd, J_{PP} = 237.7 Hz, J_{PP} = 62.6 Hz, [$t$$Bu_2$P–P–{C(H)($p$-$Me_2N$-$C_6H_4$)}–**P**$t$$Bu_2$]$^-$;
- -69.52 ppm, dd, J_{PP} = 348.2 Hz, J_{PP} = 237.7 Hz, [[$t$$Bu_2$P–**P**–{C(H)($p$-$Me_2N$-$C_6H_4$)}–P$t$$Bu_2$]$^-$;

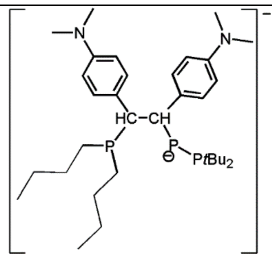

[P(nBu)$_2$–CH(p-Me_2N-C_6H_4)–CH(p-Me_2N-C_6H_4)–P–(P$t$$Bu_2$)]$^-$ (**4b”**)

- 54.84 ppm, d, J_{PP} = 328.6 Hz, [P(nBu)$_2$–CH(p-Me_2N-C_6H_4)–CH(p-Me_2N-C_6H_4)–P–(**P**$t$$Bu_2$)]$^-$;
- -22.45 ppm, d, J_{PP} = 109.6 Hz, [**P**(nBu)$_2$–CH(p-Me_2N-C_6H_4)–CH(p-Me_2N-C_6H_4)–P–(P$t$$Bu_2$)]$^-$;
- -67.41 ppm, dd, J_{PP} = 328.6 Hz, J_{PP} = 109.6 Hz, [P(nBu)$_2$–CH(p-Me_2N-C_6H_4)–CH(p-Me_2N-C_6H_4)–**P**–(P$t$$Bu_2$)]$^-$;

$t$$Bu_2$PLi

- 39.77 ppm, s;

$t$$Bu_2$PH

- 19.81 ppm, s;

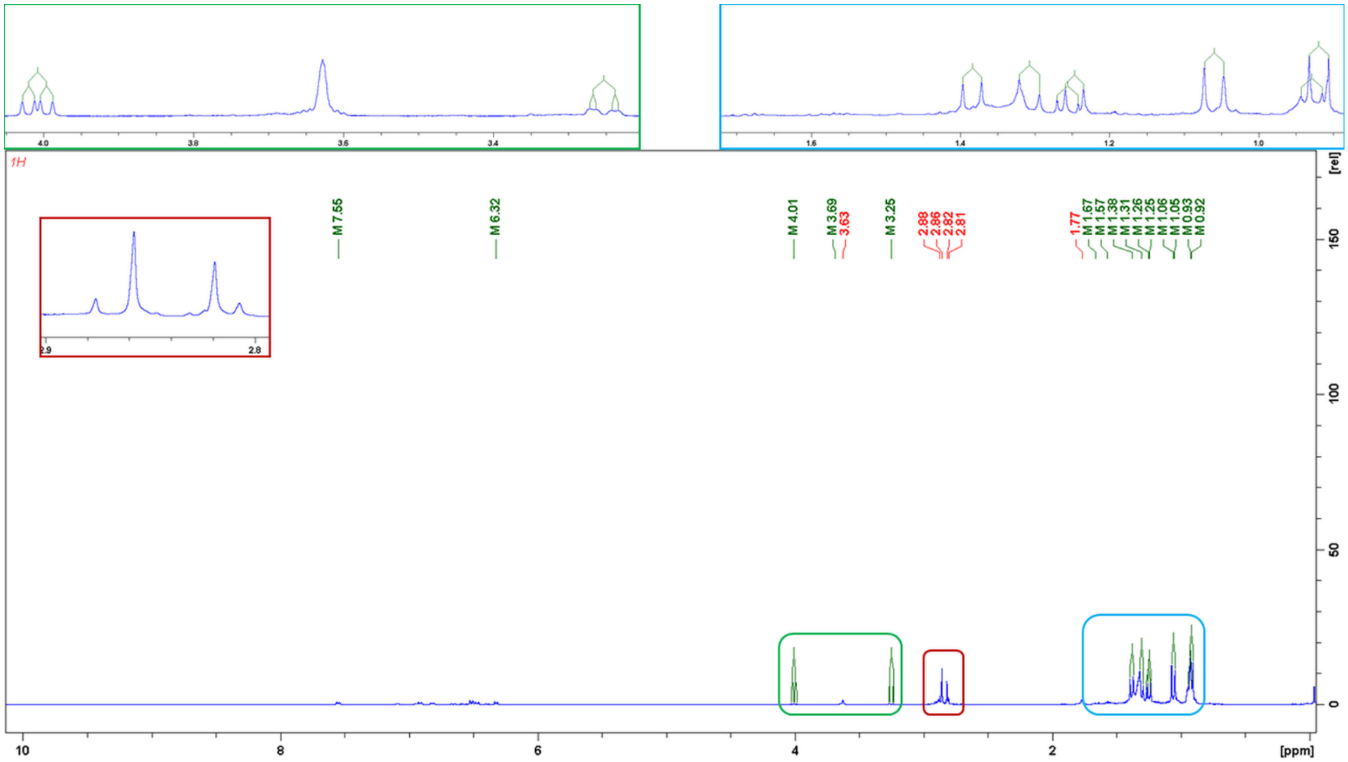

Figure S43. [1]H NMR spectrum of reaction mixture of (*p*-Me_2N-C_6H_4)(H)C=P–P*t*Bu_2 (**4**) with *n*BuLi in THF-d_8.

Table S25. Description of signals observed on the ^{1}H NMR spectrum of reaction mixture of (*p*-Me$_2$N-C$_6$H$_4$)(H)C=P–P*t*Bu$_2$ **(4)** with *n*BuLi in THF-d$_8$ – **Figure S43**.

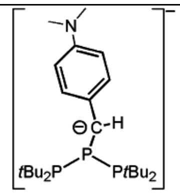

[*t*Bu$_2$P–P–{C(H)(*p*-Me$_2$N-C$_6$H$_4$)}–P*t*Bu$_2$]$^-$ **(2_4)**

- 4.01 ppm, dd, J_{PH} = 9.6 Hz, J_{HH} = 6.5 Hz [*t*Bu$_2$P–P–{C(**H**)(*p*-Me$_2$N-C$_6$H$_4$)}–P*t*Bu$_2$]$^-$;
- 2.86 ppm, s, [*t*Bu$_2$P–P–{C(H)(*p*-**Me**$_2$N-C$_6$H$_4$)}–P*t*Bu$_2$]$^-$;
- 2.82 ppm, s, [*t*Bu$_2$P–P–{C(H)(*p*-**Me**$_2$N-C$_6$H$_4$)}–P*t*Bu$_2$]$^-$;
- 1.38 ppm, d, J_{PH} = 10.0 Hz, [***t*****Bu**$_2$P–P–{C(H)(*p*-Me$_2$N-C$_6$H$_4$)}–P***t*****Bu**$_2$]$^-$;
- 1.25 ppm, d, J_{PH} = 9.8 Hz, [***t*****Bu**$_2$P–P–{C(H)(*p*-Me$_2$N-C$_6$H$_4$)}–P***t*****Bu**$_2$]$^-$;
- 1.06 ppm, d, J_{PH} = 10.4 Hz, [*t*Bu$_2$P–P–{C(H)(*p*-Me$_2$N-C$_6$H$_4$)}–P*t*Bu$_2$]$^-$;
- 0.92 ppm, d, J_{PH} = 10.5 Hz, [*t*Bu$_2$P–P–{C(H)(*p*-Me$_2$N-C$_6$H$_4$)}–P*t*Bu$_2$]$^-$

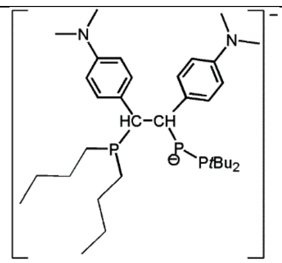

[P(*n*Bu)$_2$–CH(*p*-Me$_2$N-C$_6$H$_4$)–CH(*p*-Me$_2$N-C$_6$H$_4$)–P–(P*t*Bu$_2$)]$^-$ (**3b"**)

- 3.69 ppm, broad m, [P(*n*Bu)$_2$–CH(*p*-Me$_2$N-C$_6$H$_4$)–C**H**(*p*-Me$_2$N-C$_6$H$_4$)–P–(P*t*Bu$_2$)]$^-$;
- 3.25 ppm, broad dd, J_{PH} = 11.8 Hz, J_{HH} = 3.1 Hz [P(*n*Bu)$_2$–C**H**(*p*-Me$_2$N-C$_6$H$_4$)–CH(*p*-Me$_2$N-C$_6$H$_4$)–P–(P*t*Bu$_2$)]$^-$;
- 2.88 ppm, s, [P(*n*Bu)$_2$–C**H**(*p*-Me$_2$N-C$_6$H$_4$)–CH(*p*-Me$_2$N-C$_6$H$_4$)–P–(P*t*Bu$_2$)]$^-$;
- 2.81 ppm, s, [P(*n*Bu)$_2$–C**H**(*p*-Me$_2$N-C$_6$H$_4$)–CH(*p*-Me$_2$N-C$_6$H$_4$)–P–(P*t*Bu$_2$)]$^-$;
- 1.67 ppm, broad m, [P(***n*****Bu**)$_2$–CH(*p*-Me$_2$N-C$_6$H$_4$)–CH(*p*-Me$_2$N-C$_6$H$_4$)–P–(P*t*Bu$_2$)]$^-$;
- 1.57 ppm, broad m, [P(***n*****Bu**)$_2$–CH(*p*-Me$_2$N-C$_6$H$_4$)–CH(*p*-Me$_2$N-C$_6$H$_4$)–P–(P*t*Bu$_2$)]$^-$;
- 1.31 ppm, broad d, J_{PH} = 10.8 Hz, [P(*n*Bu)$_2$–CH(*p*-Me$_2$N-C$_6$H$_4$)–CH(*p*-Me$_2$N-C$_6$H$_4$)–P–(P***t*****Bu**$_2$)]$^-$;
- 1.26 ppm, broad d, J_{PH} = 11.2 Hz, [P(*n*Bu)$_2$–CH(*p*-Me$_2$N-C$_6$H$_4$)–CH(*p*-Me$_2$N-C$_6$H$_4$)–P–(P***t*****Bu**$_2$)]$^-$;
- 1.05 ppm, broad m, [P(***n*****Bu**)$_2$–CH(*p*-Me$_2$N-C$_6$H$_4$)–CH(*p*-Me$_2$N-C$_6$H$_4$)–P–(P*t*Bu$_2$)]$^-$;
- 0.92 ppm, broad m, [P(***n*****Bu**)$_2$–CH(*p*-Me$_2$N-C$_6$H$_4$)–CH(*p*-Me$_2$N-C$_6$H$_4$)–P–(P*t*Bu$_2$)]$^-$;

Another signals

- 3.63 ppm and 1.77 ppm THF-d$_8$;

c) with *t*BuLi

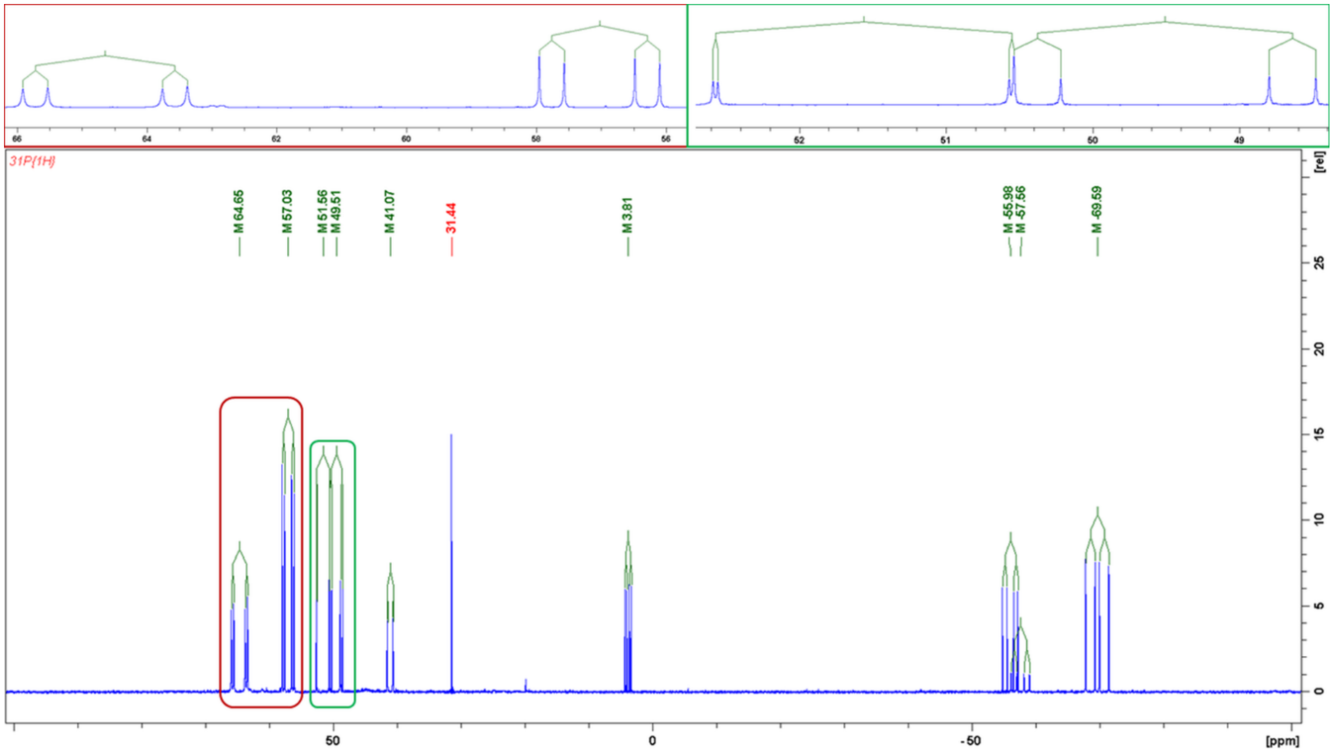

Figure S44. $^{31}P\{^1H\}$ NMR spectrum of reaction mixture of (*p*-Me_2N-C_6H_4)(H)C=P–P*t*Bu_2 (**4**) with *t*BuLi in THF-d_8.

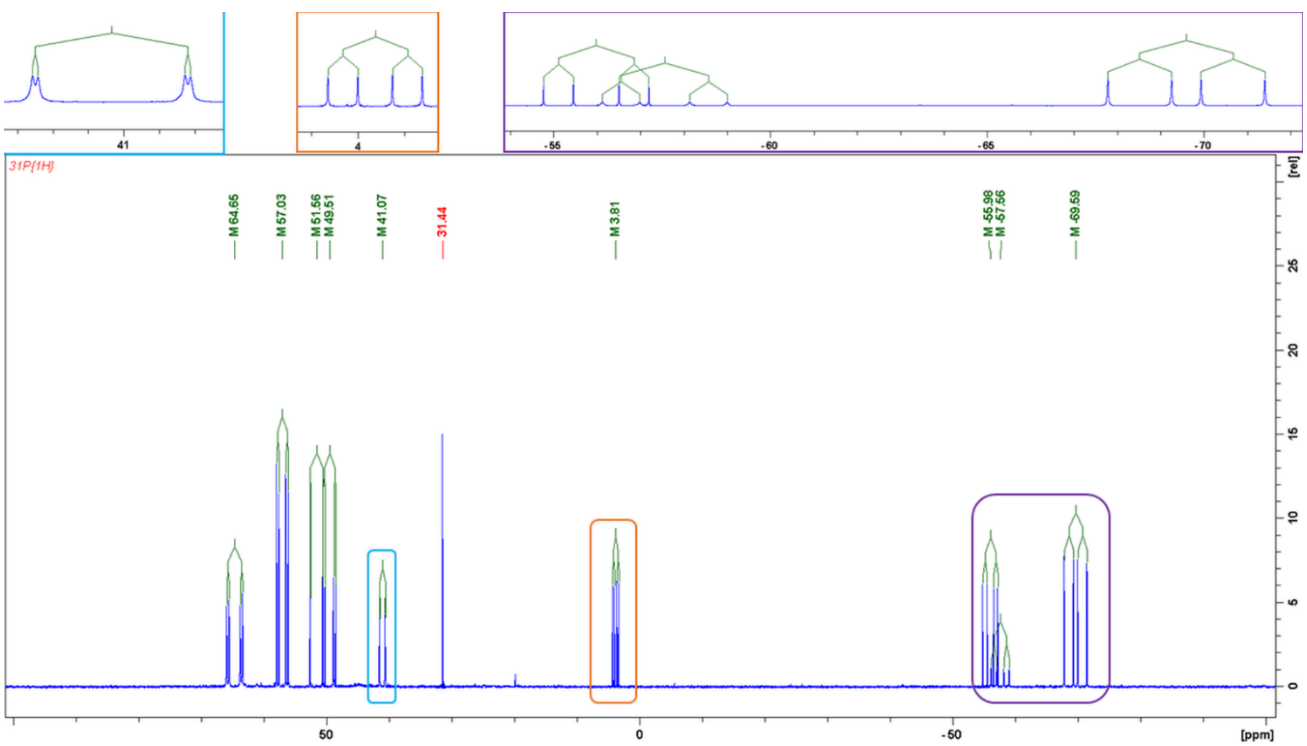

Figure S45. $^{31}P\{^1H\}$ NMR spectrum of reaction mixture of (*p*-Me_2N-C_6H_4)(H)C=P–P*t*Bu_2 (**4**) with *t*BuLi in THF-d_8.

Table S26. Description of signals observed on the ^{31}P{^{1}H} NMR spectrum of reaction mixture of (*p*-Me$_2$N-C$_6$H$_4$)(H)C=P–P*t*Bu$_2$ **(4)** with *n*BuLi in THF-d$_8$ – **Figure S44** and **S45**.

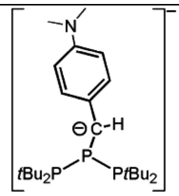

[*t*Bu$_2$P–P–{C(H)(*p*-Me$_2$N-C$_6$H$_4$)}–P*t*Bu$_2$]$^{–}$ **(2_4)**

- 64.65 ppm, dd, J_{PP} = 348.2 Hz, J_{PP} = 62.6 Hz,
- 57.03 ppm, dd, J_{PP} = 237.7 Hz, J_{PP} = 62.6 Hz, [*t*Bu$_2$P–P–{C(H) (*p*-Me$_2$N-C$_6$H$_4$)}–**P***t*Bu$_2$]$^{–}$;
- -69.59 ppm, dd, J_{PP} = 348.2 Hz, J_{PP} = 237.7 Hz, [*t*Bu$_2$P–**P**–{C(H) (*p*-Me$_2$N-C$_6$H$_4$)}–P*t*Bu$_2$]$^{–}$;

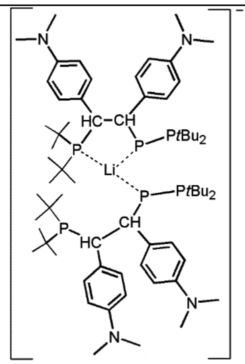

[{P(*t*Bu)$_2$–CH(*p*-Me$_2$N-C$_6$H$_4$)–CH(*p*-Me$_2$N-C$_6$H$_4$)–P–(**P***t*Bu$_2$)}$_2$Li]$^{–}$ (**4c***)

- 51.56 ppm, dd, J_{PP} = 326.9 Hz, J_{PP} = 5.3 Hz, [{P(*t*Bu)$_2$–CH(*p*-Me$_2$N-C$_6$H$_4$)–CH(*p*-Me$_2$N-C$_6$H$_4$)–P–(**P***t*Bu$_2$)}$_2$Li]$^{–}$;
- 49.51 ppm, dd, J_{PP} = 281.7 Hz, J_{PP} = 51.5 Hz, [{P(*t*Bu)$_2$–CH(*p*-Me$_2$N-C$_6$H$_4$)–CH(*p*-Me$_2$N-C$_6$H$_4$)–P–(**P***t*Bu$_2$)}$_2$Li]$^{–}$;
- 41.07 ppm, dd, J_{PP} = 139.5 Hz, J_{PP} = 5.3 Hz, [{**P**(*t*Bu)$_2$–CH(*p*-Me$_2$N-C$_6$H$_4$)–CH(*p*-Me$_2$N-C$_6$H$_4$)–P–(P*t*Bu$_2$)}$_2$Li]$^{–}$;
- 3.81 ppm, dd, J_{PP} = 111.3 Hz, J_{PP} = 51.5 Hz, [{**P**(*t*Bu)$_2$–CH(*p*-Me$_2$N-C$_6$H$_4$)–CH(*p*-Me$_2$N-C$_6$H$_4$)–P–(P*t*Bu$_2$)}$_2$Li]$^{–}$;
- -55.98 ppm, dd, J_{PP} = 281.7 Hz, J_{PP} = 111.3 Hz, [{P(*t*Bu)$_2$–CH(*p*-Me$_2$N-C$_6$H$_4$)–CH(*p*-Me$_2$N-C$_6$H$_4$)–**P**–(P*t*Bu$_2$)}$_2$Li]$^{–}$;
- -57.56 ppm, dd, J_{PP} = 326.9 Hz, J_{PP} = 139.5 Hz, [{P(*t*Bu)$_2$–CH(*p*-Me$_2$N-C$_6$H$_4$)–CH(*p*-Me$_2$N-C$_6$H$_4$)–**P**–(P*t*Bu$_2$)}$_2$Li]$^{–}$;

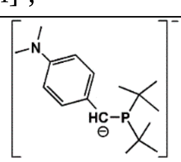

[(*p*-Me$_2$N-C$_6$H$_4$)(H)C–**P**(*t*Bu$_2$)$_2$]$^{–}$ (**4c'**)

- 31.44 ppm, s, [(*p*-Me$_2$N-C$_6$H$_4$)(H)C–**P**(*t*Bu$_2$)$_2$]$^{–}$;

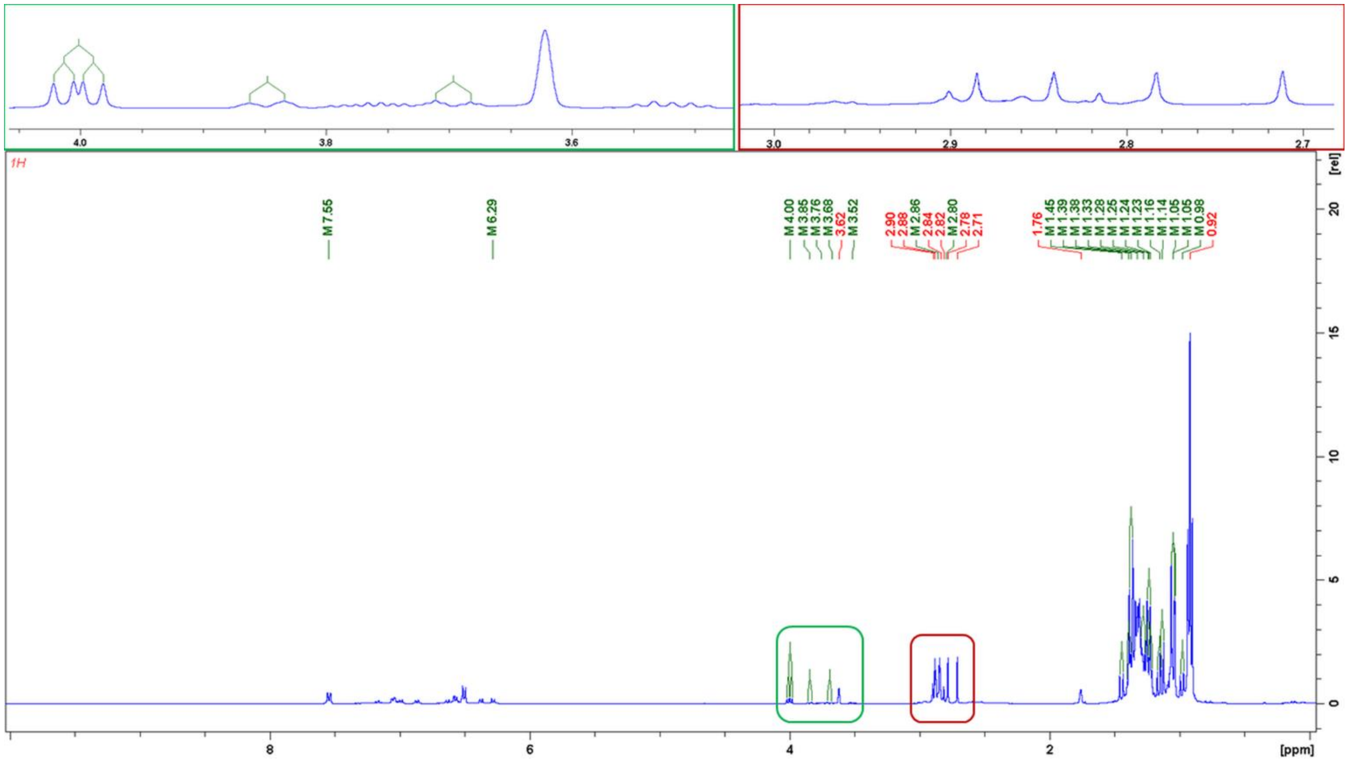

Figure S46.[1]H NMR spectrum of reaction mixture of (p-Me_2N-C_6H_4)(H)C=P–P$t$$Bu_2$ (**4**) with tBuLi in THF-d_8.

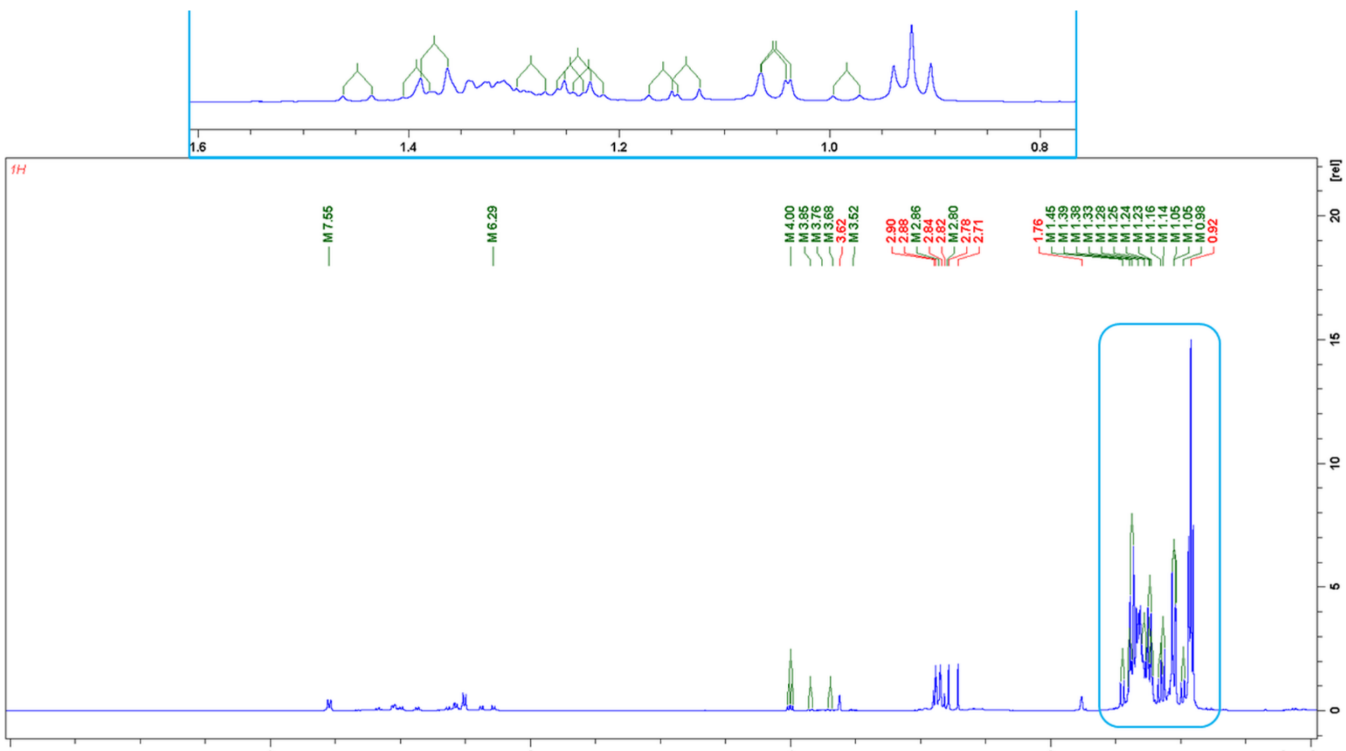

Figure S47.[1]H NMR spectrum of reaction mixture of (p-Me_2N-C_6H_4)(H)C=P–P$t$$Bu_2$ (**4**) with tBuLi in THF-d_8.

Table S27. Description of signals observed on the [1]H NMR spectrum of reaction mixture of (p-Me$_2$N-C$_6$H$_4$)(H)C=P–PtBu$_2$ **(4)** with nBuLi in THF-d$_8$ – **Figure S46** and **S47**.

➢ from 7.55 ppm to 6.29 ppm, aromatic protons;
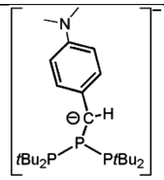 [tBu$_2$P–P–{C(H)(p-Me$_2$N-C$_6$H$_4$)}–PtBu$_2$]$^-$ **(2_4)** ➢ 4.00 ppm, dd, J_{PH} = 9.6 Hz, J_{HH} = 6.5 Hz [tBu$_2$P–P–{C(**H**)(p-Me$_2$N-C$_6$H$_4$)}–PtBu$_2$]$^-$; ➢ 2.88 ppm, s, [tBu$_2$P–P–{C(H)(p-**Me**$_2$N-C$_6$H$_4$)}–PtBu$_2$]$^-$; ➢ 2.84 ppm, s, [tBu$_2$P–P–{C(H)(p-**Me**$_2$N-C$_6$H$_4$)}–PtBu$_2$]$^-$; ➢ 1.38 ppm, d, J_{PH} = 10.1 Hz, [***t*Bu**$_2$P–P–{C(H)(p-Me$_2$N-C$_6$H$_4$)}–P***t*Bu**$_2$]$^-$; ➢ 1.24 ppm, d, J_{PH} = 9.8 Hz, [***t*Bu**$_2$P–P–{C(H)(p-Me$_2$N-C$_6$H$_4$)}–P***t*Bu**$_2$]$^-$; ➢ 1.05 ppm, d, J_{PH} = 9.8 Hz, [***t*Bu**$_2$P–P–{C(H)(p-Me$_2$N-C$_6$H$_4$)}–P***t*Bu**$_2$]$^-$; ➢ 1.05 ppm, d, J_{PH} = 10.8 Hz, [***t*Bu**$_2$P–P–{C(H)(p-Me$_2$N-C$_6$H$_4$)}–P***t*Bu**$_2$]$^-$
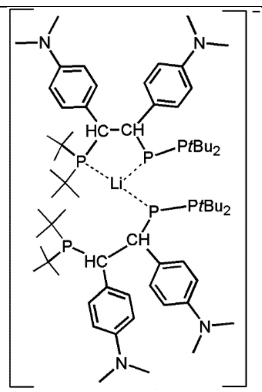 [{P(tBu)$_2$–CH(p-Me$_2$N-C$_6$H$_4$)–CH(p-Me$_2$N-C$_6$H$_4$)–P–(PtBu$_2$)}$_2$Li]$^-$ (**4c***) ➢ 3.84 ppm, broad d, J_{PH} = 10.9 Hz, [{P(tBu)$_2$–C**H**(p-Me$_2$N-C$_6$H$_4$)–CH(p-Me$_2$N-C$_6$H$_4$)–P–(PtBu$_2$)}$_2$Li]$^-$; ➢ 3.76 ppm, broad m, J_{PH} = 4.4 Hz, [{P(tBu)$_2$–CH(p-Me$_2$N-C$_6$H$_4$)–C**H**(p-Me$_2$N-C$_6$H$_4$)–P–(PtBu$_2$)}$_2$Li]$^-$; ➢ 3.69 ppm, broad d, J_{PH} = 11.5 Hz, [{P(tBu)$_2$–CH(p-Me$_2$N-C$_6$H$_4$)–CH(p-Me$_2$N-C$_6$H$_4$)–P–(PtBu$_2$)}$_2$Li]$^-$; ➢ 3.52 ppm, broad m, J_{HH} = 5.4 Hz, [{P(tBu)$_2$–C**H**(p-Me$_2$N-C$_6$H$_4$)–CH(p-Me$_2$N-C$_6$H$_4$)–P–(PtBu$_2$)}$_2$Li]$^-$; ➢ 2.90 ppm, s, [{P(tBu)$_2$–CH(p-Me$_2$N-C$_6$H$_4$)–CH(p-**Me**$_2$N-C$_6$H$_4$)–P–(PtBu$_2$)}$_2$Li]$^-$; ➢ 2.82 ppm, s, [{P(tBu)$_2$–CH(p-**Me**$_2$N-C$_6$H$_4$)–CH(p-**Me**$_2$N-C$_6$H$_4$)–P–(PtBu$_2$)}$_2$Li]$^-$; ➢ 2.78 ppm, s, [{P(tBu)$_2$–CH(p-**Me**$_2$N-C$_6$H$_4$)–CH(p-**Me**$_2$N-C$_6$H$_4$)–P–(PtBu$_2$)}$_2$Li]$^-$; ➢ 2.71 ppm, s, [{P(tBu)$_2$–CH(p-**Me**$_2$N-C$_6$H$_4$)–CH(p-**Me**$_2$N-C$_6$H$_4$)–P–(PtBu$_2$)}$_2$Li]$^-$; ➢ 1.44 ppm, J_{PH} = 10.9 Hz, [{P(tBu)$_2$–CH(p-Me$_2$N-C$_6$H$_4$)–CH(p-Me$_2$N-C$_6$H$_4$)–P–(**P***t*Bu$_2$)}$_2$Li]$^-$; ➢ 1.39 ppm, broad d, J_{PH} = 10.2 Hz, [{P(***t*Bu**)$_2$–CH(p-Me$_2$N-C$_6$H$_4$)–CH(p-Me$_2$N-C$_6$H$_4$)–P–(PtBu$_2$)}$_2$Li]$^-$; ➢ 1.28 ppm, broad d, J_{PH} = 10.8 Hz, [{P(***t*Bu**)$_2$–CH(p-Me$_2$N-C$_6$H$_4$)–CH(p-Me$_2$N-C$_6$H$_4$)–P–(PtBu$_2$)}$_2$Li]$^-$; ➢ 1.24 ppm, d, J_{PH} = 10.14 Hz, [{P(tBu)$_2$–CH(p-Me$_2$N-C$_6$H$_4$)–CH(p-Me$_2$N-C$_6$H$_4$)–P–(P***t*Bu**$_2$)}$_2$Li]$^-$; ➢ 1.23 ppm, d, J_{PH} = 10.14 Hz, [{P(***t*Bu**)$_2$–CH(p-Me$_2$N-C$_6$H$_4$)–CH(p-Me$_2$N-C$_6$H$_4$)–P–(PtBu$_2$)}$_2$Li]$^-$; ➢ 1.15 ppm, d, J_{PH} = 10.9 Hz, [{P(tBu)$_2$–CH(p-Me$_2$N-C$_6$H$_4$)–CH(p-Me$_2$N-C$_6$H$_4$)–P–(P***t*Bu**$_2$)}$_2$Li]$^-$; ➢ 0.98 ppm, d, J_{PH} = 10.0 Hz, [{P(tBu)$_2$–CH(p-Me$_2$N-C$_6$H$_4$)–CH(p-Me$_2$N-C$_6$H$_4$)–P–(P***t*Bu**$_2$)}$_2$Li]$^-$;

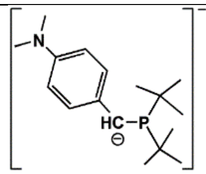

- $[(p\text{-}Me_2N\text{-}C_6H_4)(H)C–P(t\text{Bu}_2)_2]^-$ (**4c’**)

- 2.80 ppm, s, $[(p\text{-}Me_2N\text{-}C_6H_4)(H)C–\mathbf{P}(t\text{Bu}_2)_2]^-$;
- 2.86 ppm, s, $[(p\text{-}Me_2N\text{-}C_6H_4)(H)C–\mathbf{P}(t\text{Bu}_2)_2]^-$;
- 1.14 ppm, d, J_{PH} = 10.4 Hz, $[(p\text{-}Me_2N\text{-}C_6H_4)(H)C–\mathbf{P}(t\text{Bu}_2)_2]^-$;

4. NMR spectra of isolated (3,5-*t*Bu$_2$C$_6$H$_3$)(H)C=P–P*t*Bu$_2$ (**3**).

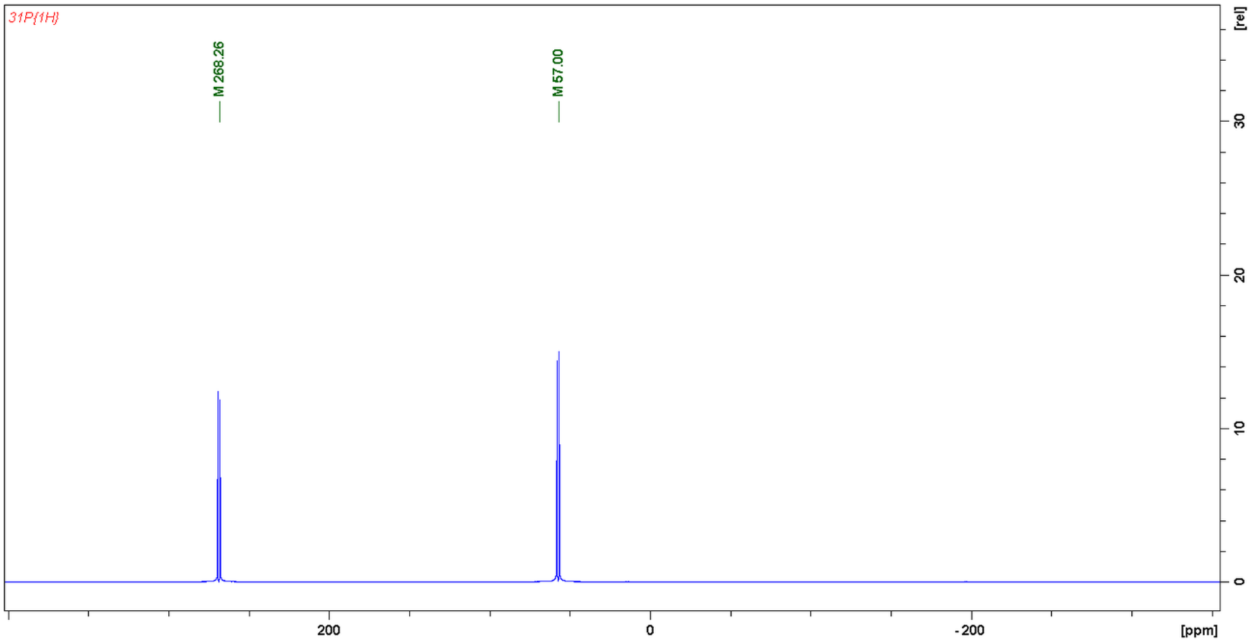

Figure S48. ^{31}P{^{1}H} NMR (400 MHz, C$_6$D$_6$, 298 K) spectrum of isolated (3,5-*t*Bu$_2$C$_6$H$_3$)(H)C=P-P*t*Bu$_2$ (**3**).

- 268.26 ppm, $J_{P\text{-}P}$ = 224.9 Hz, (3,5-*t*Bu$_2$C$_6$H$_3$)(H)C=**P**-P*t*Bu$_2$;
- 57.00 ppm, $J_{P\text{-}P}$ = 224.9 Hz, (3,5-*t*Bu$_2$C$_6$H$_3$)(H)C=P-**P***t*Bu$_2$;

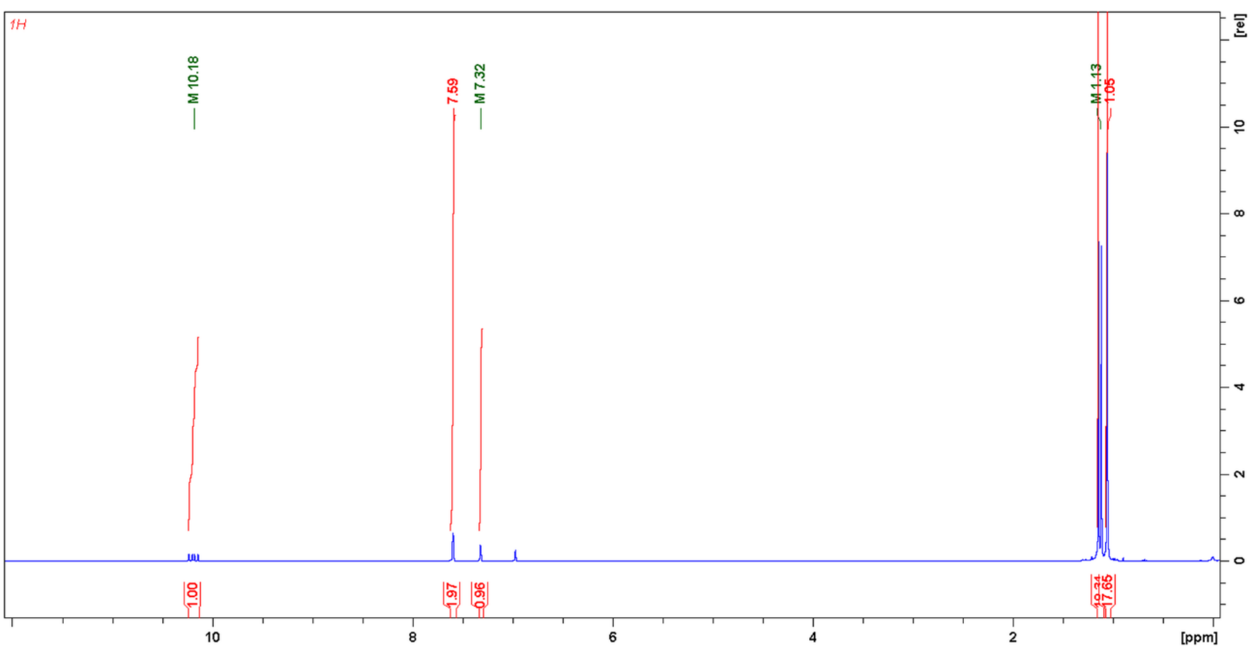

Figure S49. ^{1}H NMR (400 MHz, C$_6$D$_6$, 298 K) spectrum of isolated (3,5-*t*Bu$_2$C$_6$H$_3$)(H)C=P-P*t*Bu$_2$ (**3**)

- 10.18 ppm, dd, $J_{P\text{-}H}$ = 22.6 Hz, $J_{P\text{-}H}$ = 13.9 Hz, 1H, (3,5-*t*Bu$_2$C$_6$H$_3$)(**H**)C=P-P*t*Bu$_2$;

- 7.59 –7.32 ppm, 3H, (3,5- tBu$_2$C$_6$**H$_3$**)(H)C=P-PtBu$_2$;
- 1.13 ppm, d, $J_{P\text{-}H}$ = 11.2 Hz, 18H, (3,5- tBu$_2$C$_6$H$_3$)(H)C=P-P***t*Bu$_2$**;
- 1.05 ppm, s, 18H, (3,5-***t*Bu$_2$**C$_6$H$_3$)(H)C=P-PtBu$_2$;

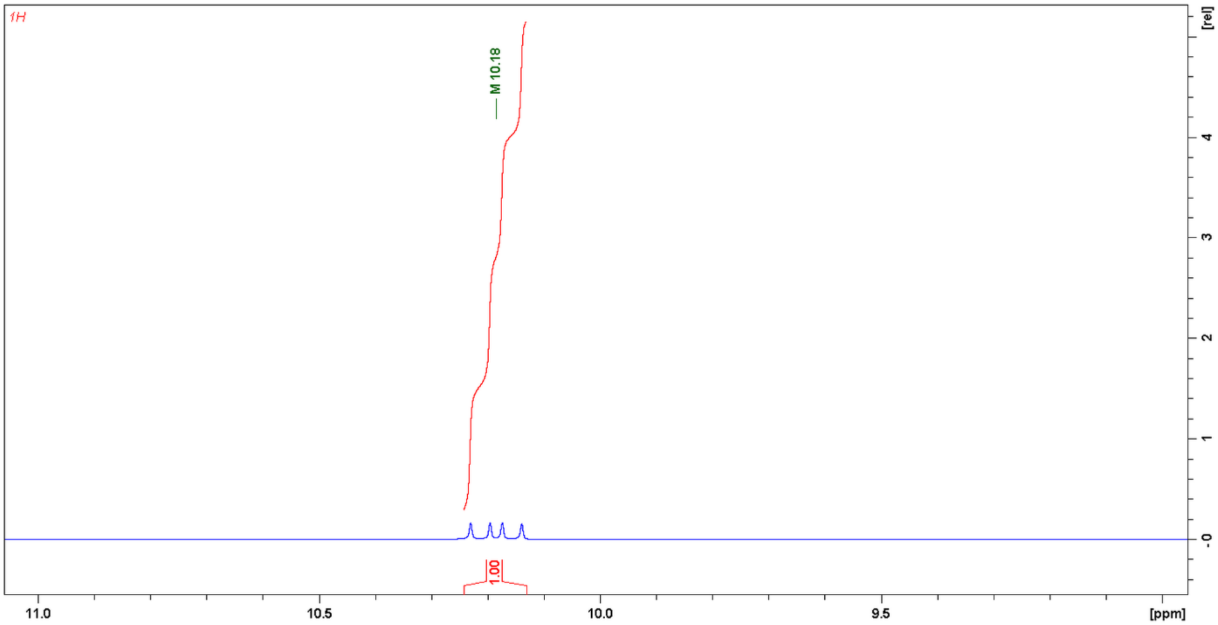

Figure S50. [1]H NMR (400 MHz, C$_6$D$_6$, 298 K) spectrum of isolated (3,5-tBu$_2$C$_6$H$_3$)(H)C=P-PtBu$_2$ (**3**) in the range from 11 ppm to 9 ppm.

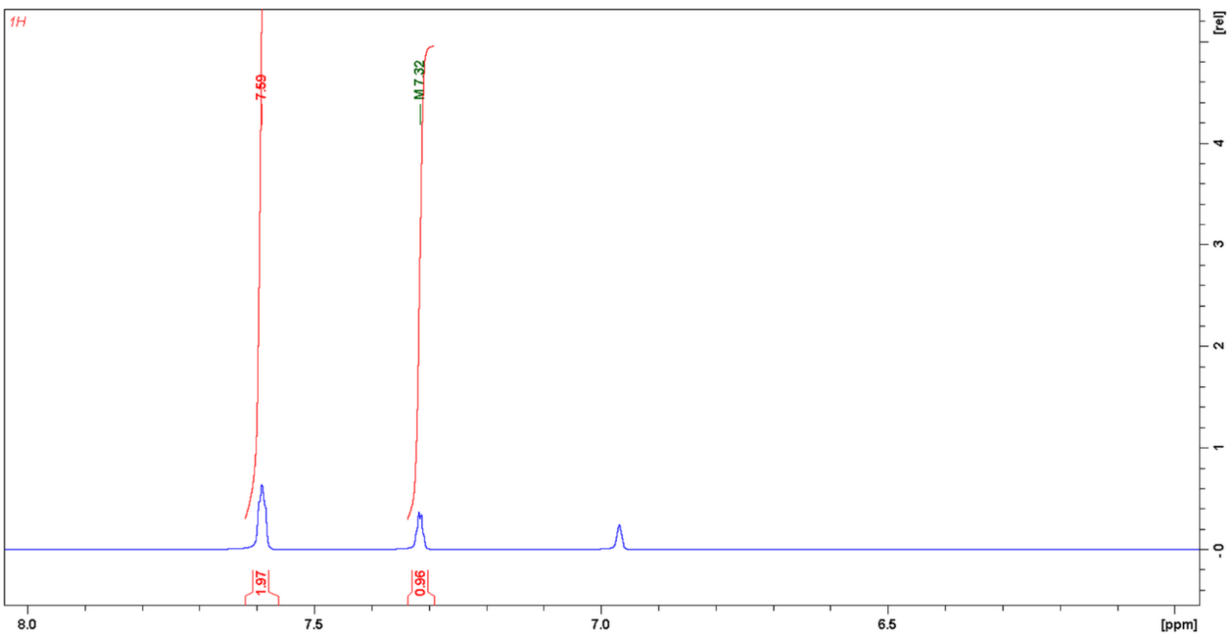

Figure S51. [1]H NMR (400 MHz, C$_6$D$_6$, 298 K) spectrum of isolated (3,5-tBu$_2$C$_6$H$_3$)(H)C=P-PtBu$_2$ (**3**) in the range from 8 ppm to 6 ppm.

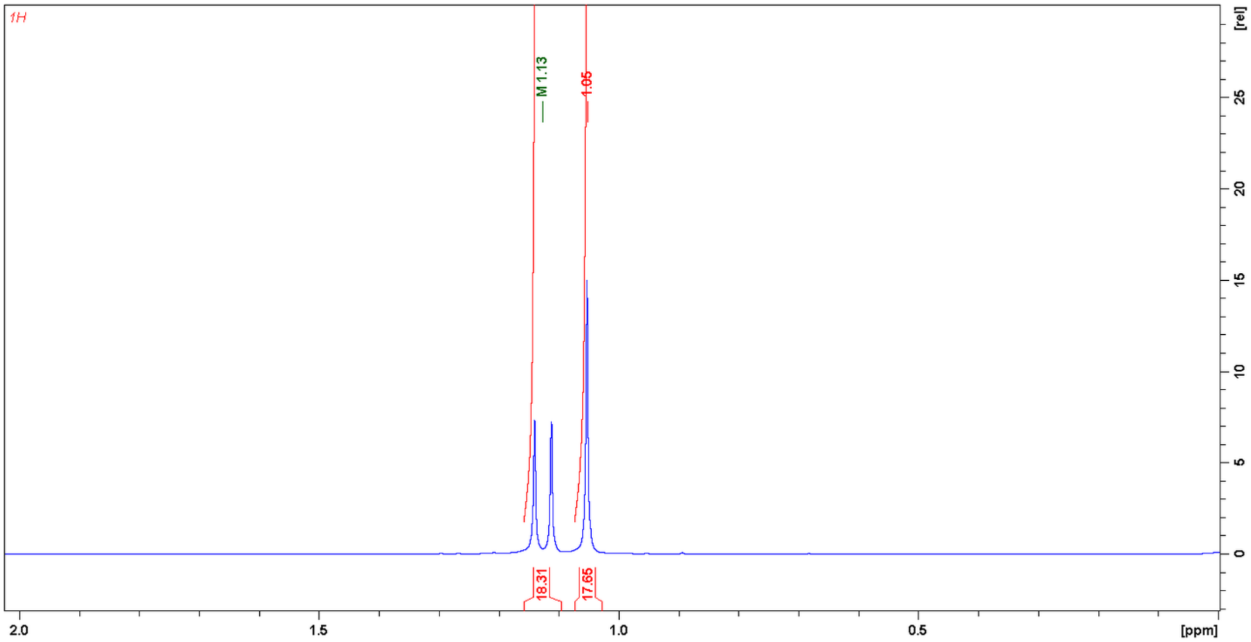

Figure S52. [1]H NMR (400 MHz, C_6D_6, 298 K) spectrum of isolated (3,5-*t*$Bu_2C_6H_3$)(H)C=P-P*t*Bu_2 (**3**) in the range from 2 ppm to 0 ppm.

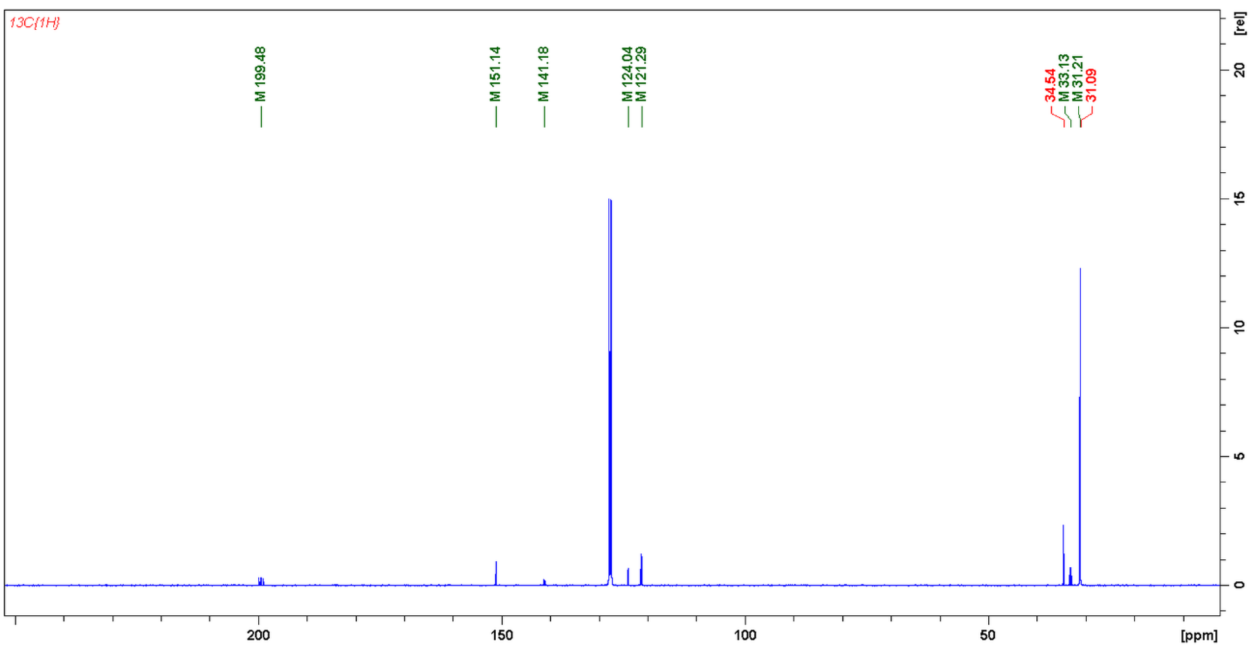

Figure S53. [13]C{[1]H} NMR (400 MHz, C_6D_6, 298 K) spectrum of isolated (3,5-*t*$Bu_2C_6H_3$)(H)C=P-P*t*Bu_2 (**3**).

- 199.48 ppm, dd, $J_{P\text{-}C}$ = 45.4 Hz, $J_{P\text{-}C}$ = 39.9 Hz (3,5-*t*$Bu_2C_6H_3$)(H)**C**=P-P*t*Bu_2;
- 151.14 ppm, d, $J_{P\text{-}C}$ = 2.7 Hz (3,5-*t*Bu_2**C_6**H_3)(H)C=P-P*t*Bu_2 (*i*-C_{Ar});
- 141.18 ppm, dd, $J_{P\text{-}C}$ = 15.4 Hz, $J_{P\text{-}C}$ = 11.8 Hz, (3,5-*t*Bu_2**C_6**H_3)(H)C=P-P*t*Bu_2 (*o*-C_{Ar});
- 124.04 ppm, d, $J_{P\text{-}C}$ = 6.3 Hz, (3,5-*t*Bu_2**C_6**H_3)(H)C=P-P*t*Bu_2 (*m*-C_{Ar});
- 121.29 ppm, d, $J_{P\text{-}C}$ = 19.9 Hz, (3,5-*t*Bu_2**C_6**H_3)(H)C=P-P*t*Bu_2 (*p*-C_{Ar});
- 34.54 ppm, s, (3,5-{**C**$(CH_3)_3\}_2C_6H_3$)((H)C=P-P*t*Bu_2;

- 33.13 ppm, dd, J_{P-C} = 27.2 Hz, J_{P-C} = 1.8 Hz (3,5-*t*$Bu_2C_6H_3$)((H)C=P-P{**C**$(CH_3)_3$}$_2$;
- 31.21 ppm, dd, J_{P-C} = 13.6 Hz, J_{P-C} = 4.5 Hz (3,5-*t*$Bu_2C_6H_3$)(H)C=P-P{C(**C**$H_3)_3$}$_2$;
- 31.09 ppm, s, (3,5-{C(**C**$H_3)_3$}$_2C_6H_3$)(H)C=P-P*t*Bu_2;

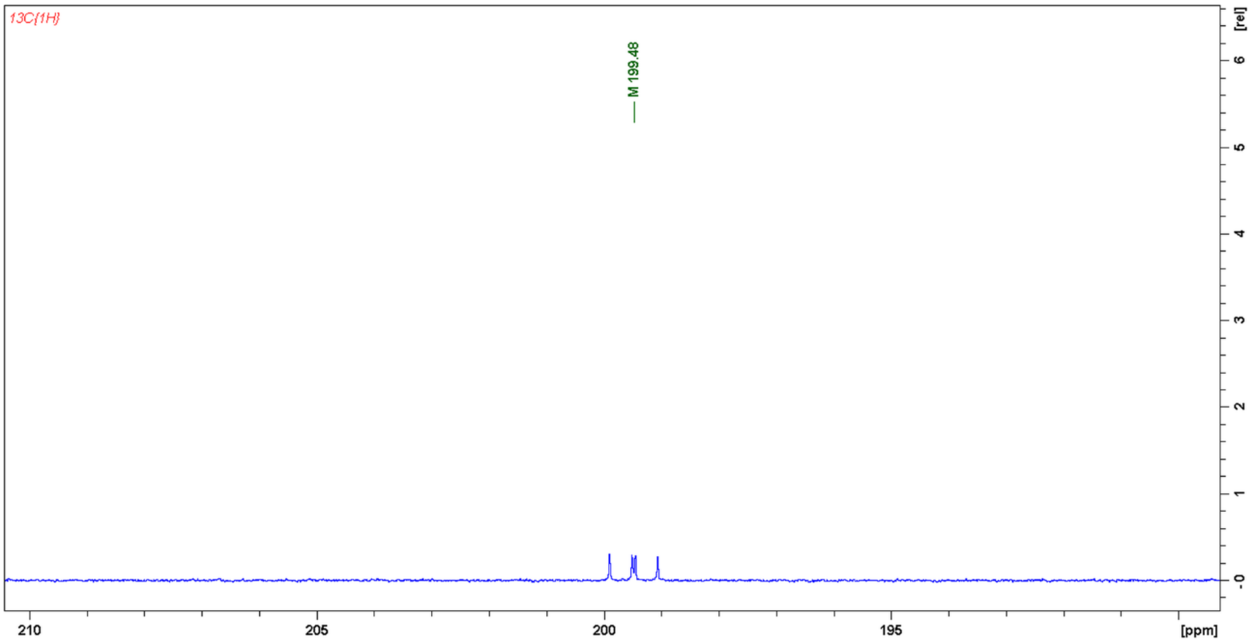

Figure S54. $^{13}C\{^1H\}$ NMR (400 MHz, C_6D_6, 298 K) spectrum of isolated (3,5-*t*$Bu_2C_6H_3$)(H)C=P-P*t*Bu_2 (**3**) in the range from 210 ppm to 190 ppm.

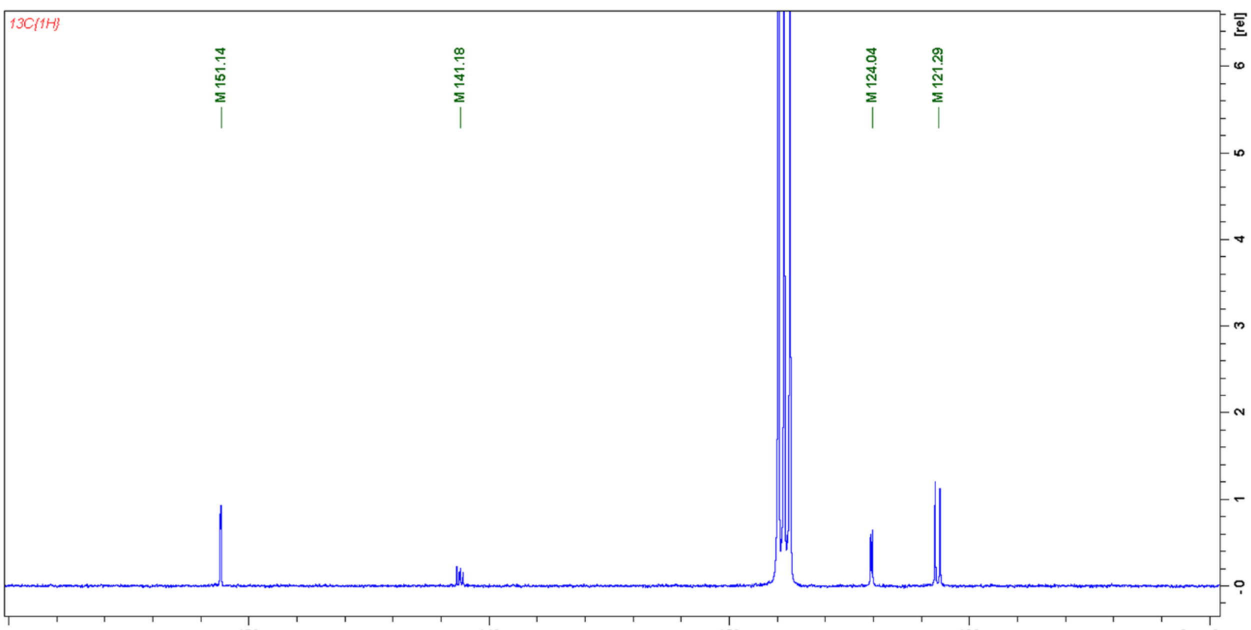

Figure S55. $^{13}C\{^1H\}$ NMR (400 MHz, C_6D_6, 298 K) spectrum of isolated (3,5-*t*$Bu_2C_6H_3$)(H)C=P-P*t*Bu_2 (**3**) in the range from 160 ppm to 110 ppm.

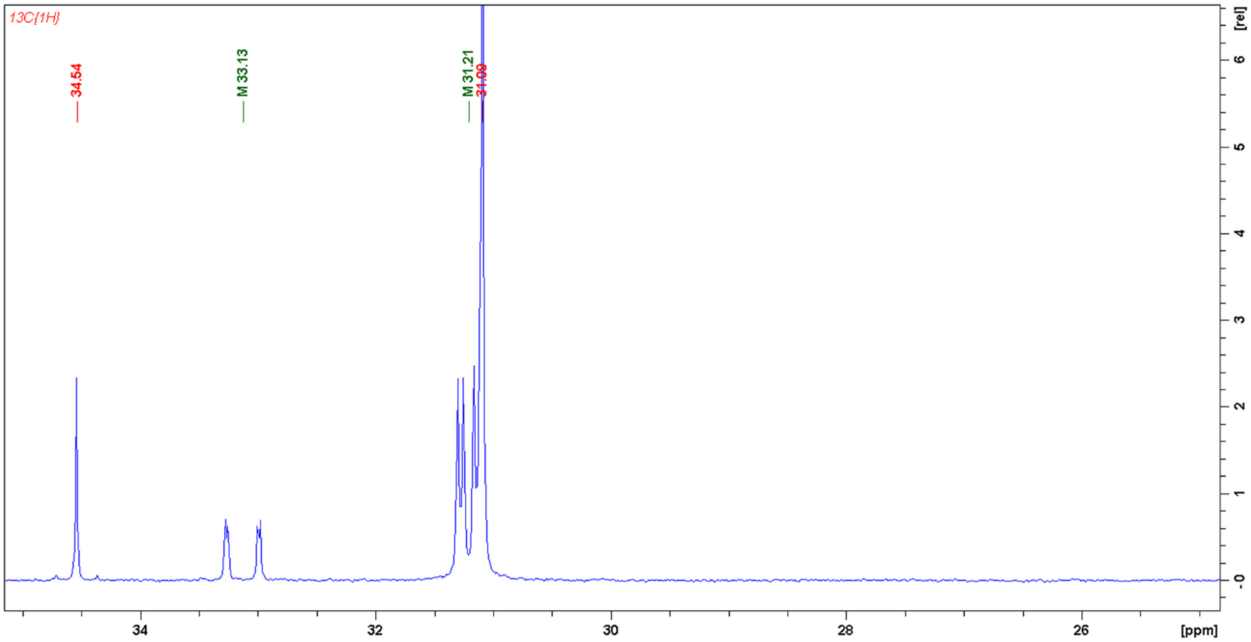

Figure S56. $^{13}C\{^1H\}$-NMR (400 MHz, C_6D_6, 298 K) spectrum of isolated (3,5-tBu$_2$C$_6$H$_3$)(H)C=P-PtBu$_2$ (**3**) in the range from 35 ppm to 25 ppm.

PART C. DFT calculation details

D.1. General methods

All calculations presented in the paper were performed using the Gaussian 09[3] program package. Molecular geometries of all compounds were optimized using density functional theory at the TPSSTPSS functional by Tao *et al*[4] with 6-31+G(d,p) basis set. The TPSSTPSS exchange-correlation functional has been chosen, as it has good overall performance for the description of kinetic and thermodynamic parameters of reactions. By adding GD3BJ keyword that includes D3 version of Grimme dispersion with Becke-Johnson[5] damping into calculations it also accounts well for long-range and dispersion interactions. Molecular geometries were energy-optimized and the most stable (the lowest energy) conformer was identified during the potential energy surface scanning. Nature of the final gas-phase geometries as local minima (no imaginary frequencies) on the potential energy surface was then validated by harmonic frequency calculations at the same level of theory. Values of calculated energies, enthalpies and Gibbs free-energies derived from thermochemical calculations were corrected for the zero-point energy (ZPE).

Table S28. Selected computational parameters obtained for considered systems (in atomic units A.U.): $\boldsymbol{\varepsilon_0}$ - electronic energy; $\boldsymbol{\varepsilon_{0 + ...}}$ - sum of electronic and: $\mathbf{E_{zpe}}$ - zero-point energies, $\mathbf{E_{therm}}$ - thermal energies, **H** – thermal enthalpies, **G** - thermal free energies calculated at TPSSTPSS//6-31+G(d,p) [TPSSTPSS//LANL2DZ for Ti] level of theory. Values of $\mathbf{\Delta H^o_{298K/273K/253K}}$ and $\mathbf{\Delta G^o_{298K/273K/253K}}$ were calculated as the difference between energy of products and substrates along the reaction path.

Compound	E_{electr} [A.U.]	$\varepsilon_0 + E_{ZPE}$ [A.U.]	$\varepsilon_0 + E_{therm}$ [A.U.]	ε_0 + H [A.U.]	ε_0 + G [A.U.]
(biph)(H)C=P–P*t*Bu_2	-2756.748730	-2755.870773	-2755.818193	-2755.817249	-2755.952186
$[Me]^-$	-576.804227	-576.615676	-576.604657	-576.603713	-576.653632
1a	-575.607850	-575.440898	-575.431082	-575.430138	-575.476274
$[tBu_2P]^-$	-669.067353	-668.880585	-668.867673	-668.866729	-668.921430
2a	-761.329100	-761.144129	-761.129331	-761.128386	-761.187795
3a	-805.909108	-805.656488	-805.640181	-805.639237	-805.701418
4	-502.981595	-502.762110	-502.749873	-502.748929	-502.801997
3a'	-4853.591621	-4852.204228	-4852.117211	-4852.116267	-4852.338227

D.2. Thermodynamics of considered reactions

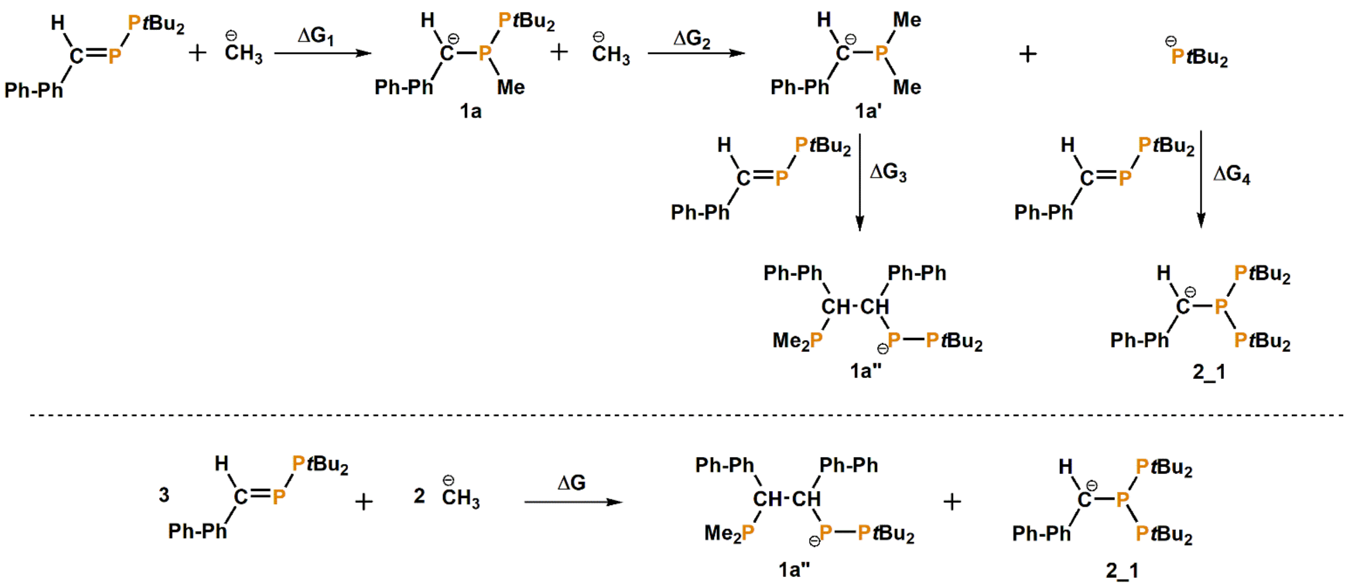

Scheme S1. Reaction of (biph)(H)C=P-PtBu$_2$ with Me$^-$ along with consecutive steps leading to formation of **3a** and **4**.

Table S29. Values of **ΔH^o_{298K}, ΔG^o_{298K}** and **K_{298K}** calculated as the difference between energy of products and substrates along the assumed reaction path (consecutive steps of formation of **1a″** and **2_1**).

Reaction Step	ΔH^o_{298K} [kcal mol^{-1}]	ΔG^o_{298K} [kcal mol^{-1}]	K_{298K}
1	-75.45	-62.72	1.20E+45
2	-36.09	-38.34	5.25E+06
3	-34.34	-18.43	1.70E+03
4	-49.05	-33.76	8.27E+05
Total	-194.93	-153.25	7.29E+26

D.3. Electrostatic potential map and Mulliken atomic charges of 1a*

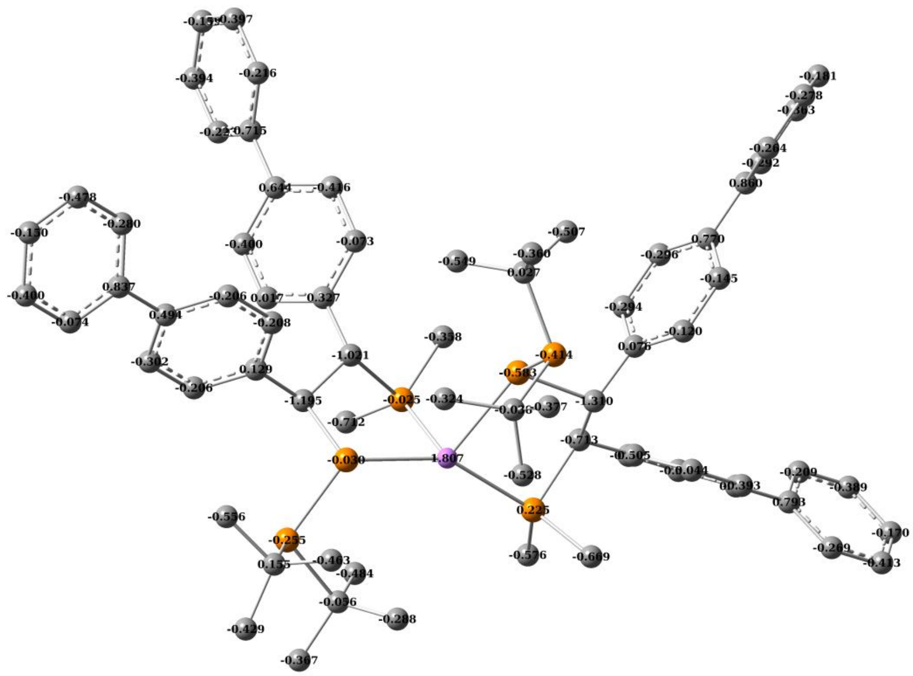

Figure S57. Optimized molecular structure of **1a*** together with charge distribution (Mulliken atomic charges).

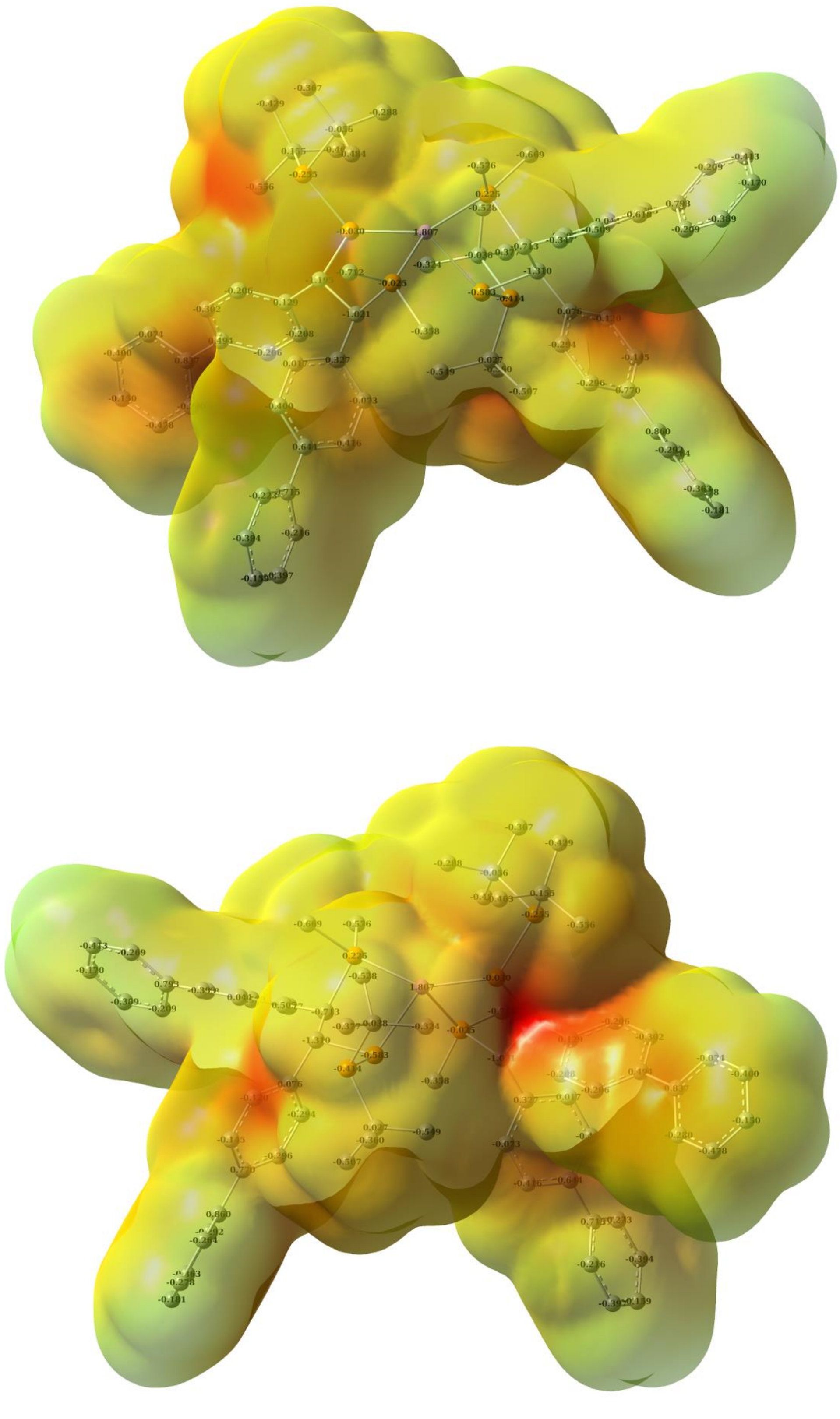

Figure S58. Electron density surface (isovalue = 0.004 e/Å^3) mapped with electrostatic potential for compound **1a***. The red areas correspond to the negative electrostatic potential and the blue areas to the positive ones (two representations along with Mullikan atomic charges).

D.4. Optimized structures and Cartesian coordinates

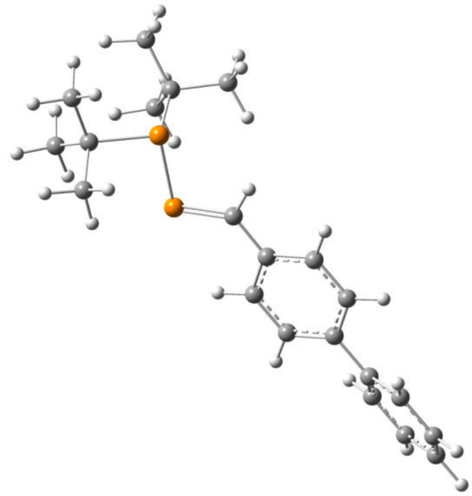

Figure S59. Optimized structure of (biph)(H)C=P–P*t*Bu$_2$.

Below are presented xyz coordinates for optimized geometry of (biph)(H)C=P–P*t*Bu$_2$:

C	0.45889400	-0.07821200	-0.58654700
C	-0.98594700	-0.06679300	-0.39822600
C	-1.60711700	-0.35256000	0.84380300
H	-0.98457200	-0.58872700	1.70579200
C	-2.99198300	-0.34515000	0.97155300
H	-3.44204300	-0.59658700	1.93038600
C	-3.83038100	-0.04730200	-0.13014700
C	-3.21577600	0.24329200	-1.36679300
H	-3.83348500	0.50634400	-2.22365500
C	-1.82679900	0.23461500	-1.49713600
H	-1.37346000	0.47125800	-2.45922900
C	-5.30456400	-0.03690800	0.01340700
C	-5.91389600	0.41234600	1.20521400
H	-5.29118300	0.78221200	2.01801300
C	-7.30680900	0.42284500	1.33980500
H	-7.75603600	0.78328900	2.26362700
C	-8.12195100	-0.01638100	0.28623700
H	-9.20519000	-0.00873200	0.39125400
C	-7.53052300	-0.46619200	-0.90348600
H	-8.15384500	-0.81934600	-1.72320700
C	-6.13772000	-0.47621700	-1.03847900
H	-5.68754700	-0.85474200	-1.95463300
C	3.91848800	1.67445200	0.01611000
C	3.67210700	1.92750100	1.51705900
H	4.26786600	1.26767800	2.15527000
H	3.94301200	2.96755700	1.75737900
H	2.61429000	1.78888500	1.77680100
C	3.01715700	2.63395800	-0.79636400
H	1.95359300	2.44664400	-0.59739100
H	3.23625800	3.67325200	-0.50789700
H	3.19038700	2.52912900	-1.87493600
C	5.39286900	1.96722400	-0.32797300
H	6.07945300	1.39191000	0.30454600
H	5.61635500	1.74477300	-1.37982000
H	5.59918900	3.03464200	-0.15602200
C	4.63738700	-1.39706100	0.06790500
C	5.92037500	-1.40293900	-0.79565100
H	5.67820300	-1.51344400	-1.86040200
H	6.50954100	-0.48819300	-0.67174900
H	6.55415500	-2.25232700	-0.49821300

C	3.91496600	-2.74803700	-0.15193900
H	3.59025900	-2.86444200	-1.19463700
H	4.60440400	-3.57164000	0.08727300
H	3.03250400	-2.84718500	0.49433100
C	5.00224900	-1.25493700	1.55660200
H	5.60525100	-0.35817200	1.74231200
H	4.10645800	-1.21033100	2.18912300
H	5.59780400	-2.12528600	1.87364300
P	1.63495300	-0.48819400	0.58703300
P	3.44469000	-0.07534800	-0.65005100
H	0.78757700	0.19946600	-1.59241900

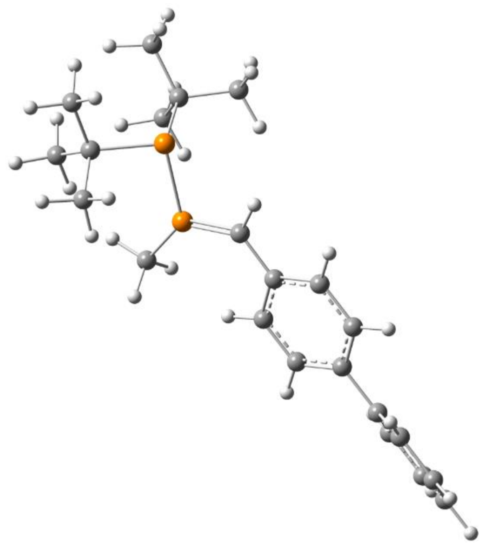

Figure S60. Optimized structure of **1a**.

Below are presented xyz coordinates for optimized geometry of **1a**:

C	0.36445200	-1.37394000	0.89495700
C	-0.96986700	-0.97956000	0.63507600
C	-1.44955300	0.37472700	0.73194300
H	-0.74339100	1.15374700	1.02000200
C	-2.77172600	0.71129900	0.49056200
H	-3.06667800	1.75406600	0.61566900
C	-3.75770900	-0.25043500	0.12565300
C	-3.29222600	-1.59176300	0.01766000
H	-3.98523100	-2.37367100	-0.29648600
C	-1.97104100	-1.94093300	0.25043500
H	-1.66558400	-2.98244400	0.13159900
C	-5.15088700	0.11526200	-0.12700600
C	-5.53502600	1.44722400	-0.45612600
H	-4.76556100	2.21099500	-0.55466400
C	-6.86762000	1.79634200	-0.68969800
H	-7.10994400	2.82902200	-0.94515500
C	-7.89085300	0.83380700	-0.61966900
H	-8.92894300	1.10618300	-0.80637800
C	-7.53720100	-0.48992700	-0.30203600
H	-8.31047800	-1.25629000	-0.22945000
C	-6.20667000	-0.83895800	-0.05660200
H	-5.97452300	-1.86556200	0.22210700
C	3.83944900	1.80996400	0.12752500
C	4.56764200	1.53230900	1.45811400
H	5.27517900	0.69929600	1.37593400
H	5.13374900	2.42788400	1.76856700
H	3.84458000	1.30083000	2.25029300

C	2.82650000	2.95707100	0.36210600
H	2.06028600	2.65685900	1.08819800
H	3.35384100	3.84282300	0.75524500
H	2.32336200	3.23541100	-0.57289100
C	4.85946300	2.27679800	-0.93045100
H	5.66396300	1.54476000	-1.07739700
H	4.37406400	2.45713300	-1.89896400
H	5.32650900	3.22069200	-0.60038900
C	3.89907300	-1.02130600	-1.23152400
C	4.30980100	-0.64509300	-2.67592200
H	3.42524300	-0.41837400	-3.28433900
H	4.97477300	0.22592900	-2.70387400
H	4.84379200	-1.49231700	-3.14124500
C	2.99263200	-2.27044600	-1.31845900
H	2.04702400	-2.04131200	-1.82643300
H	3.51147500	-3.06340600	-1.88303400
H	2.74466400	-2.66093500	-0.32618900
C	5.16206000	-1.36165600	-0.41977900
H	5.87062900	-0.52375100	-0.40010500
H	4.91810500	-1.63051700	0.61307300
H	5.67982700	-2.22024000	-0.88206800
P	1.66304700	-0.26462400	1.36657800
P	2.75047800	0.37101200	-0.55301100
H	0.61665700	-2.42404000	0.71720600
C	2.79952400	-1.45903700	2.27209200
H	2.31873700	-1.68165900	3.23369500
H	2.93849100	-2.40795900	1.73610400
H	3.78120900	-1.00947500	2.46473700

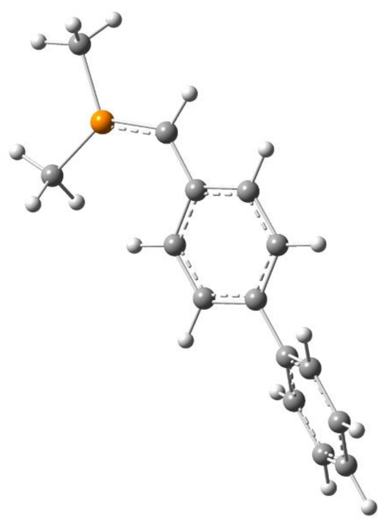

Figure S61. Optimized structure of **1a'**.

Below are presented xyz coordinates for optimized geometry of **1a'**:

C	2.89225800	-0.63998100	0.12048000
C	1.49442800	-0.44959900	0.08286400
C	0.84217100	0.81059300	-0.18564100
H	1.46814000	1.67900900	-0.39065900
C	-0.53551100	0.94477100	-0.20504200
H	-0.94839700	1.92629100	-0.44307400
C	-1.42619200	-0.14617100	0.02624700
C	-0.79368100	-1.39694700	0.28670000
H	-1.40888800	-2.27134300	0.50481800
C	0.58304900	-1.54487700	0.31933200

H	1.00800800	-2.52491100	0.54639600
C	-2.87740400	0.00711000	-0.00020600
C	-3.50893600	1.28045800	0.12543900
H	-2.89217100	2.16506400	0.27436700
C	-4.89778300	1.42632300	0.09511200
H	-5.32924700	2.42306300	0.20169100
C	-5.74207800	0.31015900	-0.05111200
H	-6.82526400	0.42479200	-0.07038200
C	-5.14546000	-0.95849700	-0.17210800
H	-5.77189900	-1.84327700	-0.29795200
C	-3.75661100	-1.10629100	-0.15343100
H	-3.33379300	-2.10094500	-0.28474400
P	4.12114200	0.62690200	-0.13904500
H	3.24751900	-1.65709700	0.33280900
C	5.25370800	0.39814400	1.35689600
H	4.73421000	0.75955700	2.25302500
H	5.50595800	-0.66392500	1.50602900
H	6.18533400	0.97229100	1.23504600
C	5.28514900	-0.20058500	-1.37605300
H	5.53168100	-1.22819200	-1.06420700
H	4.79026500	-0.24514100	-2.35414100
H	6.21877900	0.37358000	-1.48019400

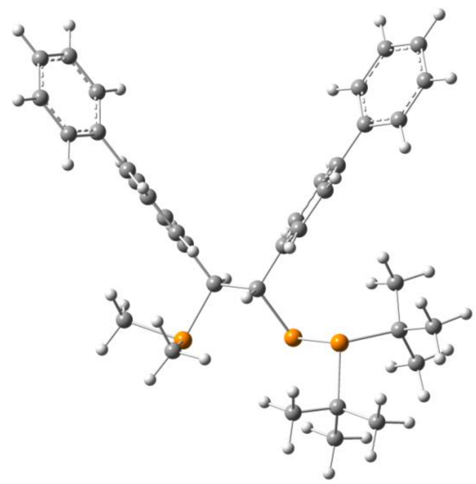

Figure S62. Optimized structure of **3a**.

Below are presented xyz coordinates for optimized geometry of **3a**:

C	0.23907600	-4.17709100	0.71583200
H	-0.67200200	-3.83944900	1.23044900
H	1.11830200	-3.70116700	1.16291700
H	0.33205500	-5.26354300	0.84672100
C	-1.49289500	-4.56909800	-1.45510800
H	-1.37876700	-5.66155800	-1.41950000
H	-1.82830600	-4.30062700	-2.46530200
H	-2.26728600	-4.26437500	-0.73724400
C	4.71865200	0.81443900	-0.15970400
C	5.72924400	0.40358100	-1.24421100
H	6.13562900	1.30195800	-1.74184600
H	5.23978900	-0.21788900	-2.00636500
H	6.57771500	-0.15339800	-0.82548000
C	5.42113600	1.61885800	0.95665900
H	6.22844800	1.05614200	1.43897500
H	4.69962000	1.91146000	1.73163000
H	5.86125000	2.53818100	0.53286600
C	3.66406000	1.73766400	-0.80601100
H	4.16263000	2.63591100	-1.20865100

H	2.91069400	2.06015500	-0.07603400
H	3.14196900	1.21765200	-1.61810800
C	4.96575700	-2.06697500	1.03029700
C	5.50635600	-2.83924000	-0.18996300
H	6.16064900	-2.22057500	-0.81403700
H	4.67052700	-3.19539200	-0.80765900
H	6.08972300	-3.71337000	0.15029000
C	6.14034700	-1.56096300	1.88935900
H	6.70707100	-2.42044900	2.28710900
H	5.78641600	-0.96241500	2.74055000
H	6.83930900	-0.95056000	1.30349900
C	4.13171300	-3.05463900	1.87756700
H	3.28384100	-3.42336100	1.28535800
H	3.74331700	-2.57246200	2.78534700
H	4.75439300	-3.91613400	2.17397000
C	0.79957000	-1.16345700	-0.27006900
H	0.78178000	-1.53315600	0.76494400
C	0.50803400	0.31360000	-0.23340900
C	0.24756700	1.05969900	-1.40284400
H	0.27177500	0.55443400	-2.36746800
C	0.01762100	2.43293100	-1.35270800
H	-0.14858200	2.98013400	-2.28056800
C	0.05471300	3.14003200	-0.12597000
C	0.31913100	2.39616500	1.04301800
H	0.32801500	2.90038400	2.00944200
C	0.52953400	1.01531700	0.99010200
H	0.73692400	0.46425600	1.90621400
C	-0.17072300	4.59998500	-0.07350400
C	-1.05872200	5.23920400	-0.97037200
H	-1.60438900	4.63575700	-1.69405200
C	-1.27090700	6.62164300	-0.92187500
H	-1.96710700	7.08344800	-1.62184900
C	-0.60669000	7.41036500	0.03076800
H	-0.77265700	8.48611000	0.07004000
C	0.27676100	6.79278000	0.93021400
H	0.81092200	7.39185500	1.66745300
C	0.49480800	5.41155500	0.87528700
H	1.21058900	4.95160700	1.55461600
C	-0.24963900	-1.94490500	-1.10136200
H	-0.13098300	-1.66388300	-2.15961100
C	-1.67351800	-1.66470900	-0.69642100
C	-2.06457300	-1.54460200	0.65335500
H	-1.30716700	-1.58955400	1.43271500
C	-3.39799500	-1.32181700	1.00685300
H	-3.65705500	-1.19816800	2.05795500
C	-4.40448800	-1.19741900	0.02616800
C	-4.01468000	-1.30067200	-1.32594900
H	-4.76825300	-1.22410700	-2.10944700
C	-2.68127500	-1.52956100	-1.67293000
H	-2.40733900	-1.61099500	-2.72511200
C	-5.81731300	-0.95503600	0.40191200
C	-6.37493000	-1.54330400	1.55880500
H	-5.75874000	-2.20403700	2.16654300
C	-7.70888800	-1.31375900	1.91619300
H	-8.11534300	-1.78509100	2.81040200
C	-8.52433800	-0.49324900	1.12223600
H	-9.56238100	-0.31520300	1.39907900
C	-7.98620200	0.09731600	-0.03114500
H	-8.60396800	0.74708100	-0.65008800
C	-6.65042200	-0.12815300	-0.38399400
H	-6.23404200	0.36164700	-1.26270400
P	2.54983200	-1.52799800	-1.01455600
P	3.70600000	-0.64495800	0.62748200
P	0.20454800	-3.81345500	-1.11695300

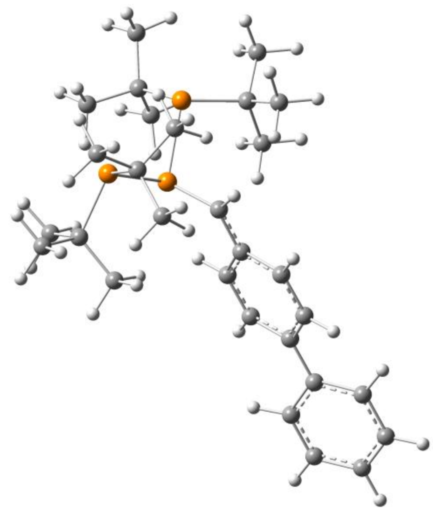

Figure S63. Optimized structure of **2_1**.

Below are presented xyz coordinates for optimized geometry of **2_1**:

C	-3.41326500	-2.19673800	1.42844600
C	-3.93380800	-0.92661300	2.13692800
H	-4.44786300	-1.22000200	3.06764000
H	-4.63614100	-0.36496100	1.50880600
H	-3.11012600	-0.25380200	2.40063200
C	-2.36044800	-2.85431900	2.33715300
H	-1.46821100	-2.22006700	2.41688000
H	-2.05910200	-3.84248100	1.96857400
H	-2.77894500	-2.99095400	3.34889400
C	-4.62286100	-3.14097500	1.23712400
H	-4.34355700	-4.09641800	0.78028900
H	-5.38614600	-2.67018400	0.60336400
H	-5.07614000	-3.35747000	2.21936700
C	-1.64020300	-3.02184000	-1.00352800
C	-0.27869400	-3.22813600	-0.30737800
H	0.28409100	-4.00631600	-0.85021200
H	-0.39075400	-3.55972000	0.72929700
H	0.31932700	-2.31220900	-0.32240800
C	-2.40952400	-4.36040200	-1.02053600
H	-3.40956100	-4.24908600	-1.46239200
H	-2.51648100	-4.78404000	-0.01405000
H	-1.84614500	-5.08835800	-1.62741100
C	-1.38297800	-2.60425700	-2.47163500
H	-0.80816400	-3.39574100	-2.98034400
H	-0.79661900	-1.67915000	-2.50968800
H	-2.32688400	-2.45359000	-3.01358300
C	-0.02512000	0.11766600	-0.93671300
H	-0.28788500	0.32696000	-1.97424300
C	1.36403600	0.05803300	-0.64815600
C	2.33645500	0.28109000	-1.68459500
H	1.97476700	0.51387300	-2.68803500
C	3.70216900	0.23042100	-1.44962400
H	4.37819000	0.44183900	-2.27914300
C	4.24278500	-0.03909800	-0.16149500
C	3.29035900	-0.26120000	0.87064800
H	3.64034500	-0.51012600	1.87330800

C	1.92147000	-0.22383700	0.64721700
H	1.23753500	-0.42716600	1.47188800
C	5.68653000	-0.08589700	0.08426800
C	6.61867000	-0.34232000	-0.95950000
H	6.24800700	-0.54078200	-1.96381500
C	7.99619300	-0.38021300	-0.72563700
H	8.67242100	-0.58675800	-1.55623900
C	8.51394800	-0.17663600	0.56529800
H	9.58722100	-0.21095900	0.74797400
C	7.61229600	0.07222400	1.61476800
H	7.98749000	0.24462400	2.62434500
C	6.23536600	0.12240100	1.38017300
H	5.56656300	0.35349700	2.20754900
C	-1.68323100	2.92375900	1.32188700
C	-2.28172200	4.34276000	1.22598400
H	-1.84248700	4.97705800	2.01362000
H	-3.37171300	4.32953800	1.36558300
H	-2.06060600	4.81570400	0.26124300
C	-0.15958100	2.98244700	1.08894000
H	0.28873700	3.67708900	1.81995700
H	0.09904600	3.33132300	0.08524700
H	0.30531100	1.99956200	1.22610600
C	-1.92866300	2.39677500	2.75647900
H	-1.51132500	1.38831000	2.87433300
H	-3.00073700	2.36268600	2.99330500
H	-1.43031300	3.06128100	3.48115200
C	-2.68318700	2.40873700	-1.60105000
C	-3.86341200	3.40594800	-1.70693800
H	-3.71233700	4.29618100	-1.08559000
H	-4.80506000	2.93164400	-1.40051400
H	-3.96620000	3.73929600	-2.75362700
C	-1.39099400	3.09069000	-2.08792700
H	-1.48321600	3.32149000	-3.16309900
H	-0.51928100	2.44493600	-1.94093800
H	-1.21378800	4.03811500	-1.56296600
C	-3.01714900	1.20844400	-2.51498100
H	-3.90800200	0.67311800	-2.16272900
H	-2.19729800	0.48475100	-2.55680800
H	-3.20791400	1.57426100	-3.53761200
P	-2.79730300	-1.63658900	-0.31867600
P	-1.27510100	-0.03636100	0.31041300
P	-2.68377500	1.71959800	0.19642100

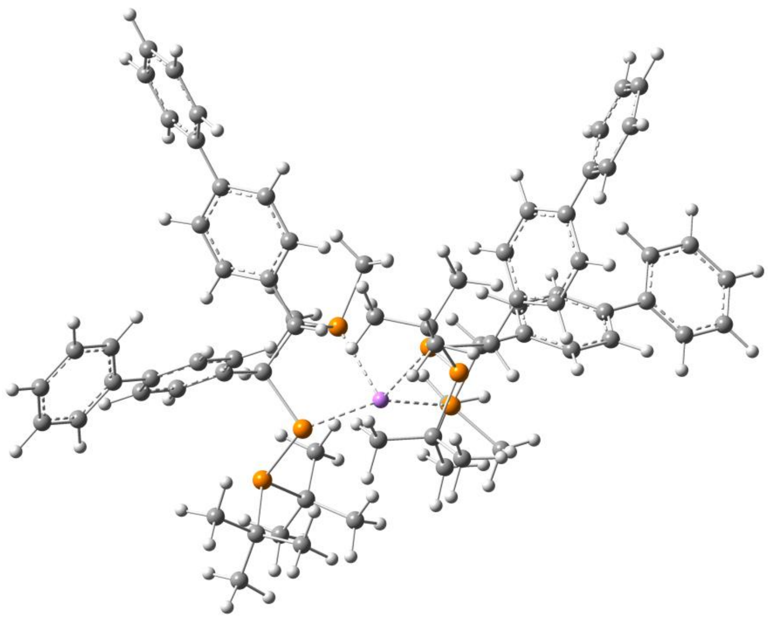

Figure S64. Optimized structure of **1a***.

Below are presented xyz coordinates for optimized geometry of **1a***:

C	-0.11508700	-1.67252000	4.02381400
C	-1.03406800	-0.73567800	-3.71240300
H	-1.51934300	0.16191100	-4.11917300
H	-1.73374800	-1.57743000	-3.74263900
H	-0.17024100	-0.99017000	-4.34033200
C	0.54897300	1.09628900	-2.23288800
H	1.45317600	0.84360900	-2.80403500
H	0.85127300	1.47579700	-1.24868200
H	-0.01447700	1.86724100	-2.77393200
C	0.43619300	-2.93758500	3.33258300
H	-0.05065100	-3.83139500	3.75380700
H	1.52198500	-3.03064700	3.48269200
H	0.24236500	-2.91160800	2.25310700
C	2.75997900	-3.48480600	-2.18083300
H	3.85257200	-3.53420600	-2.27385300
H	2.35662800	-2.83935300	-2.97072400
H	2.33312800	-4.48615700	-2.31612000
C	0.11891800	-1.83572400	5.54484300
H	-0.26134700	-0.98201000	6.11691300
H	1.18923600	-1.94359300	5.76758400
H	-0.40312500	-2.73822600	5.90378400
C	-1.61984400	-1.56403800	3.72918100
H	-2.12772600	-2.49011100	4.04630600
H	-1.81448500	-1.43879300	2.65673700
H	-2.08231000	-0.73413500	4.27823100
C	0.06523400	1.44355500	3.75442000
C	-0.34070600	1.55854900	5.23675300
H	0.50725200	1.34144300	5.90112100
H	-1.16374000	0.87858700	5.48964600
H	-0.68356700	2.58514700	5.44571600
C	-1.15971200	1.69670300	2.85335200
H	-1.96934500	0.98400300	3.04087800
H	-0.86295100	1.61869700	1.79895200
H	-1.55049400	2.71341700	3.02825400
C	1.12384900	2.52863400	3.44621300
H	0.68297900	3.52806000	3.59610600
H	1.46748100	2.44864200	2.40653000

H	1.99884200	2.42962200	4.10152800
C	2.90061400	-0.59912200	1.01368700
H	3.19685200	-1.33574400	1.77299200
C	3.67565200	0.66835800	1.26733400
C	3.73380800	1.71348200	0.32209700
H	3.22517900	1.59887200	-0.63371100
C	4.39990600	2.90610500	0.60113100
H	4.40182500	3.70378000	-0.14120400
C	5.03045000	3.11652300	1.84949100
C	4.97303300	2.07207400	2.79377000
H	5.47160500	2.19047200	3.75556300
C	4.31847600	0.87081300	2.50398600
H	4.27844600	0.08104600	3.25233100
C	5.72444500	4.38896400	2.15317000
C	6.42991800	5.09447400	1.15263100
H	6.48360100	4.67746900	0.14818300
C	7.08348700	6.29860600	1.43987800
H	7.62591200	6.81814100	0.65059400
C	7.05503700	6.82878200	2.73876600
H	7.56429900	7.76485400	2.96308300
C	6.36036900	6.13963800	3.74455400
H	6.31892600	6.54547200	4.75479200
C	5.70128400	4.93927600	3.45452200
H	5.13689000	4.43078100	4.23452800
C	3.13939700	-1.18964200	-0.39925000
H	2.60977600	-0.56421800	-1.13462900
C	4.58791700	-1.28316500	-0.81024900
C	4.97059200	-1.01370500	-2.13871200
H	4.20672700	-0.72105000	-2.85948500
C	6.30225300	-1.11531900	-2.55025300
H	6.55928400	-0.92164800	-3.59102400
C	7.31349800	-1.49279700	-1.64247200
C	6.93381100	-1.75449700	-0.30919000
H	7.69819100	-2.00259400	0.42606800
C	5.60135700	-1.64870500	0.09799300
H	5.34707200	-1.81633400	1.14245000
C	3.17216100	-3.94752300	0.60269900
H	2.76543500	-4.96286400	0.51585000
H	3.04080600	-3.61879800	1.63943500
H	4.24098900	-3.96210200	0.35191500
C	8.72876000	-1.60105500	-2.07197200
C	9.27320300	-0.70643900	-3.01885000
H	8.64904000	0.09293900	-3.41492400
C	10.60828800	-0.81170900	-3.42658800
H	11.00718200	-0.10355800	-4.15167700
C	11.43480700	-1.81198400	-2.89336500
H	12.47397900	-1.89235700	-3.20821200
C	10.90936900	-2.70634300	-1.94901200
H	11.53817000	-3.49253800	-1.53320100
C	9.57278400	-2.60307500	-1.54563600
H	9.16686200	-3.31900400	-0.83269700
C	-4.14272900	-4.98948900	0.49273200
C	-3.31624900	-5.02270100	1.79401200
H	-3.93693200	-5.41867100	2.61572700
H	-2.99241000	-4.00922100	2.06349400
H	-2.42953100	-5.66083900	1.70591700
C	-4.58439100	-6.41869200	0.12342000
H	-3.73147200	-7.10847100	0.08510000
H	-5.09943100	-6.44612200	-0.84696500
H	-5.27947500	-6.79888200	0.88998600
C	-5.40366700	-4.13020200	0.74802600
H	-5.96603000	-4.54457500	1.60098400
H	-6.06178700	-4.11608700	-0.13110300
H	-5.12315100	-3.09537800	0.98325700

C	-1.81376000	-5.18108400	-1.61410000
C	-0.82596900	-5.62786700	-0.52374400
H	-1.27031100	-6.37807300	0.14193600
H	-0.50309000	-4.77018500	0.08305400
H	0.07185600	-6.07722200	-0.98276000
C	-2.34374100	-6.40672200	-2.39151700
H	-1.50722200	-6.90885500	-2.90620200
H	-3.07655800	-6.09956300	-3.15019300
H	-2.81982700	-7.14419100	-1.73725600
C	-1.06780500	-4.28621400	-2.62536500
H	-0.64629500	-3.39950700	-2.13431300
H	-1.74505300	-3.94706400	-3.42195300
H	-0.24715400	-4.85609900	-3.09100900
C	-3.05705300	-0.95378700	-1.09410800
H	-3.20615600	-1.34810000	-2.10780800
C	-4.39837000	-0.51258700	-0.56210300
C	-4.51696500	0.31129500	0.57655700
H	-3.61803600	0.65822300	1.08290900
C	-5.76654900	0.66534000	1.08363800
H	-5.82267200	1.28225300	1.98003600
C	-6.95938500	0.20253500	0.48185900
C	-6.83967600	-0.62432300	-0.65409700
H	-7.73921700	-0.97678500	-1.15848700
C	-5.58559600	-0.96635400	-1.16824200
H	-5.51518100	-1.61189500	-2.04351600
C	-8.28628400	0.57370200	1.02443300
C	-8.51351700	1.84757600	1.59240200
H	-7.70275600	2.57421500	1.60506900
C	-9.76717300	2.19774700	2.10733900
H	-9.91580200	3.18954800	2.53318600
C	-10.83250700	1.28544600	2.06322100
H	-11.80843900	1.55806000	2.46227300
C	-10.62441800	0.01689200	1.50053100
H	-11.43869000	-0.70646900	1.47030600
C	-9.36832900	-0.33480200	0.99251800
H	-9.20930400	-1.33358000	0.58904300
C	-2.00326800	0.18514200	-1.11286500
H	-1.64146500	0.35669400	-0.08630800
C	-2.48848400	1.49935300	-1.67127500
C	-3.38146600	1.57018300	-2.75872400
H	-3.78650700	0.65178600	-3.17900900
C	-3.79534600	2.80154800	-3.27461000
H	-4.51734600	2.82312200	-4.09010000
C	-3.33776800	4.01554000	-2.72064100
C	-2.44954000	3.94474800	-1.62643200
H	-2.06157200	4.86332900	-1.18785100
C	-2.03571000	2.71239400	-1.11525500
H	-1.34347300	2.68138900	-0.27448100
C	-3.78306300	5.32148400	-3.26364500
C	-3.99850700	5.49891400	-4.64790100
H	-3.80901300	4.66773000	-5.32532500
C	-4.42074200	6.73089500	-5.16152000
H	-4.57287900	6.84349500	-6.23430400
C	-4.63372900	7.82015500	-4.30350800
H	-4.96044400	8.77919200	-4.70245300
C	-4.42197200	7.66049700	-2.92589100
H	-4.59356600	8.49502500	-2.24722400
C	-4.00477800	6.42659700	-2.41298300
H	-3.87243500	6.30516600	-1.33919100
Li	-0.03920300	-2.04303500	-0.05123400
P	1.01139500	-0.23589000	1.22960100
P	0.99492100	-0.21196300	3.41458600
P	2.20153500	-2.83795000	-0.52691800
P	-2.41797600	-2.38612300	0.03319700

P	-3.29919500	-4.09421200	-1.00132600
P	-0.43330200	-0.46419200	-1.96982900

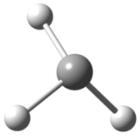

Figure S65. Optimized structure of [Me]$^-$.

Below are presented xyz coordinates for optimized geometry of [Me]$^-$:

C	0.00001700	0.00000400	-0.12526200
H	-0.58142900	0.86693100	0.25051400
H	-0.46017600	-0.93694800	0.25050700
H	1.04150100	0.06999300	0.25054900

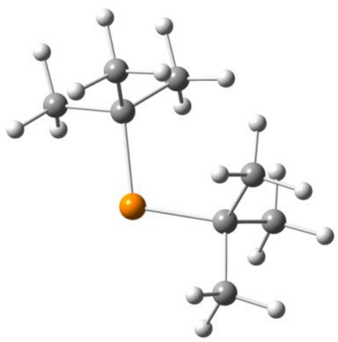

Figure S66. Optimized structure of [P*t*Bu$_2$]$^-$.

Below are presented xyz coordinates for optimized geometry of [P*t*Bu$_2$]$^-$:

C	1.55742800	0.02301300	0.00181300
C	1.89225500	0.61258100	-1.39166500
H	1.11105700	1.30044100	-1.73692600
H	2.85107700	1.17247200	-1.37085100
H	1.97241000	-0.19441700	-2.13101400
C	2.71873100	-0.92293500	0.38999200
H	2.75923600	-1.78534900	-0.29178700
H	3.68871600	-0.39306300	0.33474000
H	2.58108000	-1.30601000	1.40986900
C	1.52856200	1.17188400	1.03227300
H	0.76466100	1.92106100	0.78279400
H	1.30804100	0.78275900	2.03509200
H	2.50480300	1.69718400	1.06459200
C	-1.55742600	0.02301200	-0.00181400
C	-1.89225600	0.61258100	1.39166500
H	-1.97241300	-0.19441700	2.13101300
H	-1.11105800	1.30044000	1.73692800
H	-2.85107800	1.17247300	1.37084900
C	-2.71873000	-0.92293500	-0.38999200
H	-2.75923600	-1.78534900	0.29178800
H	-3.68871500	-0.39306300	-0.33474100
H	-2.58107900	-1.30601200	-1.40986800
C	-1.52856200	1.17188400	-1.03227300
H	-0.76466100	1.92106100	-0.78279600
H	-1.30804200	0.78276000	-2.03509200
H	-2.50480400	1.69718200	-1.06459000
P	0.00000000	-1.13364400	0.00000000

PART D. References

1. G. Sheldrick, A short history of SHELX, *Acta Crystallogr. A*, 2008, **64**, 112-122.
2. L. Farrugia, WinGX and ORTEP for Windows: an update, *J. Appl. Cryst.*, 2012, **45**, 849-854.
3. M. J. Frisch, G. W. Trucks, H. B. Schlegel, G. E. Scuseria, M. A. Robb, J. R. Cheeseman, G. Scalmani, V. Barone, G. A. Petersson, H. Nakatsuji, X. Li, M. Caricato, A. V. Marenich, J. Bloino, B. G. Janesko, R. Gomperts, B. Mennucci, H. P. Hratchian, J. V. Ortiz, A. F. Izmaylov, J. L. Sonnenberg, Williams, F. Ding, F. Lipparini, F. Egidi, J. Goings, B. Peng, A. Petrone, T. Henderson, D. Ranasinghe, V. G. Zakrzewski, J. Gao, N. Rega, G. Zheng, W. Liang, M. Hada, M. Ehara, K. Toyota, R. Fukuda, J. Hasegawa, M. Ishida, T. Nakajima, Y. Honda, O. Kitao, H. Nakai, T. Vreven, K. Throssell, J. A. Montgomery Jr., J. E. Peralta, F. Ogliaro, M. J. Bearpark, J. J. Heyd, E. N. Brothers, K. N. Kudin, V. N. Staroverov, T. A. Keith, R. Kobayashi, J. Normand, K. Raghavachari, A. P. Rendell, J. C. Burant, S. S. Iyengar, J. Tomasi, M. Cossi, J. M. Millam, M. Klene, C. Adamo, R. Cammi, J. W. Ochterski, R. L. Martin, K. Morokuma, O. Farkas, J. B. Foresman and D. J. Fox, Gaussian 16 Rev. B.01.*Journal*, 2016.
4. J. Tao, J. P. Perdew, V. N. Staroverov and G. E. Scuseria, Climbing the Density Functional Ladder: Nonempirical Meta--Generalized Gradient Approximation Designed for Molecules and Solids, *Phys. Rev. Lett.*, 2003, **91**, 146401.
5. S. Grimme, S. Ehrlich and L. Goerigk, Effect of the damping function in dispersion corrected density functional theory, *J. Comput. Chem.*, 2011, **32**, 1456-1465.